HYDROGEOMORPHOLOGY OF LAVA RISE PITS IN THE LAKI LAVA FIELD, SOUTHEAST ICELAND

TEDDY D'MOI KEEN

A THESIS SUBMITTED TO

THE FACULTY OF GRADUATE STUDIES

IN PARTIAL FULFILLMENT OF REQUIREMENTS

FOR THE DEGREE OF

MASTER OF SCIENCE

GRADUATE PROGRAM IN GEOGRAPHY

YORK UNIVERSITY

TORONTO, ONTARIO

July 2023

Abstract

In Southern Iceland, Lava Rise Pits (LRPs) can be found within the volcanic landscape of the Laki lava field. LRPs are a natural occurrence in pahoehoe lava flows and are formed when the lava in the underlying lava tubes ceases to flow and causes the surface to collapse. The goal of this thesis was to better understand the geomorphology and hydrology of lava rise pits over a Fall-Winter season. Three LRPs were selected for this study based on depth and openness to the atmosphere. A differential GPS was used to map their 2- and 3-dimentional structure. A range of sensors and measurements were made to track their thermal regime, rainfall, and soil moisture regime. Surveys of vegetation and soils were also made.

Ash and surface coverage varied amongst the pits. The deepest of the three pits (-7 m) had the least ash coverage while the shallowest pit (-2 m) had the most. The study also noted significant differences in surface coverage between the lava rise pits and with depth. Thermal regimes were primarily impacted by depth, pit openness and relations between the ground and air temperature signals. In pits that were more open and exposed to the atmosphere, the near surface above-ground temperatures, and below-ground temperatures mimicked the trends in air temperature. Precipitation (rainfall) was the most important input of water into these depressions, and soil moisture fluctuations were linked to ground temperature conditions. When ground temperatures were below 0°C and frozen, soil moisture levels were low despite large precipitation events. However, once ground temperatures increased, soil moisture levels rose due to snow and ice melt infiltrating into the ground.

While rainfall was the primary input of water into the lava rise pit system, other water pathways, such as overland flow, and groundwater may play a significant role in water movement in these features. Therefore, further hydrologic studies in this unique volcanic area are warranted.

Acknowledgements

I would like to thank my supervisor Dr. Kathy L. Young for her guidance, counselling, and support throughout my time at York University as both an undergraduate, and graduate student. Professor Young has been a great mentor and inspiration, who has taught me many well needed skills to situate myself in the fields of physical geography and hydrology. I would like to thank Professor Richard Bello, who also offered time and support when needed throughout this thesis. I am grateful for Patrick Modjehi who helped me by loaning field equipment, ensuring that it was calibrated, and in working order. He also provided useful advice on different field methods.

This study was accomplished through funds from the Northern Scientific Training Program (NSTP), as well as the Research Cost Fund grant issued by York University, in addition to research funds from Dr. Kathy L. Young. While at York University, I received support through a Teaching Assistant for which I'm most grateful.

In Iceland, I would like to thank Finnur Pálsson at the University of Iceland (Háskóli Islands) for his time and generosity with equipment support, as well as those from the Icelandic Institute of Natural History and the Meteorological office.

I am grateful for the friends who created my support system; Jessica Opoku, Rebecca Gasman, Amanda Little, Aiesha Aggarwal, Wesley Wu, and Elizabeth Perera, who have helped me along the way with their guidance, support, and knowledge.

And finally, I would like to thank those who never failed to cheer me on in addition to their infinite love and support, my family; Marjorie, Debbie, Ingvar Örn, and Fríða Ólöf, you are all appreciated beyond words, thank you!

To my Aunt Denise, we love you and we miss you.

Table of Contents

List of Tables

List of Figures

.

Chapter 1: Introduction

Iceland is found in the Low Arctic between 63°- 66°N and 13° - 24°W. Temperatures in Iceland are moderate due to the Gulf Stream bringing warm waters to Iceland's southern coast (Arnalds, 2016). The climate is mainly controlled by the Icelandic Low (IL), which is an area of low pressure in between Greenland and Iceland. The IL influences wind patterns and the amount of precipitation received across the country. Winters in Iceland often experience strong hurricane like winds with lots of precipitation (rain and snow), while summers in Iceland are the least active (Hanna, 2004). Regional and local weather patterns and temperatures are strongly controlled by the surrounding topography, resulting in micro-climates.

Icelandic deserts cover 35-45% of the country (35,000 - 45,000 km^2), making it the most dominant landscape type (Arnalds and Kimble, 2001). In this case, the term "desert" means an area that is desolated or abandoned (Arnalds and Kimble, 2001). Lava fields are one of the types of deserts in Iceland. Throughout the history of Iceland, volcanic activity has continuously reshaped landscapes here by ejecting large amounts of tephra into the atmosphere, which then falls to the land, smothering vegetation. Landscapes can also be covered over with massive lava flows. In 1783, a volcanic fissure 27 km long opened in Southern Iceland. This was the largest observed lava flow in Icelandic history (Thórdarson and Seif, 1993). At the time of the eruption, the lava flow completely decimated the land. Today this area is known as the Laki lava field. A common characteristic of basaltic lava fields are rapid soil infiltration rates, dry surface conditions and rough surfaces (Arnalds *et al.*, 2001; Kiernan *et al.*, 2003; Arnalds, 2004). Basaltic lava fields, such as the ones found in Iceland are highly permeable, making it likely that underground springs, aquifers and groundwater systems could be replenished with rainfall (Kiernan *et al.*, 2003).

Lava rise pits are a natural occurrence in basaltic pahoehoe lava flows and can be found in Skaftáreldhraun - a section of the Laki lava field in Southern Iceland. They are formed when the roofs of the underlying lava tubes collapse under the immense weight of the surface above creating large circular depressions (Walker, 1991). The geomorphology of these pits has been extensively researched in Hawaii (Walker 1991), Australia (Whitehead and Stephenson, 1998; Keirnan *et al*., 2002) and New Mexico, USA (Keszthelyi and Pieri, 1993; Hamilton et al., 2020) but there are gaps in knowledge about hydrological flow characterises in these volcanic features (Keirnan et al.,2002).

A conceptual diagram of the possible hydrological pathways of a lava rise pit in Southeast Iceland, outlining the gains, losses and storages of water can be seen in Figure 1.1.

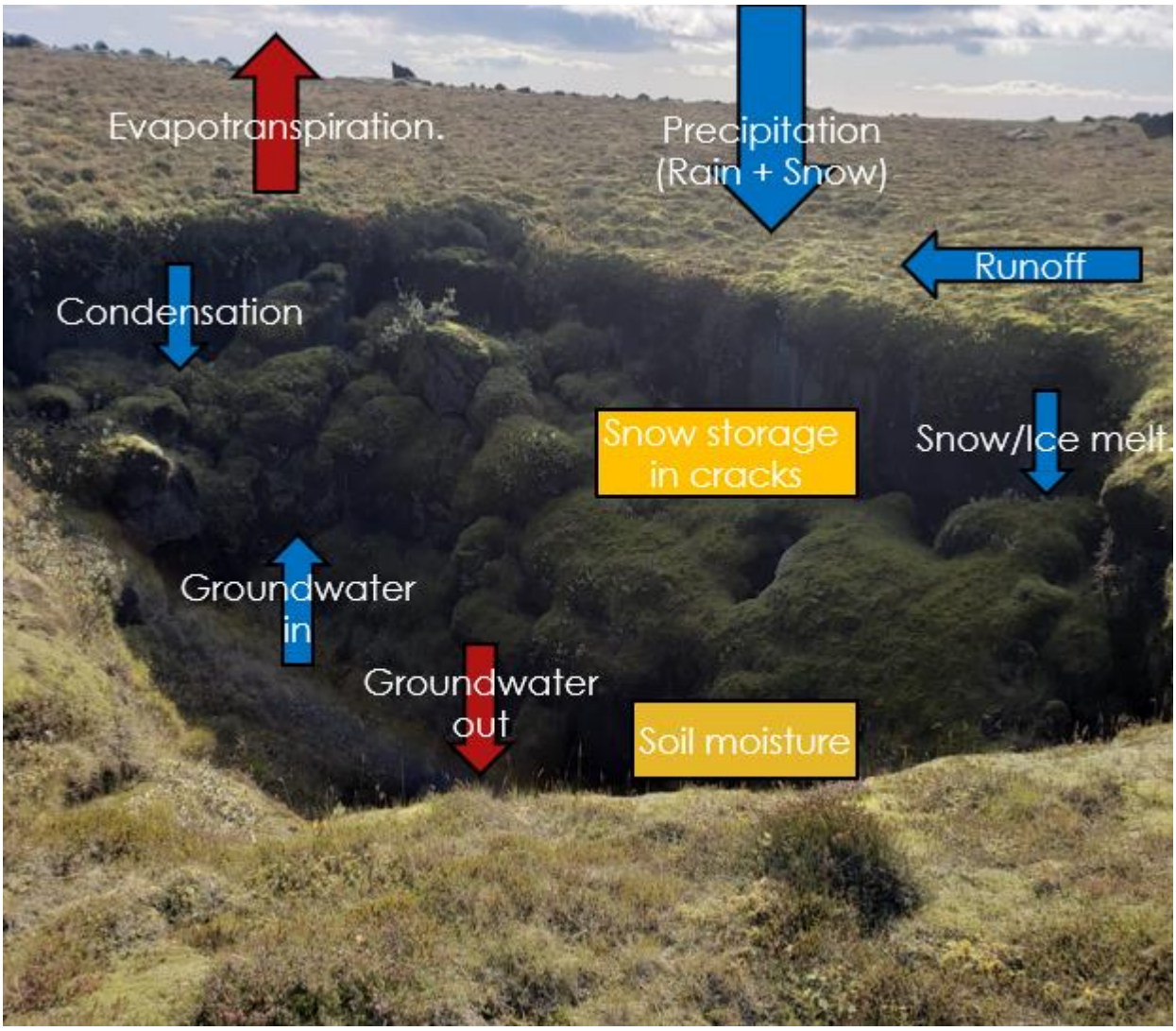

Figure 1.1 A conceptual diagram outlining the hydrological inputs, outputs and water storage of an Icelandic lava rise pit, Southeast Iceland. Possible gains of water are represented by blue, losses are red, and areas of water storage are yellow. Photograph of a lava rise pit taken September 16, 2019.

Local and regional winds in Iceland cause sediments (ash and dust) from various Icelandic sandar (fluvial outwash plains) to become airborne and transported, and this process is referred to as aeolian activity. Aeolian activity can be detrimental to areas as it can erode agriculture lands, riverbanks, and ditches, making these areas prone to floods. Lava rise pits are both a source and sink for ash and dust, thus driving local and regional aeolian activity (Walker, 1991). While it is known that ash and dust affect infiltration (Orradóttir, 2008), it is not known how ash and dust affect groundwater and its recharge-discharge processes, particularly in these lava depressions.

Groundwater in Iceland is one of the most important sources of drinking water (Klove *et al.,* 2016). Approximately 95% of Iceland's drinking water comes from groundwater sources (Klove *et al.,* 2016), that are recharged by rain, snowmelt, and streams/rivers that flood periodically. While groundwater is critical in the daily lives of all Icelanders, detailed water budgets and management strategies tend to neglect the role that lava fields play in the hydrological system through their potential to store, infiltrate and add water to groundwater reserves (Kiernan *et al.,* 2003).

This field-based study aims to improve our understanding of lava rise pits in Southeast Iceland both in terms of examining their geomorphological features and their hydrologic function, including water gains, losses, and storage. The manuscript is broken down into several chapters. Chapter 1 is the introduction. The second and third chapters contain the literature review, research questions and study objectives. The study site and field and lab methodologies are outlined in the 4th and 5th chapters respectively. The results and discussion are found in the 6th and 7th chapters, while chapter 8 outlines the conclusions of the study.

Due to limited hydrological knowledge about lava rise pits occurring in Iceland and despite their potential importance in groundwater flow systems, the primary question of this research study is: *What is the hydrological function of Icelandic Lava Rise Pits?* The following research objectives will aid in the understanding both their geomorphology and hydrology:

(1) Describe the geomorphology of lava rise pits (small to large) including their thermal regimes;

(2) Assess seasonal hydrology of lava rise pits, by examining areas of water inputs, losses, and storage of water from Fall to Spring (2020-2021) and,

(3) Evaluate the role of the lava rise pit structure (cracks, crevasses), and the occurrence of ash/dust, in enhancing water storage, drainage and loss.

Chapter 2: Literature Review

2.1 Volcanic Activity

Iceland is located on the Mid-Atlantic Ridge, making it one of the most volcanically active areas in the world. Historical records indicate that on average 20 eruptions occur per century or one every five years in Iceland (Óladóttir *et al.*, 2011). However, due to recent volcanic events (2021 – 2022 eruptions), it is likely that a new volcanic eruption period may begin, and it is predicted to last for centuries (Bindeman, Deegan, Troll *et al.*, 2022) Iceland is sectioned off into different volcanic zones, with 30 active volcanoes. Currently, the most active volcanic zone in Iceland is the Eastern Volcanic Zone (EVZ) with Grímsvötn showing recent activity (Figure 2.1). The Eastern Volcanic Zone (EVZ) has been responsible for 87% of the eruptions that have occurred historically — releasing the largest amounts of magma and tephra (Thorhallsdottir, 2007). Grímsvötn (Last Recorded Eruption-LRE, 2011), Katla (LRE, 1918), Hekla (LRE, 2000), Bárðarbunga (LRE, 2014-2015), Eyjafjallajökull (LRE, 2010) and the Vestmannaeyjar (Eldfell-Heimaey) volcano (LRE, 1973) reside in the EVZ zone and have all erupted within the last 150 years (Thórdarson and Larsen, 2007). Overall, about 60% of Icelandic volcanoes tend to be housed underneath icecaps (Bjornsson and Palsson, 2008). Underneath Vatnajökull, Europe's largest ice cap, are some of Iceland's most historically active volcanoes such as Grímsvötn (LRE, 2011), Bárðarbunga (LRE, 2014-2015) and Kverkfjöll. The latter is geothermally active but has not erupted within the last century (Óladóttir *et al.*, 2011). Fagradalsfjall in the Reykjanes Peninsula (Reykjanes Volcanic Belt - RVB), was the most recent eruption to occur in Iceland, which erupted on March 19th, 2021, and ended on September 18th, 2021 (Pedersen *et al*., 2022) and then again on August 3rd, 2022. Prior to these eruptions, the last eruption on record was approximately 781 years ago (Pedersen*et al.*, 2022; Bindeman *et al.*, 2022). The Laki lava field,

the study area of interest in this thesis is 40 km from Grímsvötn, 85 km from Bárðarbunga and 100 km from Kverkfjöll.

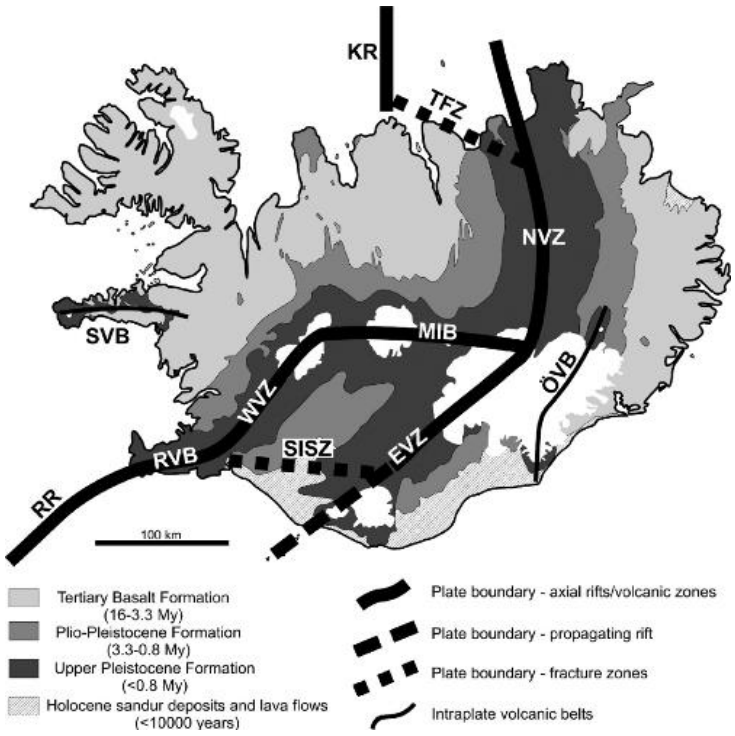

Figure 2.1. Volcanic zones and belts found in Iceland. RR, Reykjanes Ridge; RVB, Reykjanes Volcanic Belt; SISZ, South Iceland Seismic Zone; WVZ, West Volcanic Zone; MIB, Mid-Iceland Belt; EVZ, East Volcanic Zone; NVZ, North Volcanic Zone; TFZ, Tjörnes Fracture Zone; KR, Kolbeinsey Ridge; ÖVB, Öræfi Volcanic Belt; SVB, Snæfellsnes Volcanic Belt. (Thórdarson and Larsen (2007), Modified from Thórdarson and Höskuldsson (2002)).

Eruptions in Iceland can be characterized as explosive (Thórdarson and Larsen, 2007) and produce large amounts of tephra (Davies, 2010). Volcanoes positioned underneath ice caps commonly present more dangers than those opened to the atmosphere. ‘Wet’ eruptions are a result of hot volcanic magma interacting with the ice, creating explosive or ‘wet’ eruptions. ‘Dry’ eruptions occur when the tops of the volcano are ice free. ‘Wet’ eruptions are significantly

more dangerous when compared to ‘dry’ eruptions. Based on historical records, three out of every four eruptions are explosive, and of these explosions, 86% are ‘wet’, and 14% are ‘dry’ (Thórdarson and Höskuldsson, 2008).

Many eruptions that occur under ice caps are dangerous and can trigger jökulhlaups, which are flash floods that occur when the ice is rapidly melted. These floods can have catastrophic results and cause extensive damage impacting both humans and the landscape. However, eruptions do not need to occur under a glacier for a jökulhlaups to occur. Jökulhlaups also arise when the underlying volcano releases significant geothermally heat and ice melts. Glacial outwash plains (sandar - plural of sandur) can be expanded upon or created during jökulhlaups, as sediment trapped on the glacier, along with melt water, ash and tephra are all flushed out and deposited downstream on the land (Björnsson and Einarsson, 1990; Roberts *et al.,* 2001*;* Magillian *et al.,* 2002).

Volcanic eruptions in Iceland can either be basaltic, silicic or a mixture of the two. However, most of the eruptions are basaltic (79% — Thorhallsdottir, 2007). The difference between the two rock types is commonly noticed in soil stratigraphies. Dating volcanic eruptions based on the colour of tephra and ash has been used in many studies (Arnalds, 2008; Óladóttir *et al.,* 2011). Silicic ash tends to be lighter in colour (such as greys), whereas basaltic tephra is darker (black) (Arnalds, 2008).

Beyond altering the physical landscape, volcanoes can alter the soils found in all areas of Iceland. The soil properties of volcanic soils have lower organic content, high pH levels in comparison to organic material, and are easily eroded restricting vascular plant growth. As basaltic volcanic rocks are the dominant parent material in Iceland, soils found here are of an

andic nature, otherwise classified as andosols. Andosols are formed from tephra (ash and dust) from volcanic eruptions and through the erosion of volcanic rock. These soils are fine and glassy, making them poorly adhesive (Arnalds, 2004). The largest volume of andosols globally can be found in Iceland. Due to the consistent deposition of volcanic ash and tephra, Icelandic soils are the youngest, and are considered unique on a global scale (Arnalds, 2004). These soils can impact the hydrological cycle in volcanic areas as they generally exhibit high infiltration rates, have low bulk densities, and still have the potential to hold much water (Arnalds, 2004).

Aeolian activity occurs when sediments found in glacial or volcanic landscapes become airborne due to wind activity. Approximately 60-70% of the surface area in Iceland is covered by glacial or volcanic landscapes, and these areas experience sizeable and persistent wind. Consequently, these two landscapes act as both sinks and sources for ash and dust. With little to no vegetation present, aeolian transport and deposition, along with wind erosion in these areas are frequent, and severe (Gisladóttir *et al.*, 2005). Iceland has the largest active aeolian areas when being compared to other Arctic and European areas (Arnalds *et al*., 2016)

The aeolian processes in Iceland that are driven by volcanic eruptions, are impactful as they can remove vegetation and cause the erosion of ditches and riverbanks. Volcanic eruptions that eject large amounts of tephra can modify landscapes both locally and globally. In 2010, the eruption of Eyjafjallajökull released fine grains of tephra (ash and dust) into the atmosphere. The tephra was than dispersed by the northwesterly and westerly winds into the upper atmosphere to areas over 1000´s of kilometers (Davies, 2010). The eruption heavily interrupted air traffic across mainland Europe causing flights to be cancelled due to unsafe flying conditions (Davies *et al.*, 2010).

2.2 Laki lava field

In May of 1783, one of largest fissures in historical time erupted in Southern Iceland and it is called Laki. The 27 km long fissure with 140 vents opened and erupted for eight months (Guilbaud, 2005), resulting in the largest basaltic lava flow in history (147 km^3) (Thórdarson and Seif, 1993). At the same time, Grímsvötn was also active (1783-1785), resulting in a two-year long volcanic episode (Thórdarson and Seif, 1993; Guilbaud *et al.*, 2005). The continuous flow of lava inundated both the Skaftá and Hverfisfljót river gorges, redirecting the flow of water.

The Laki lava field was created when the lava flow in both river gorges overflowed onto the outwash plain of the Skaftá river and travelled eastwards (Thórdarson and Seif, 1993). During the lava flow, all known types of pahoehoe lava surfaces were formed; shelly pahoehoe, spiny pahoehoe, slabby pahoehoe and rubbly pahoehoe. Shelly pahoehoe, is characterized as large flat-topped sheet lobes with smooth vesicular surfaces. Slabby pahoehoe, can be identified by their tubular curved pieces of crust, and lava rise pits can be found in this landform. Rubbly pahoehoe can be identified by lava piled into mounds, which can range from 0.2 m to 0.5 m in thickness and 1-2 m in length. Finally, spiny pahoehoe ranges from 5-20 m long sheet lobes and have coherent crusts that are rarely fragmented. It is also common to see lava rise pits in this type of pahoehoe formation (Guilbaud *et al.*, 2005). The formation of these land types depends heavily on topography, amount of lava available to further extend the lava field, and the distance from the fissure (Guilbaud *et al.*, 2005).

The fine particles of tephra and haze (a combination of gases and aerosols) deposited into the atmosphere were dispersed locally and across Iceland, however, the tephra and haze were not only limited to Iceland (Thórdarson and Seif, 1993). At the time of the eruption, the westerly winds were the dominating current between 5-17 km above the surface (Thórdarson and Seif,

1993). At the most intense moment of the eruption, the plumes from the eruptions reached 10-15 km above the surface (Thórdarson and Seif, 1993). The regional winds caused the most damage to the area as it allowed the ash and haze to stay at lower levels in the atmosphere and be deposited with precipitation. During the 1783-1784 eruption of the Laki, no lives were directly lost, however the low-lying ash and haze from the eruption resulted in a long-lasting famine from 1783-1786. It is often referred to as the Haze Famine and contributed to the French Revolution (Thórdarson, 2003). The haze and ash deposition affected plant and crop growth, destroyed the livestock population by 50%, decimated the fish populations found in lakes and rivers and caused the death of 10,521 Icelanders or 22% of the population (Thórdarson and Seif, 1993).

2.3 Lava Rise Pits

Lava rise pits can be found in volcanic areas where the lava flow type is characterized as pahoehoe (Rowland and Walker, 1990). The two types of lava flow are pahoehoe and aa. The determining components of whether the lava flow will be a pahoehoe or an aa are the volcanoes eruption style and duration, magma chemical composition, gas to water ratio, temperature and volume, and viscosity and flow of lava (Rowland and Walker, 1990).

Aa lava flows at a high volumetric rate of > 5-10 m^3/s and creates rough surfaces, whereas pahoehoe has a volumetric flow of < 5-10 m^3/s resulting in smooth surfaces (Rowland and Walker, 1990). Typically, volcanoes that produce aa lava flows are powerful and exert a large amount of lava at a quicker rate (Rowland and Walker, 1990). Since aa has a higher volumetric flow, the formation of lava tubes is not common, and due to the higher volumetric flow rate, aa lava tends to flow above the surface in open channels instead of lava tubes (Rowland and Walker, 1990). There is less cooling time for the lava to form a roof, and in cases

where lava tube roofs are created, they tend to be torn away by continuing lava flows (Rowland and Walker, 1990).

Pahoehoe lava flows are generally associated with basaltic eruptions and have longer flow duration. Pahoehoe lava flow spreads horizontally or sheet like over larger distances in comparison with aa lava, which flow in narrow pathways (Walker, 1991; Self *et al.*,1998; Glaze *et al.*, 2004). As pahoehoe lava flow is slower (< 5-10 m^3/s), the surface can cool in sufficient time to create lava tubes. The Laki lava field is characterized as a pahoehoe lava flow field (Self *et al.*, 1998).

There are two ways in which lava rise pits can be created. The first is through the failure of lava rises. Lava rises occur when the lava being injected underneath cause the ground to lift upwards (hydrostatic pressure) (Walker, 1991). Lava rise pits created by this process occur when the lava rises above the elevated ground surface and then subsides forming depressions, or the ground fails to rise causing the lava to flow around it and grow in height (Walker, 1991). These forms of lava rise pits were observed in the Wapi lava field by Champion and Greeley (1977). It was also observed that lava rise pits formed in this process were not connected to lava tubes (Walker, 1991; Scheidt *et al.*, 2014) and instead are considered as products of inflation, in areas where lava failed to rise (Scheidt *et al.*, 2014).

The second way in which lava rise pits can be created occurs when the ground surface above the lava tubes collapses into the hollowed lava tubes, creating large depressions (Walker, 1991). However, lava rise pits created in this manner have a lava tube system attached (Walker, 1991), which is the situation in the Laki lava field (Kiernan *et al.*, 2003).

The depressions associated with lava rise pits can range from 1 m to > 20 m in depth, and vary in length and width (Walker, 1991; Glaze *et al.*, 2005). Lava rise pits created through the first process, have flatter surfaces with little to no mosaic blocks, which occur when the lava rise pit collapses into a lava tube (Walker, 1991). For lava rise pits that were formed through the second process, they tend to have complex flooring that occurs from the collapsed ground surface. These collapses are characterized by multiple ground surface lows (e.g. cracks and crevices) (Walker, 1991). The pits can also have flat edges, steep or overhanging escarpments (Walker, 1991; Scheidt *et al.*, 2014). Wide and deep pits can be potentially dangerous to humans and animals. A lava rise pit > 5 m in depth is shown in Figure 2.2.

Figure 2.2. A typical lava rise pit in the Laki lava field. A mosaic of ground surfaces: ash, vegetation, cracks and rocky overhangs can be observed in the depression. Photograph taken September 16, 2019. The person in the foreground is facing southwest.

The ground coverage for lava rise pits and adjacent lava field tend to be dominated by primary successors, such as graminoids (grasses), moss- e.g., Woolly Fringe Moss (*Racomitrium lanuginosum*) and salix- Tea Leaved Willow (*Salix phylicifolia)*. It is common to find these types of vegetation in Icelandic volcanic and glacial landscapes (Vilmundardóttir *et al.*, 2018),

including areas with much ash and dust (Glaze *et al.*, 2014). For the lava rise pits in Iceland's Skaftáreldahraun, dust and ash are often found in the cracks and crevices. The dust and ash are deposited during volcanic eruptions and through aeolian activity, the sediments are carried from Skeiðarársandur -the nearby sandur (glacial outwash plain), as well as from the nearby riverbeds of Hverfisfljót, Djúpa, and Bruná, glacial-fed rivers.

2.4 Climate of Iceland

2.4.1 Icelandic Low (IL) Pressure System

The Icelandic Low (IL) is an area of low pressure over the Northern Atlantic Ocean at 60 – 70°N, in between southern Greenland, and Iceland (Jónsdóttir and Uvo, 2009; Zhang and Walsh, 2004) (Figure 2.3).

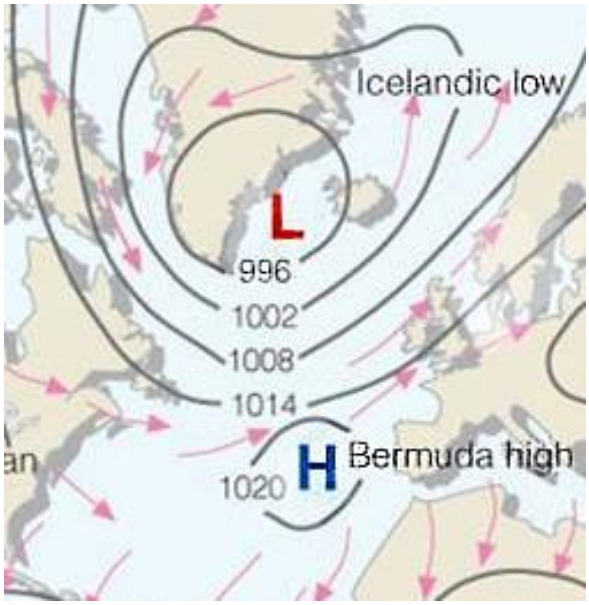

Figure 2.3. Diagram illustrates the occurrence of low-pressure systems in Iceland. The Icelandic low-pressure system can be spotted with the surface isobars. The west and southwest sections of Iceland show the lowest pressure contours (Photo: North Carolina Climate Office, https://climate.ncsu.edu/edu/NAO, March 1, 2020).

The Gulf Stream brings a continuous influx of warm water to the area. The temperature contrast between the cold atmosphere and warm water from the Gulf Stream create the Icelandic Low-pressure system (Hameed and Piontkovski, 2004; Phillips and Thrope, 2006). In low pressure systems it is very common for strong winds to occur (Serreze *et al.*, 1997). The most recent cyclonic event to hit Iceland and parts of Western Europe was Hurricane Dennis, with gale force winds reaching 108 – 144 km/h (IMO, 2020). Westerly winds arriving in Iceland are amplified during the winter months (Dec, Jan, Feb-DJF) and weakened in the summer (June, July, Aug-JJA) (Serreze *et al.*, 1997). The IL pressure system also influences the temperature and precipitation in Iceland creating dramatic changes both locally and nationally, thus making Iceland's climate extremely sensitive to any changes in the IL pressure system (Phillips and Thrope, 2006).

2.4.2 Temperature

Long term temperature data has been recorded continuously since 1845 in Stykkishólmur, West Iceland (Hanna *et al.*, 2004). Temperatures in Iceland are considerably moderate, with mild winters and cool summers in comparison to other sub-arctic regions (Ólafsson *et al.*, 2007). Mean winter temperatures in Iceland tend to stay at or slightly below freezing (0°C), while mean summer temperatures stay between 8 -10°C (Hanna *et al.*, 2004; Ólafsson *et al.*, 2007). The Gulf Stream plays a critical role in Iceland's temperature range. As the Gulf Stream brings warmer waters to Iceland's southern shores, it helps to warm the atmospheric temperatures and reduces the effects of arctic winds as they move west (Lyon, 2017). Within the last 30 years, there has been a significant increase in atmospheric temperature. Since 2000, warming in Iceland has been about 1.0ºC, which is directly linked to increases in temperature in the atmosphere and oceanic systems surrounding Iceland (Björnsson *et al.*, 2013).

2.4.3 Precipitation

Like temperature, precipitation data have been collected continuously for more than a century, starting in 1884 (Hanna, 2004; Jónsson, 1994). This longevity in record collection is critical as predicting changes and detecting trends in precipitation is significantly harder in comparison to temperature (Phillips and Thrope, 2006). Southern Iceland and areas where orographic influences are dominant receive the greatest amount of precipitation in Iceland (Ólafsson *et al.*, 2007). The annual mean precipitation in Southern Iceland is > 1000 mm, mainly aided by the southerly winds (Hanna *et al.*, 2004; Phillips and Thrope, 2006), and these values are significantly lower in the north (Phillips and Thrope, 2006; Ólafsson *et al.*, 2007). The summer months in Iceland (JJA) tend to have the lowest amounts of precipitation, whereas winter (DJF) and autumn (Sept, Oct, Nov-SON) have the highest followed by spring (Mar, April, May-MAM) (Hanna *et al.*, 2004). Precipitation can fall as snow in any season; however, it rarely occurs in July and August. Precipitation as snowfall reaches its peak during January and February (Jónsdóttir and Uvo, 2009). While precipitation changes seasonally, topography and wind direction are key factors in the amounts of received precipitation, thus resulting in precipitation being extremely local and sporadic (Hanna *et al.*, 2004; Ólafsson *et al.*, 2007).

2.5 Water Balance Theory

A water budget framework can be utilized to analyse and evaluate how much water is stored, gained, and lost over time (Young and Woo, 2004). When used over time, a water budget can display changes that have occurred due to significant weather events (i.e., extreme rainfall or droughts). Weather and climate change can significantly affect many hydrological processes (Du *et al.*, 2015), such as snowmelt, thawing of permafrost, evaporation rates (Xu *et al.*, 2018), and in

defining what form precipitation occurs (liquid - rain or frozen - snow). The largest hydrological input in the Icelandic lava rise pit system is precipitation (rain). As noted in section 2.4.3, Iceland receives high amounts of rainfall, which is driven by the Icelandic Low and regional topography. In the south, Iceland can receive >1000 mm of rainfall (Hanna, 2004). To better understand the hydrological cycle of these lava pits, the gains, losses, and storage of water need to be identified and examined (Figure 1.1). Ideally this can be approached using a water balance framework (eq. 3):

$$\underset{\textbf{Inputs}}{P\ (Sn + R) + Dr\ + Ls + GWin} \underset{\textbf{- Outputs}}{=\ E\ +\ GWout} \underset{\textbf{}}{= \pm \Delta S + \zeta} \underset{\textbf{}}{\pm \Delta \textbf{Storage+Error}} \quad (3)$$

where P is precipitation and is the total amount of snow (Sn) and rainfall (R), Dr is amount of water drip (condensation) that occurs under the overhang of the lava rise pit, Ls is the lateral surface flow that enters into the pits from the surrounding upland area, GW_{in} is the amount of groundwater entering the lava pits, E is evaporation loss and GW_{out} is the amount of groundwater leaving the lava rise pit system. The term ΔS represents the sum or loss of different water storages in the pits (e.g. snow storage in cracks), soil moisture (unsaturated zone) and groundwater (saturated zone). Finally, ζ represents the residuals or errors found in the measurement or estimation of these water budget constituents.

It can be difficult to accurately measure the individual water budget components due to inaccuracies with calculations, data and instrument errors, adverse weather conditions and the accessibility of the study site (Young and Woo, 2004; Montanari *et al.*, 2009). Errors in precipitation measurements are one of the most common problems, primarily due to wind activity (Wang *et al.* 2015), leading precipitation to be under or overestimated (Hanna *et al.*,

2004). In terms of snowfall, Wang *et al.,* (2015) found that snowfall can have errors of up to 50%. Young *et al.* (2010) observed errors in evaporation from wetlands, which they determined stemmed from a constant $\alpha' = 1.26$ in the Priestley-Taylor equation, often applied to wet surfaces. Groundwater estimates also often cause large uncertainties and errors in the water budget (Hunt *et al.* 1996) because groundwater is generally inaccessible and difficult to quantify in most areas (Khan *et al.*, 2016).

Chapter 3: Study Area

3.1 Iceland

Iceland is an island of 103,000 km^2 in area. It is located in the North Atlantic Ocean and is located in the Mid-Atlantic Rift zone where both the American and Eurasian tectonic plates are separating. Hence, it experiences much volcanic activity, which is a primary resource for geothermal energy and responsible for providing heated groundwater directly to taps and heaters in homes and businesses.

Glaciers are also a common landscape feature in Iceland and cover 11% of the surface (Jónsdóttir and Uvo, 2009). The watersheds from these glaciers take up another 35% of Iceland's surface area, making flooding from them widespread and significantly dangerous. Climate change however has negatively impacted Icelandic glaciers since the 1990s, and in the early 2000's all Icelandic glaciers were in a state of ablation. Since Icelandic glaciers are warm based, they are quite vulnerable to small variations in temperature and precipitation. The visual effects of climate change were evident in 2014, when the Icelandic glacier Okjökull was declared officially deceased by Dr. Oddur Sigurðsson, the head glaciologist at the Icelandic Meteorological Office (RUV.is, 2019). For glaciers that have underlying volcanoes, eruptions and geothermal activity can result in extremely dangerous flash floods (Sigurðsson *et al.*, 2007; Einarsson, 2009) inflicting extensive damage to both the environment, roads, homes, and agricultures. These jökulhlaups can also occur after the sudden drainage of ice-dammed glacial lakes.

3.1.1 Skaftáreldahraun

The Skaftáreldahraun (Eldahraun) is a 565 km^2 lava field located in Southeast Iceland at the southern-most tip of the Laki lava field, where more than 180 lava rise pits of various dimensions could be identified (Figure 3.1). The Skaftáreldahraun is boarded by two glacial rivers in the area, the Skaftá (Eldvatn) to the west and, the Hverfisfljót to the east (see Figure 3.1). The Skaftá (Eldvatn) river is both spring and glacier fed whereas the Hverfisfljót is only glacier fed (KGP, 2017). It is also the largest monitored glacial river in the area. However, both rivers are fed by glacial tongues from the Vatnajökull glacier. Approximately every two years, both rivers flood into the lava field, during high flow, with the Hverfisfljót River spilling water into the lava tubes in the Skaftáreldahraun (Kiernan *et al.,* 2003).

The lava field is intertwined with lava pits both deep (>5 m) and shallow (< 2 m) many with small and large cracks. Field observations in October 2019 showed that deeper pits had a larger temperature range (2-6°C) from top to bottom in comparison to the shallow pits (1-3°C). In December 2019, field observations indicated that several deeper pits had a little ice, if any, compared to the shallow pits. These observations were noted again in October 2020, and in January 2021. In May 2015, field observations by Dr. Kathy L. Young (York University) indicated that snow was stored in the cracks and crevices of the lava pits, insulated by thick layers of ash with ice water dripping from icy moss and shaded rocky, vertical walls.

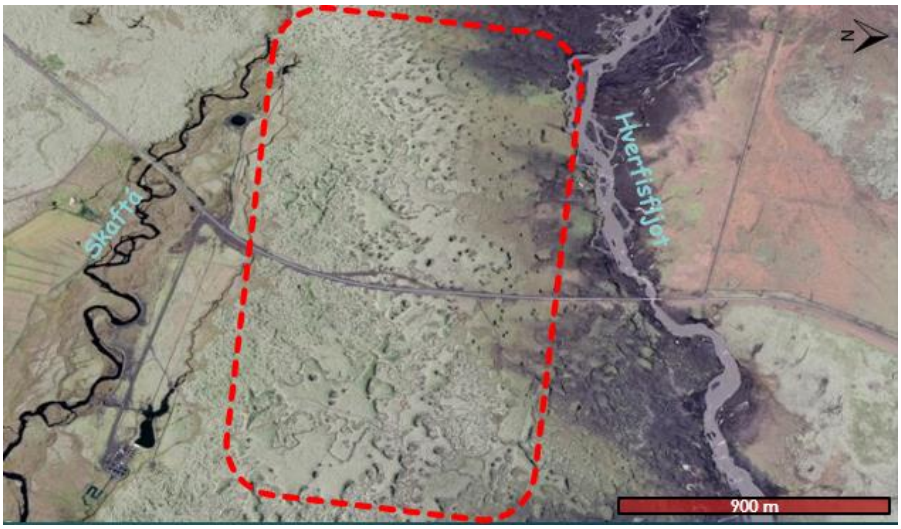

Figure 3.1. Lava rise pits (depressions) found in the Laki lava field can be found within the red dotted lines. Two glacial rivers, the Skaftá and the Hverfisfljót are identified (Photo: Google Maps, March 10, 2020).

To the south of the Skaftáreldahraun lies the world's largest glacial outwash plain- Skeiðarársandur, created by sediment depositions from glacial rivers and jökulhlaups. Being a volcanic landscape, ash and dust are the main surface cover types, along with Icelandic moss. Aeolian deposition in the study site would be significantly higher as the sediment from the Hverfisfljót river along with aeolian material from the sandur can frequently be carried into the lava rise pits and collect in the vegetation or be directly stored in cracks. While a little covering of ash on snow can enhance snowmelt by reducing the albedo, thick coverings can prolong insitu snow (insulation). Thick sediments on vegetation and other rocky surfaces will also modify water infiltration and storage in these geo-systems (Poesen *et al*., 1994; Thompson *et al*., 2010; Dubbert and Werner, 2019).

As this is a volcanic landscape, surface types can either consist of vegetation (primary succession), ash and dust, or bare rock. The Laki Lava field is considered a sandy lava, due to the high amounts of aeolian activity (Thorarinsdóttir and Arnalds, 2012). The sediments that are

deposited into the lava field can originate from tephra (ash and dust), as well as sediment from the near-by sandur and riverbanks of glacial rivers (Thorarinsdóttir and Arnalds, 2012). For this study, three lava pits were selected for further study. Due to the varying physical characteristics of lava rise pits, three lava rise pits were selected based on their depth: – 2 m, –5 m, and –7 m (see Figure 3.2).

Figure 3.2. Selected lava rise pits used for this study found at the edge of the Laki lava field, SE Iceland. a) 2 m deep, b) 5 m deep and c) 7 m deep. Photo: Shallow Pit September 16, 2019, Deep Pit December 26, 2019.

3.2 Vegetation

Unlike sand deserts, sandy lavas like the Laki Lava field can still have a strong presence of vegetation. The vegetation found here are typically *graminoids* (grasses), *Racomitrium lanuginosum* (Woolly Fringe Moss*)* and *Salix phylicifolia* (Tea Leaved Willow*)* (Bjarnason, 1991). The landscape processes behind volcanic and glacial landscapes strip the land of all soils and nutrients leaving bare ground. The vegetation that grows soon after are considered "R" species or primary succession species (Tsuyuzaki and Moral, 1995). While these three species are abundant in the lava field, based on field observations, the distribution of these plants along with the other plants identified could be dependent on one or more of the following factors, such as, aeolian activity, soil type, sunlight, climate, infiltration, and/or surface structure of the lava (Vilmundardóttir *et al*., 2018).

While *Graminoids (*grasses*), Racomitrium lanuginosum (*Woolly Fringe Moss*) and Salix phylicifolia (*Tea Leaved Willow*)* make up a majority of the lava fields vegetation coverage, other plants are also present (Figure 3.3). *Empetrum nigrum* (Crowberry), *Juncus ranarius* (Frog Rush), *Cladonia rangiferina* (Reindeer Lichen), *Thymus praecox* (Wild Thyme), *Alchemilla alpine* (Alpine Lady's Mantle), and *Festuca richardsonii* (Arctic Fescue) were identified within the lava rise pits as well as at the lava field surface. The vegetation found within the lava field were verified using Hörður Kristinsson's book, Flowering Plants and Ferns of Iceland (2010) and by experts from the Icelandic Institute of Natural History (IINH).

Figure 3.3. Vegetation found within the lava field and within the three lava rise pit used for this study. a. Thymus praecox (Wild Thyme), b. Alchemilla alpina (Alpine Lady's-Mantle), c. Juncus ranarius (Rush Frog), d. Cladonia rangiferina (Reindeer Lichen), e. Racomitrium lanuginosum (Woolly Fringe Moss), f. Graminoid (Grass), g. Empetrum nigrum (Crowberry), h. Salix phylicifolia (Tea Leaved Willow), and i. Festuca richardsoni (Arctic Fescue).

Chapter 4: Methodology

4.1 Geomorphology

The physical characteristics of lava rise pits have been studied in detail by many geologists (e.g., Walker, 1991; Self and Keszthelyi, 1998; Kiernan *et al.*, 2003; Glaze *et al.*, 2005; and Scheidt *et al.*, 2014) focussing on Hawaii, resulting in limited literature on the lava rise pits found in Iceland. As mentioned in Section 2.3, lava rise pits are formed when the roof of lava tubes collapses under the weight of the surface, or lava rises above the ground and then collapses due to lack of lava flow (Walker, 1991). Kiernan *et al*., (2003) identified that lava tubes in Skaftáreldahraun have also been used by overflow by the glacier river Hverfisfljót. This suggests that the lava rise pits in the Skaftáreldhraun (Laki Lava field) are created by the collapsing of the roofs of the lava tubes, rather than lava rising above the ground that failed to rise under hydrostatic pressure. A summarised table outlining number of samples collected per pit, type of parameters/variables measured, location within the pit and the sampling approach can be found in Appendix I.

4.1.1 Physical Characteristics

In this study, the physical dimensions and distribution of cracks of Icelandic lava rise pits were analyzed. Using a roving Differential GPS system (Trimble R7 ±10 cm), the length, width and elevation (X, Y and Z) of the lava rise pits was recorded. As there is limited geomorphological data on the lava rise pits, using a Differential GPS system was necessary for this study as it has a higher level of accuracy (± 10 cm) compared to standard GPS technology (Kuter and Kuter, 2010). The waypoints collected were uploaded into ArcGIS where both a 2D and 3D model of the lava rise pits were produced to better show the rugged terrain of these features.

4.1.2 Surface Type and Coverage

As this is a volcanic landscape, surface types can either consist of vegetation, ash and dust, or bare rock. The sediments that are deposited in this area are from tephra and ash from volcanic eruptions, as well as from glacial sediment from sandar and glacial riverbanks (Thorarinsdóttir and Arnalds, 2012). Aeolian activity largely determines where and what surface type will persist (Gísladóttir *et al.,* 2005). Aeolian activity can both deposit sediment (i.e. dust, ash and sand) and use sediment suspended in the air to erode the land and vegetation during wind activity. Specifically, moss and vascular plants in these areas can be destroyed overtime with wind erosion through burial or abrasion (Gisladóttir *et al.,* 2005). The Laki lava field and other sandy lava fields are known as sediment sinks, as large amounts of airborne sediments get trapped and settle into the depressions because of surface roughness (Gisladóttir *et al.*, 2005). The sediment can be deposited onto the landscape from glacial riverbanks, eruptions, and glacial sediment from sandar (Thorarinsdottir and Arnalds, 2012). As surfaces become less vegetated, the role of ash, dust and glacier sediment become more dominating and aeolian activity becomes stronger over time (Gisladóttir *et al.*, 2005; Thorarinsdottir and Arnalds, 2012).

For this study, surface coverage was analyzed using the stratified random sample approach. Each pit was subjectively sectioned off by depth (top, middle, bottom); the vegetated and non-vegetated surface types were then sampled with quadrats (0.25 m x 0.25 m). The quadrat was thrown within the sectioned depths of the pit, for a total of 90 quadrat readings per pit (30 samples per section). For the sampling of plants and surfaces, the minimum size for a quadrat is 0.25 m x 0.25 m (Phukan and Boruah, 2021). Since the surface cover distribution frequently changed, especially within the pits, and the vegetation was pre-established, (following

Phukan and Boruah, 2021) the choice of a 0.25 m x 0.25 m quadrat was deemed appropriate to realistically represent the areas.

4.1.3 Vegetation

Using the samples collected from the stratified random samples (5.1.3), vegetation density was examined. Within the quadrats (0.25 m x 0.25 m), vegetation type was recorded (following after Muller-Dombois and Ellenberg, 1974). These data were then used to calculate vegetation density, which indicates how many individual plants are in an area. The vegetation that was identified in the field was also compared to the botany textbook by Kristinsson, (2010). Photos of the different vegetation types were also sent to the Icelandic Institute of Natural History and were verified by Starri Heiðmarsson, an expert botanist for Iceland.

A photo was taken of each quadrat and the area of the quadrat was divided into sections using a grid overlay (5 cm x 5 cm per grid), which was then used to calculate the surface coverage within each quadrat (Chen *et al.*, 2010). The percentage of the surface type (e.g. plant, dust, rock) was identified within the quadrat. To calculate how much area each surface type covered, the area of the entire quadrat and each individual cell within the grid was determined.

This method documented how the surface coverage changed within the different depths of the pits and indicated what the dominating surface and/or vegetation type was. Combining the density and coverage data served to address links between the physical characteristics of the lava rise pits and erosion/deposition factors. Specifically, this approach confirmed whether the spatial patterning of vegetation was in response to erosion (aeolian activity), or the physical features of the lava rise pit itself through modification of moisture and the micro-climatic conditions (e.g. temperature, shade and wind).

4.1.4 Soil Properties and Characteristics

Soils are a critical feature in lava fields and lava rise pits. Soils can modify infiltration rates and can determine what types of aeolian material are being deposited. Soils found within volcanic landscapes are known as Andosols or Andic soils. These soils have a parent material of basaltic volcanic glasses that are ejected from volcanoes in the form of tephra and ash (Arnalds, 2016), or from the erosion and weathering of volcanic rocks (Arnalds *et al.,* 2001; Arnalds, 2010). Compared to andosols found in other volcanic areas i.e. New Zealand, parent material of andosols found in Iceland are more diverse (Arnalds, 2004). Andosols in Iceland are some of the youngest soils in the world due to frequent volcanic eruptions, aeolian deposition and glacial sediment inputs (Arnalds, 2004). At this specific site, aeolian deposits consist of volcanic ash and dust, glacial sediment from nearby glacial outwash fields (sandar) and glacial riverbanks. Andosols tend to have very low bulk densities with high porosity, along with very high-water holding capacities when saturated (Arnalds, 2008). In accordance with the simplified soil map of Iceland developed by Arnalds and Grétarsson (2001), the specific andic soil type found in the Laki Lava field is characterized as vitrisols, a sub-category of andosols found in cool and moist areas. They are characterized by high infiltration rates especially in the summer season (Arnalds, 2008).

For this study, due to restrictions of a soil import licence, only six soil samples of 200-350g from each lava rise pit were collected in soils tins with known weights and volumes. These soils were collected at the surface, middle and bottom of the lava pits. Soil samples of greater than 200g are required as it is the total amount needed for the accurate completion of the following soil testing. As noted each pit had six samples analyzed (n= 6 per lava rise per pit surface, center and bottom) for a total of 18 soil samples collected during the study. Using the six

samples per pit, the following tests were conducted: bulk density, porosity, particle size and grain distribution (Ward and Robinson, 2001; Carter and Gregorich, 2007 and Koc *et al.*, 2008).

4.1.5 Bulk Density and Porosity

Bulk density ρb (g/cm^3) is used to identify compaction within the soils, whereas porosity (Φ) (%) is the number of open spaces or voids in between soils that can either be filled with air or water (Ward and Robinson, 2000). Bulk density and porosity tend to be analyzed together due to their shared relation. If bulk density is high, porosity tends to be low and vice versa.

To obtain bulk density, lab testing methods followed those of Koc *et al.* (2008). Soil samples in tins of a known volume (31.1 cm^3) were weighed and dried for 24 hours at 104°C. After 24 hours, the dried soils were reweighed *Mt* (g). Bulk density ρb (g/cm^3) was then calculated where the weight of the dried soil sample *Mt* (g) is divided by total volume of the soil *Vt* (cm^3):

$$\rho b = \frac{Mt}{Vt} \quad (1)$$

Soil porosity (Φ) is a volumetric measurement as it measures the volume of pores (Vp) (void spaces) per volume of soil sample (Vt) (Ward and Robinson, 2000). Soil porosity (Φ) can be obtained by the following equation:

$$\Phi = \frac{Vp}{Vt}\ x\ 100 \quad (2)$$

4.1.6 Particle Size and Distribution

Soil particle size is an important characteristic of soils, especially found in areas of higher aeolian activity. Particle size can be found using the sieving and gradation method. The sieving method is used to separate sands from fines (silts and clay) through the utilization of different sized sieves (see Carter and Gregorich, 2007).

Soils were weighed and dried for 24 hours, at which point they were lightly separated and sieved. The following sieves were used: no. 10 (2 mm), no. 18 (1 mm), no. 35 (500 μm), no. 60 (250 μm), no. 120 (125 μm), and no. 230 (63 μm). Carter and Gregorich (2007) indicate that sieve no. 230 (63 μm) is critical as it is used to separate gravels and sands from fines (silts and clays). Following sieving, the amount of the retained soil per sieve was calculated for a cumulative total. The retained amounts (*Rw*) of soil sample (g) from each sieve was then be divided by the original weight (*Ow*) of the soil sample (g), to obtain the percentage of gravels, sands and fines (silts and clays):

4.2 Micro-climatology of Lava Rise Pits

Climate and weather in Iceland are not uniform, in fact precipitation, temperature and windspeeds are controlled by regional topography, resulting in dramatic changes in areas relatively near each other.

4.2.1 Precipitation

Precipitation was recorded in both the lava field, and the Kirkjubæjarklaustur weather station. To measure precipitation in the field one automatic ONSET HOBO RG3-M tipping-bucket rain gauge (± 0.25 mm) was placed at the bottom of each lava rise pit (n=3), as well as two placed at the surface in the surrounding lava field. One ONSET HOBO RG3-M tipping bucket rain gauge was also placed under an overhang in the 7 m lava rise pit to intercept precipitation under a moss overhang. Precipitation was measured at the Kirkjubæjarklaustur weather station with a Lambrecht Type 15183H tipping-bucket rain gauge, placed 1.5 m above ground.

As the rain gauges in the lava field dropped in accuracy below 0°C, the precipitation for these days were estimated. A ratio was used to calculate the relationship between total rainfall collected in Kirkjubæjarklaustur and in the lava field on days that were $\geq$ 0°C. This ratio was then applied to days below 0°C to estimate precipitation and is referred to as adjusted precipitation. A partial rainfall record was measured for the -5 m pit until the raingauge failed.

As measuring snowfall can be difficult in the field, it was not possible to know the exact amount of snow collected in the pits.

4.2.2 Air Temperature and Light Intensity

Temperatures within the pit can significantly vary from the temperatures found at the ground surface. This was confirmed during preliminary field observations using a Fluke infrared thermometer (± 1.5ºC), in both October and December 2019. As freeze-thaw cycles are common in Iceland (Hall, 2007; Arnalds, 2015), it was important to capture seasonal ground temperature changes to identify links between snow and ice melt, and soil infiltration.

For continuous measurements (hourly) and to capture the changes to the temperature regimes over the seasons (Fall to Spring), HOBO Pendant MX Temperature/Light Data Loggers (±0.5°C, 0 to 320,000 lux (x0.0079 Wm^{-2}) were placed 8 cm above the ground, within the lava rise pit, at the surface, middle and bottom zones. Changes in light levels indicated where the pit surfaces were in shade or in the open.

4.2.3 Surface Type Temperature

Preliminary field observations in October 2019 indicated that surface temperatures for grass, vascular plants, moss, and bare ground varied at different depths within the pits. As air temperature, ground temperature and shading play a large role in determining the temperatures of the pits, it was important to assess near-surface temperatures to examine spatial patterns. Using the stratified random sample approach, each surface type was spot sampled at different levels (upper, middle, lower) in the lava rise pits using an infrared thermometer (± 3ºC). To monitor continuous near-surface ground temperature changes, a HOBO Smart Temperature Sensor (±0.2°C) was placed at the bottom of each pit at a depth of -0.05 m. These near-ground temperatures were recorded every 15 minutes.

4.2.4 Relative Humidity and Wind Speed

A Kestrel 3000 (handheld windspeed, temperature and humidity monitor) was used when in the field to record spot measurements of windspeed (m/s) (including averages, gusts), relative humidity (%) (± 3%), air temperature and dew point (± 0.5ºC) at the top and bottom of each pit once a day. Spot measurements in the lava field were taken twice a day. Continuous relative humidity measurements were also recorded with three (3) HOBO MX2301A Temperature and Relative Humidity (RH) sensors (Temperature: ±0.2ºC, RH ± 1%). One was placed at the lava field surface on a pole (70 cm) above the lava field surface while the other two were placed at the bottom of the -2 m (shallow) and -7 m (deep) lava rise pits, again 70 cm above the ground surface. Continuous wind measurements were not collected in the field. Instead, daily wind data (speed and direction) along with other supplementary climate information (air temperature and precipitation) were obtained at the Kirkjubæjarklaustur – Stjórnarsandur (63.793N, 18.0119W) (IMO) weather station (18 km away). Wind was measured with a Young Marine Wind Monitor (±0.3 m/s) placed 10 m above ground, and temperature was measured with a Logan PT-100 temperature sensor placed 2.0 m above ground. These government climate data collected from an open field provided verification for the field data collected. These data were also used as supplementary data for site conditions.

4.3 Hydrological Methods

The hydrological processes of a lava rise pit can be identified by water gains, losses, and storage. This section addresses these three processes.

4.3.1 Drip and condensation

Overhang drip and condensation within the cracks can be considered as water inputs in the hydrological system of these lava rise pits. It is critical to know the surface type and slope of the

overhangs. These two characteristics can either hinder or accelerate drip activity. Drip primarily occurs when the vegetation has reached its maximum storage capacity, at which point water either drains (drips) into the pits or evaporates (a loss). When dripping into the pits, the water can be absorbed by the underlying sand and porous rocks.

The original method to collect overhang drip and condensation was through the utilization of a rain trough system that would be fastened to the walls of the pits directly underneath the overhang. In a study conducted by Gomez *et al.* (2018), troughs were used to catch runoff and funnel it into a storage system to create a small-scale irrigation system in arid areas. Utilizing this technique, troughs would drain into manual rain gauges, where they would be measured daily during the in-field portion of this study (May 3rd to May 22nd, 2020). However, due to the uneven surfaces of the lava rise pits, it was not possible for the rain trough system to be implemented. Instead, a container (60 cm x 40 cm x 22 cm – water holding capacity of 45L) with a tube leading directly to an ONSET HOBO RG3-M tipping-bucket rain gauges (± 0.25 mm) was utilized. Seven manual rain gauges (dia. = 15cm) that could hold 1000 ml, drained twice per day were placed under the over hangs of each pit to collect dripping water during the study period. Due to the variation in wind, precipitation and temperature, the amount of water collected in the rain gauges were not reliable as they would overflow depending on the weather conditions resulting in inaccurate readings. These data are not reported.

4.3.2 Infiltration

Infiltration can be defined as a process that moves water from one place to another in a lava rise pit, for example from the surface into bare ground, sediment, vegetation and ultimately into the underlying groundwater system. The soils in Icelandic lava fields tend to drain relatively well, even when vegetated (Arnalds and Kimble, 2001) in comparison to non-volcanic landscapes

(Arnalds, 2004). The soil's ability to infiltrate quickly is due to the parent material and the soil being of volcanic or 'andic' nature — having high permeability (Arnalds, 2004).

As this study took place over several seasons including the winter, frozen ground was probable. As the temperatures in Iceland are dependent on local topography and microclimate, multiple freeze-thaw events are also not uncommon. Freeze-thaw occurs when in a short period of time the frozen ground (<0°C) rapidly warms up (>4°C) and then refreezes (Arnalds, 2004; Orradóttir, 2008). Arnalds (2004) found, that andosols have a fast infiltration rate, and high-water holding capacity, however, this significantly changes when the soils are frozen.

Infiltration was monitored using the double ring infiltrometer method (Bouwer, 1986; Orradóttir, 2008). The rings were 40 cm in height and had a 39 cm diameter outer ring and 22.9 cm (inner) diameter. The rings were hammered 39 cm in the ground, leaving 1 cm above the surface with a water head of 5 mm, in both the inner ring and outer ring (Orradóttir, 2008). Changes in water level (1 mm) and time was then recorded for an hour, or until infiltration reached a plateau (Orradóttir, 2008). Due to the soil type, the duration of the infiltration tests was between 100 to 120 minutes. Infiltration readings were taken at the bottom of each pit (n=3) as well as at the surface in rock free areas before and after a rainfall event. Prior to conducting the double ring infiltration tests, the surface coverage was recorded with quadrats (0.25 m x 0.25 m). The surface (6 cm) volumetric moisture content of the soils was also recorded with a Theta soil moisture probe (%), as the degree of soil saturation could modify infiltration into the ground. Infiltration rates (mm/min) and cumulative infiltration (mm) both before and after a rainfall event were then calculated and analysed.

4.3.3 Depression storage (Water Pooling)

While it is uncertain where water pooling can be found in lava rise pits, a continuous HOBO water level logger was placed where water pooling was anticipated. As noted, lava rise pits have cracks and crevices that can collect snow, ash, and dust. Ash and dust that has been deposited on top of snow can either insulate snow, decreasing its melt rate, or significantly increase the melting rate with just a thin covering of sediment by lowering its albedo (Dragosics, 2016). Cracks and crevices are also areas where pooling is likely to occur once snow and ice melt begins, or sites in the pit where the soil would be susceptible to rapid freeze and thaw. As mentioned earlier, Arnalds (2016) found that andic soils can infiltrate water quickly and have a high-water holding capacity, which was important when considering where water pooling might occur. Previous preliminary field observations indicated that the pooling of water or its absence is influenced by seasonal climate (snowmelt, heavy rainfall, or periods of drought).

In the 2 m lava rise pits, an ONSET HOBO U20 Water Level Pressure Transducer (± 0.075 % per 0.3 cm water) was utilized to record water level every 15 minutes in water pools. Another water level pressure transducer was placed 1.0 m above the level ground surface and was fastened to a pole and measured atmospheric pressure. This approach would allow water level to be determined at the water pool based on the differences between atmospheric pressure and water pressure (Scheffel and Young, 2021). The elevation and GPS coordinates of the Hobo sensors were also recorded.

4.4 Soil Moisture

Soil moisture (θ) considers water storage in the unsaturated zone. For these andic soils (dust, ash — tephra), their water holding capacity is considered high (Arnalds, 2004). A stratified, random sampling approach was used to measure volumetric soil moisture (θ %) at different depths in the

lave rise pit and surfaces (grass, moss, vascular plants, and bare ground). Spot soil moisture (θ%) were measured with a 6 cm long, Theta Probe (± 1%), and a 10 cm long, HOBO 10HS Smart Moisture Sensor (± 3%). A HOBO 10HS Smart Soil Moisture Sensor (± 3%) was placed at the bottom of each pit and at the lava field surface allowing for continuous soil moisture measurements over the study period. Soil moisture estimates were then analysed in relation to surface conditions and measured precipitation.

4.4.1 Volumetric Soil Moisture Content and Degree of Saturation

Soil samples at the different depths were collected in soil tins as noted in section 5.1.5. These samples were then be brought back to the lab where volumetric soil moisture tests were completed (θ), using the following equation (Black, 1965), where *Vw* is the volume of water and *Vs* is the volume of soil:

$$\theta = \frac{Vw}{Vs} \tag{3}$$

Degree of saturation identifies the proportion of pores that contain water and is typically presented as a percentage (%) (Dingman 2015; Bordoni *et al.*, 2018). Using the following equation, the degree of saturation (Θ) was calculated (Dingman 2015; Bordoni *et al.*, 2018), where θ is the volumetric moisture content and Φ is porosity:

$$\Theta = \frac{\theta}{\Phi} * 100 \tag{4}$$

Chapter 5: Results

In this section, the information and data collected from the three lava rise pits, and the lava field during the study period: September 26th, 2020 – March 30th, 2021, will be presented. Section 5.1 will examine the morphology of the lava rise pits and their soil characteristics. Section 5.2 will further analyse the distribution of ash and surface coverage within the lava rise pits. Section 5.3 will focus on the microclimatology within the lava field and compare these data with the nearest government weather station at Kirkjubæjarklaustur (approximately 18 km away). Section 5.4 will analyze the thermal response of the lava rise pits, followed by Section 5.5, which will focus on the seasonal hydrology of the lava rise pits.

5.1 Geomorphology

5.1.1 2D Geomorphology of Lava Rise Pits

The dimensions (depth and diameter) of the Lava Rise Pits were measured using a Trimble7 (±10 cm). During preliminary data collection, the depths of the pits were measured using a traditional Garmin 62cs GPS (±10 m). GPS data was collected on September 26 and 27th, 2021 and again on August 25th, 2022.

The 2D spatial maps of the pits show the change in depth for each of the pits along with their circumference (Figure 5.1). The -7 m pit was the largest of the three pits in both depth and diameter. The -2 m pit had the second largest circumference followed by the -5 m pit. What can be observed in the -7 m pit is that there were two prominent deep points.

The 3D spatial maps help understand the distribution of elevations within the three pits and shows the complex shapes that these lava rise pits have, which can be seen in Figures 5.2 a, b and c. The complex geomorphology of these pits, specifically in the -7 m pit made digital mapping difficult. The entry ways into the lava tubes (sub-surface) were deeper than the bottom of the pit. Since it was not possible for the DGPS to connect with the satellite, it was not possible to record the lowest part of the pit (Figure 5.2). Using a measuring tape, the depth from the bottom of the pit – deepest point the DGPS could measure to the lava tube entry was approximately 154 cm lower than the deepest point collected by the GPS.

Field observations indicated that the distribution and sizes of pits found within the lava field varied. Pits that were located on the edge of the lava field (closer to the road and the glacial river Hverfisfljót) had more sand deposition and rockier surfaces. The lava rise pits that were found in the further into the interior of the lava field had more mature vegetation i.e. more vascular and non-vascular plant material, with less sandy surfaces. This could be seen when examining the surface type findings (figures 5.4 – 5.7) as the -7 m pit was the furthest inland from the peripheral of the lava field, compared to the -2 m pit that was approximately 50 m from the Hverfisfljót river, and the -5 m pit, which was approximately 20 m from the road. The positioning of the lava rise pits did not impact depth or circumference, as both deep and shallow pits were scattered throughout the lava field.

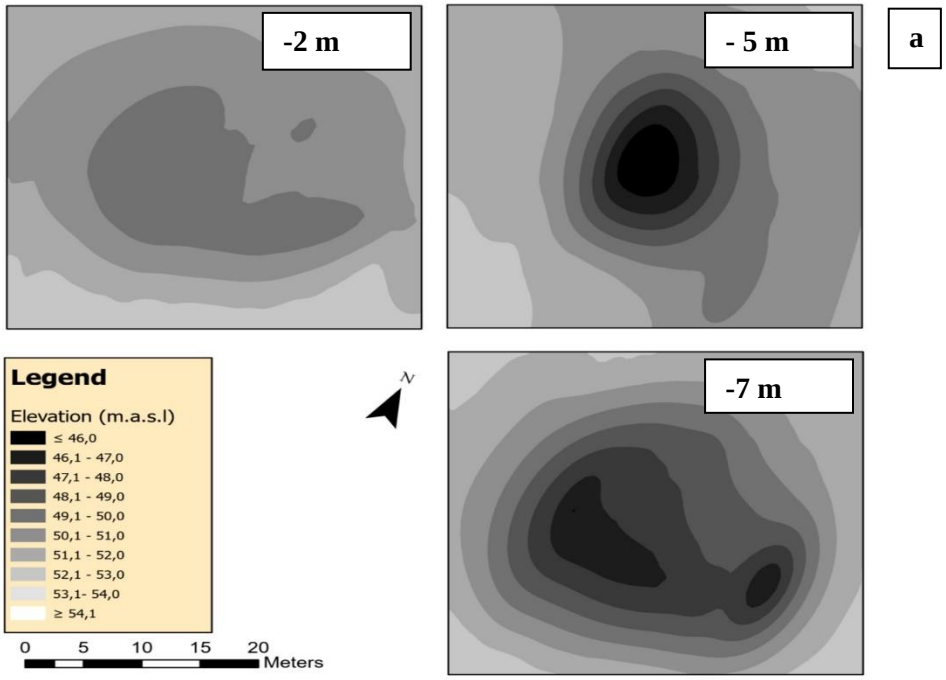
-2 m
- 5 m
a
Legend
Elevation (m.a.s.l)
≤ 46,0
46,1 - 47,0
47,1 - 48,0
48,1 - 49,0
49,1 - 50,0
50,1 - 51,0
51,1 - 52,0
52,1 - 53,0
53,1- 54,0
≥ 54,1
0 5 10 15 20
Meters
N
-7 m

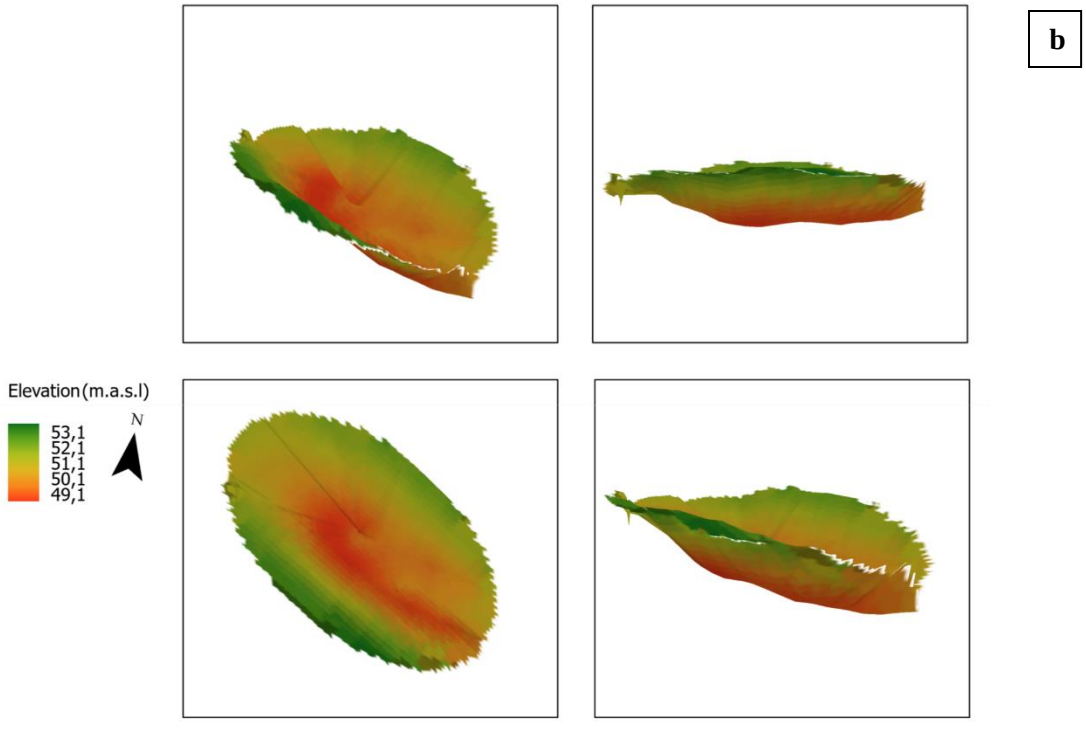
b
Elevation (m.a.s.l)
53,1
52,1
51,1
50,1
49,1
N

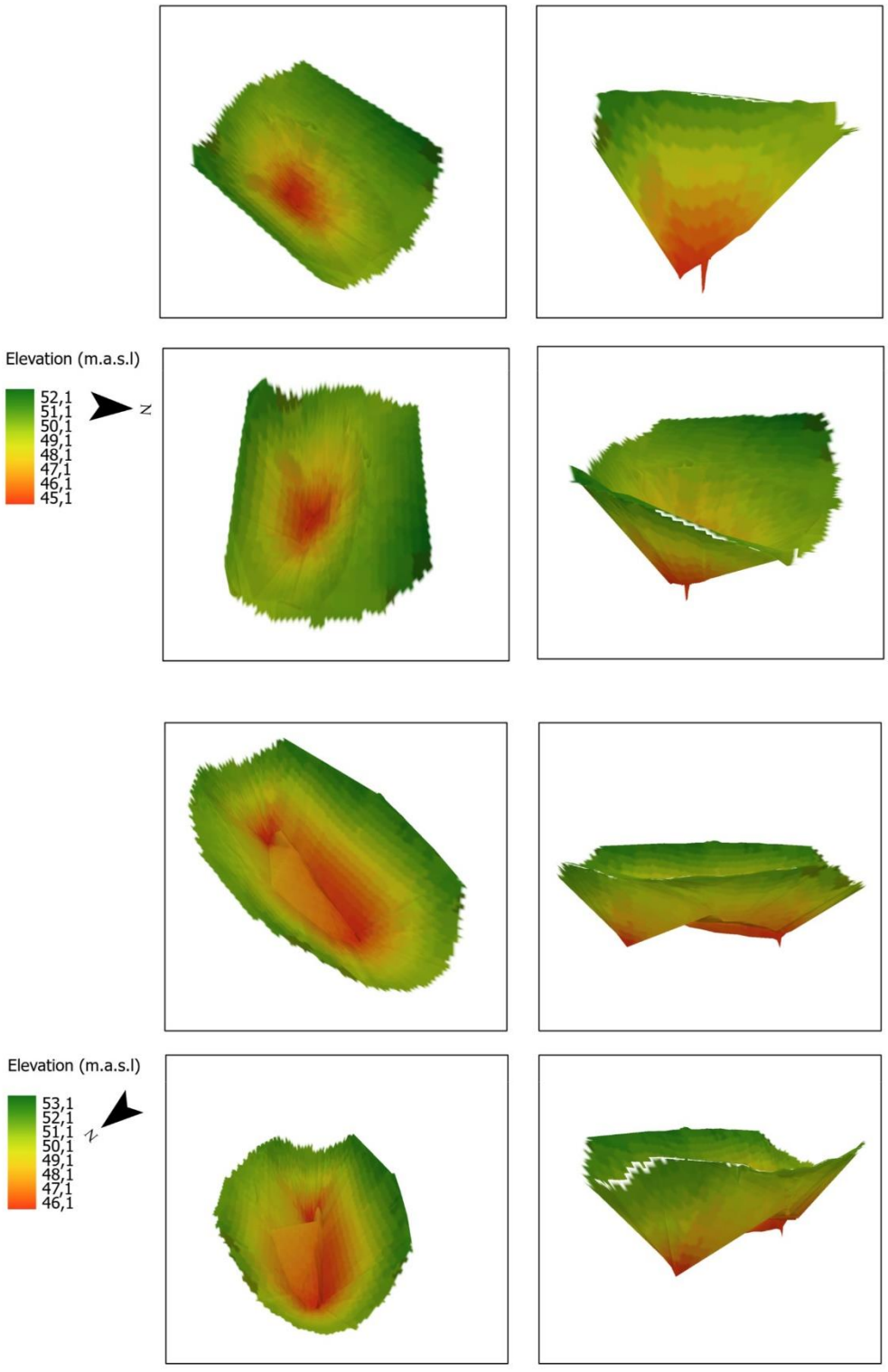

Figure 5.1 a-d, 2D and 3D images of the lava rise pits showing the changes in depth (m.a.s.l) a) 2D GIS image indicating the changes in depth, where the 3D images display multiple views of the lava rise pits - inside, front and side of each pit. b) -2m, c) -5m and d) -7m.

Figure 5.2 Entry ways into the below ground lava tubes that the DGPS could not record due to an unreachable satellite signal. Photo taken on August 25th, 2022.

5.1.2 Soil Properties

Six soil property samples per pit were taken on September 27th, 2020, to identify bulk density, porosity, degree of saturation (shown in Table 5.1)

The -2 m lava rise pit had the highest mean bulk density (1.10 g/cm^3) followed by the -5 m lava rise pit (1.01 g/cm^3). The lowest average bulk density value (0.82 g/cm^3) and the smallest range recorded in the study was observed in the -7 m pit.

Table 5.1 Soil Properties and soil moisture for all Lava Rise Pit sites. The min, max, mean and SD for the soil samples collected have been indicated from each Lava Rise Pit. Where σ = standard deviation and $\bar{x}$ = mean. Data were taken on September 28th, 2021, in the field. Total sample size was 18 (201 cm^3 per tin) - 6 samples per pit, using the stratified-random sampling approach.

Physical Properties	2 m Lava Rise Pit (n=6)			5 m Lava Rise Pit (n=6)			7 m Lava Rise Pit (n=6)		
	Range	$\bar{x}$	σ	*Range*	$\bar{x}$	σ	*Range*	$\bar{x}$	σ
Bulk Density (g/cm^3)	0.8 – 1.37	0.82	0.31	0.53 – 1.30	1.01	0.33	0.69 – 0.95	0.82	0.13
Porosity (%)	12 – 25	20	6	12 – 26	17	6	22 – 48	34	9
Degree of Saturation (%)	39 – 56	44	8	22 – 36	29	6	43 – 78	60	16
Volumetric Water Content (%)	13 – 15	14	1	21 – 32	26	5	9 – 23	16	7

However, an ANOVA indicated that the difference between the bulk density values were not statistically significant (n=18, p = 0.38). Bulk density estimates in Table 5.1 were similar to those reported in Arnalds (2004), suggesting the soil found in this location is a mixture of brown andosols and vitrisols.

Porosity values from each pit were measured in the lab using soil samples. The -7 m pit had the highest porosity value (34%), followed by the -2 m pit (17%) and finally the -5 m pit (17%) (Table 5.2). An ANOVA indicated that there was a statistically significant difference between the pits (n=18 p = 0.03). Volumetric moisture content (Table 5.1) within each pit was below 100%, indicating that the pits were not completely saturated. However, the -5 and -2 m pits had a lower degree of saturation percentage, while the -7 m was partially saturated (60%).

*Table 5.2 Properties and ranges of soil characteristics (area covered km^2, soil coverage %, organic carbon %, bulk density (g/cm^3) and water holding capacity %), for the five (5) soil types. The total area is only based on the five types displayed in the table. The table was created based on the approximate values where each variable should fall within (Arnalds 2004[1] and 2015[2]). The remaining soil types and the area they covered can be referenced in the full table created by Arnalds (2004). * Cambic and Arenic Vitrisols have been grouped together to align with the simplified soil map based on Arnalds and Gretarsson (2001).*

Soil Type	Symbol [1,2]	Total area (km^2) [1,2]	Total Soil (%) Coverage [1,2]	Organic Carbon (%) [1,2]	Bulk Density (g cm^3) [1,2]	Water Holding Capacity (%) [2]
Histosols	H	1,090	1.2	20-40	0.15 – 0.4	80 – 200
Histic Andosols	HA	4,920	5.5	12-18	0.2 – 0.4	50 – 125
Gleyic Andosols	WA	2,390	2.6	1-12	0.3 – 0.8	15 – 40
Brown Andosols	BA	13,360	14.8	2-7	0.5 – 0.8	15 – 40
Vitrosols *	V	22,190	24.5	<1	0.8 – 1.2	5 – 15

Volumetric water content was also obtained using the soil samples from the field. In the -2 m lava rise pit, the average volumetric water content was 14 %, with the smallest range among the three sites (13-15 %). The -5 m pit had the largest average volumetric water content (26 %) with the largest range of 11 %. The -7 m lava rise pit had an average value of 16 % with a range of 9 %. When comparing the soil properties recorded during the testing process to Arnalds (2004, 2015) (Table 5.2), all the pits fell within the range for Brown Andosols, Vitrosols or both (considering other variables identified in the study). The -2 m lava rise pit would be considered a Vitrosol, the -5 m lava rise pit could be considered in the Brown Andosol category, and the -7 m pit has results reflecting both Vitrosol and Brown Andosol ranges set by Arnalds (2004, 2015).

5.1.3 Soil Grain Size Analysis

Soil texture tests were completed for each study pit (6 soil samples per pit), and the averages of particles passing (%) were plotted against particle size (mm) (Figure 5.3). The -7 m lava rise pit had a higher passing percentage compared to both the -5 and -2 m lava rise pits. The 0.063 mm

(sieve #230) was utilized to separate gravels and sands from silts and clays (Carter and Gregorich, 2007). The higher passing percentage indicates that there were more silt and clay material present within the soil sample.

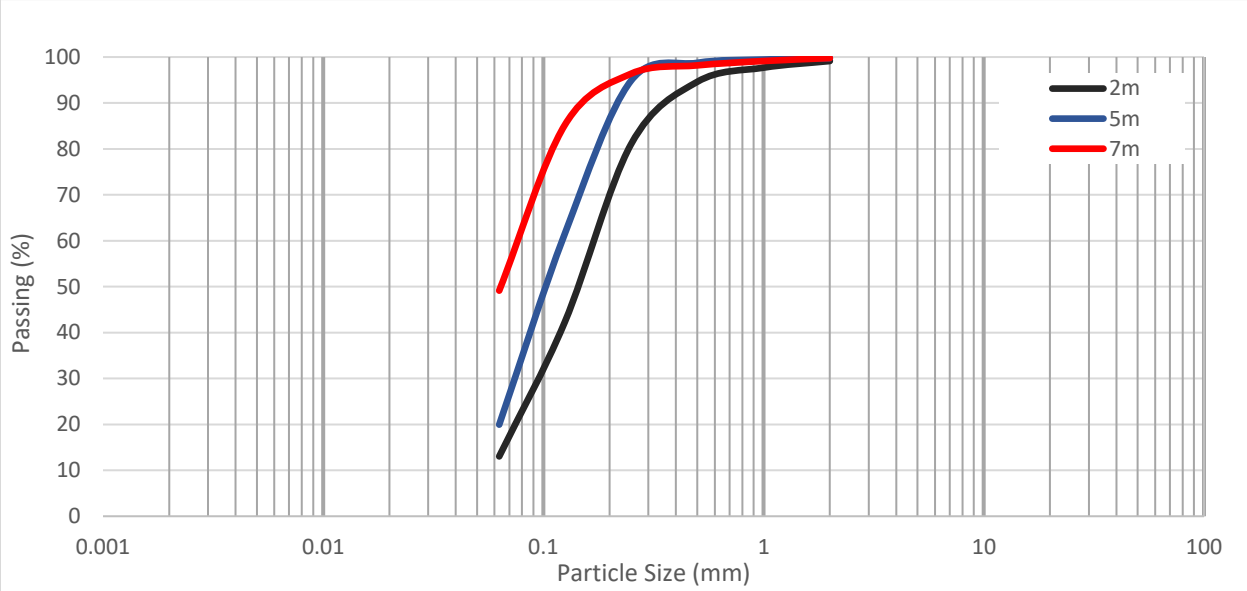

Figure 5.3 Particle passing of soils found within the three pits. Particle passing is the amount that passed through each sieve.

For this study, both silt and clay were combined during the texture analysis (Table 5.3). The -7 m pit had the largest percentage of silt and clay (85%) followed by sand (15%), with no gravel recorded during the sieving. The -5 m pit had the second largest amount of silt and clay retained (61%), with 38 % sand and 1% gravel. Finally, the -2 m pit had the lowest percentage of silt and clay (42%) with the highest amount of sand recorded in the study (57%) and 1% gravel. Soil texture sieving indicated that the soils were quite fine, with very little gravel or particles above 2 mm.

Table 5.3 The grain size analysis for each Lava Rise Pit (n = 6 per pit) has been displayed. Silt and Clay have been grouped together to indicate one value.

Lava Rise Pits	Gravel (> 2.0 mm)	Sand (0.002 – 2.0 mm)	Silt & Clay (> 0.002 mm)
		%	
2 m Lava Rise Pit (n=6)	1	57	42
5 m Lava Rise Pit (n=6)	1	38	61
7 m Lava Rise Pit (n=6	0	15	85

*The values are based on the average grain size retained during sieving.

5.2. Ash Distribution and Surface Coverage

As this is a sandy lava field, near a glacial river and sandur, it is expected that the soil found in this area would be primarily ash and sandy glacial material. Deposition of ash, dust and sand in this area would be a result of aeolian activity, including deposits left from nearby eruptions and jokulhlaups. The deposition of ash can also impact the types of surface coverage found in the lava field.

5.2.1 Ash Distribution

Ash coverage is an important characteristic of the lava rise pits, especially due to their geographical location (Figure 5.4). An ANOVA test indicated that there was a statistical significance between the depth of the pits and how much surface was covered by ash (n = 270, p= 0.006). The trend showed that with the increase in pit depth, there was a decrease in ash coverage.

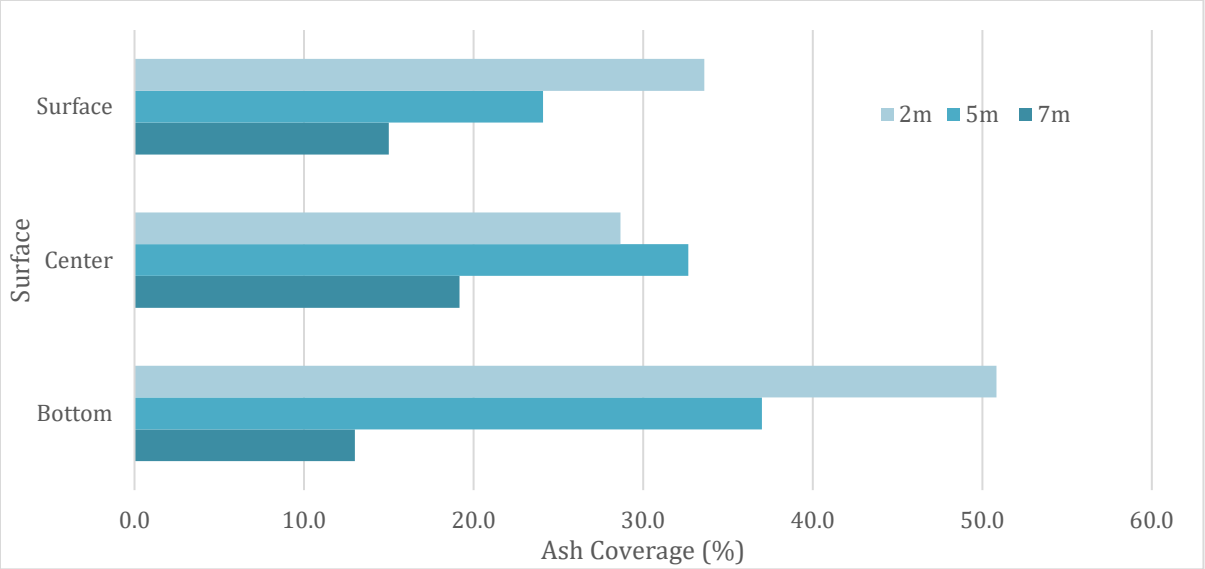

Figure 5.4 Ash cover within the three lava rise pits based on results collected from a stratified-random sampling approach n=90 per pit.

The -2 m pit had the greatest cover of ash at the bottom of the pit, with 50.1% (95.3 m^2) followed by the surface with 33.6% (63 m^2) and 28.7% (50.8 m^2) in the center. The bottom of the -2 m pit had the greatest percentage of ash coverage recorded during this study. In the -5 m pit, ash increased with depth with 24.1% (45.3 m^2) at the surface, 32.7% (61.3 m^2) measured in the center, and 36.7% (68.8 m^2) at the bottom. Finally, the -7 m pit had the least amount of ash coverage, with the center 19.2% (35.9 m^2), followed by the surface of the pit with 15% (28.1 m^2), and 13% (24.4 m^2) at the bottom. While there was an overall trend of ash decreasing with depth, individually, each pit had a different distribution pattern.

5.2.2 Surface Cover Distribution

The -7 m lava pit surface coverage was dominated by vascular and non-vascular plants (Figure 5.5). At the surface of the lava pit, vascular plants were the most common surface type, covering more than 50% of the total area examined. Following vascular plants were non-vascular plants and bare ground. The surface coverage for both the middle and bottom of the pit followed a

similar trend, where the non-vascular plants were the most dominating surface type followed by vascular plants and bare ground. An ANOVA indicated that there was a statistically significant difference (n = 90, p= 0.009) between the surface covers within the pit.

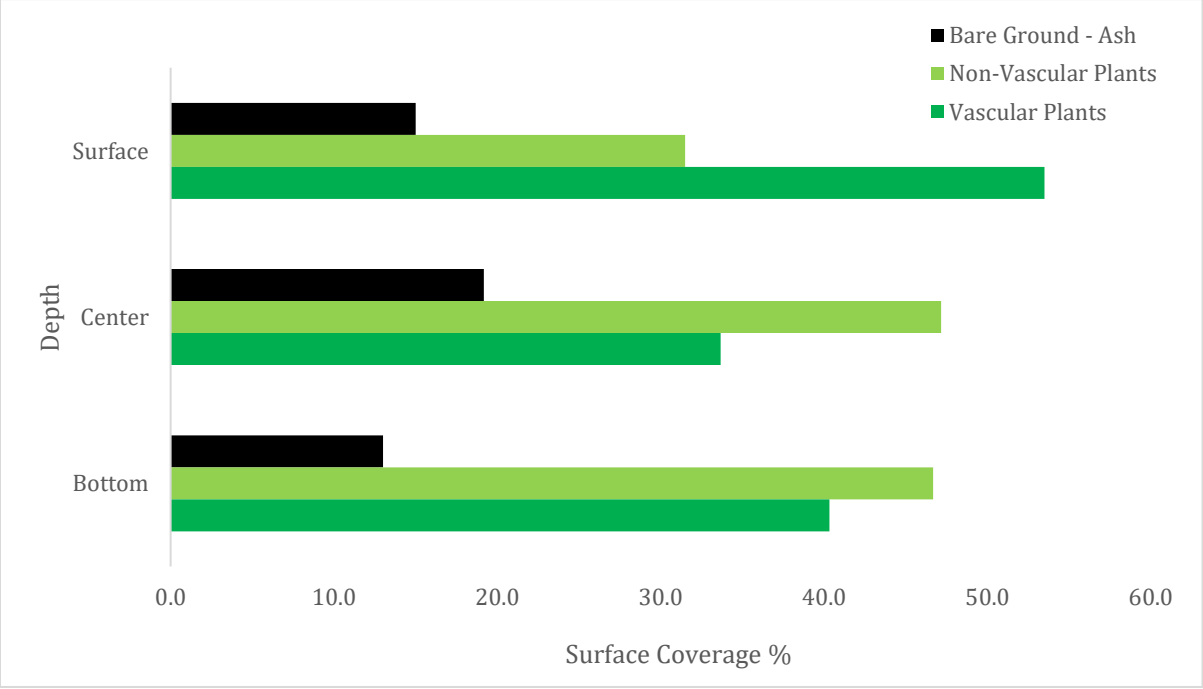

Figure 5.5 Surface coverage (%) measured within the -7 m lava rise pit using the stratified-random sampling approach. Surface types identified were bare ground, non-vascular plants, and vascular plants. Percentage is calculated based on total samples collected per zone (bottom, center and surface)

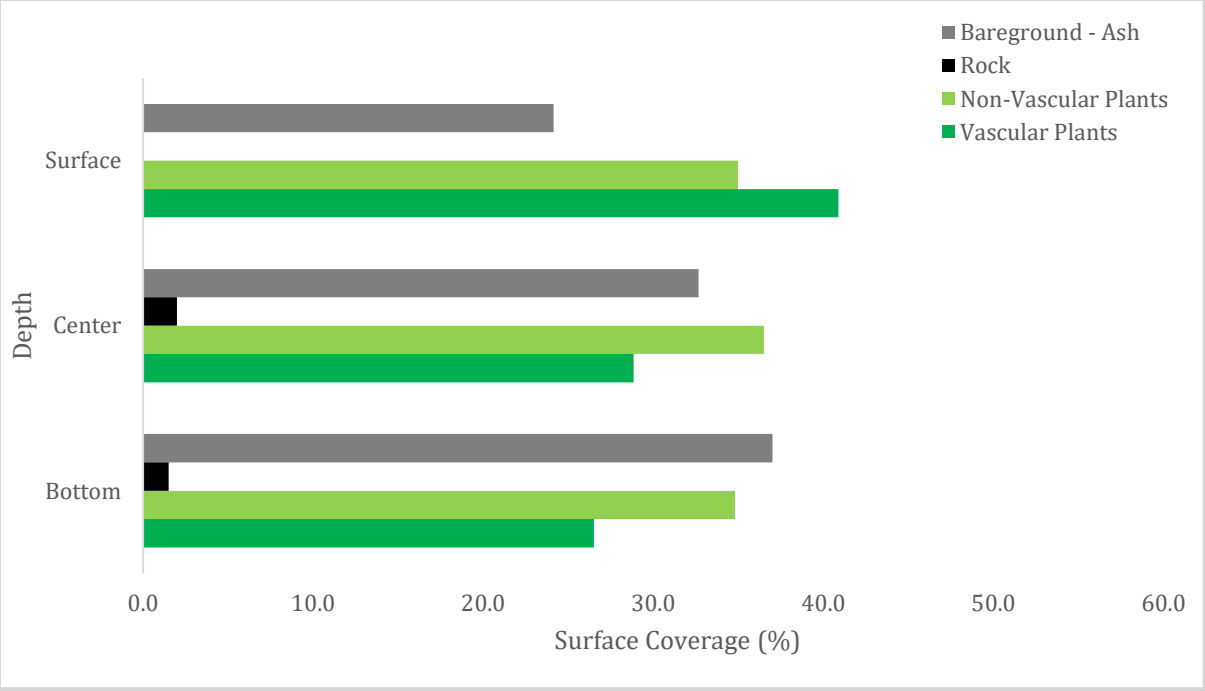

Figure 5.6 Surface coverage (%) measured within the -5 m lava rise pit using the stratified-random sampling approach. Surface types identified were bare ground, rock, non-vascular plants, and vascular plants.

The -5 m pit had four surface types: bare ground, rock, non-vascular plants, and vascular plants. In this pit vascular plants tended to decrease with depth, however, the difference between the middle and the bottom was small, only 2.3% (Figure 5.6). Unlike the -7 m pit, the amount of bare ground coverage began to increase with depth. Rocky surfaces only appeared in the middle and bottom of the pit, and these were only 2 and 1.5% of the areas quantified. An ANOVA indicated that there was a statistically significant difference (n= 90, p=0.008) between the surface types measured within the pit. Non-vascular plant coverage was consistent throughout the depths with very minor fluctuations between the three zones.

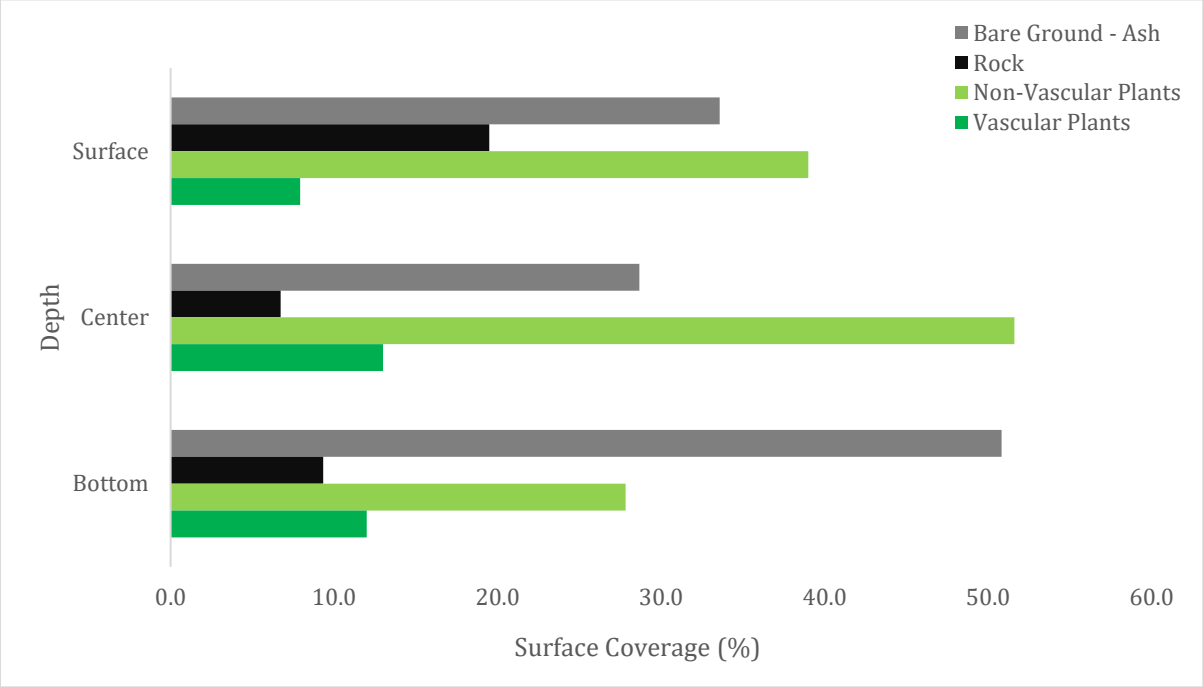

Figure 5.7 Surface coverage (%) measured within the -2 m lava rise pit using the stratified-random sampling approach (n=90). Surface types identified were bare ground, rock, non-vascular plants, and vascular plants.

Surface coverage in the -2 m pit was different from both the -5 and -7 m lava rise pits. Both bare ground and non-vascular plants were the dominating surface types (Figure 5.7). At the surface the vascular plants were predominant with 39% of the area, followed by bare ground (33.6%). Rocky ground was 19.5% of the area at the surface, which was the highest for all three pits. In the middle of the -2 m pit, non-vascular plants continued to be the dominating surface with 51.6%, followed by bare ground (28.7%). There was a decrease in both bare ground and rocky ground, However, there was a small increase in vascular plant coverage (8%). At the bottom of the -2 m lava pit, there was a shift to bare ground being the most dominating surface type (50.8%), with non-vascular plants continuing to be one of the two dominating surface types. However, there was a large decrease (28.3%) in surface coverage from what was recorded in the

middle of the pit. An ANOVA indicated that there was a significant difference (n= 90, p =0.001) within the pit. Rocky and vascular plant coverage also experienced slight changes at the bottom, Rocky ground increased, and the percentage of vascular plants decreased.

5.3 Microclimate and Weather Patterns

5.3.1 Air Temperature

Daily air temperature was recorded over the study period (September 26th, 2020 – March 30th, 2021) in the lava field (yellow) and Kirkjubæjarklaustur (blue) (Figure 5.8). Kirkjubæjarklaustur data was monitored by the Icelandic Meteorological Office (IMO) using an automatic weather station that recorded temperature, precipitation, windspeed and relative humidity (for specifications of IMO equipment, see section 4.2)

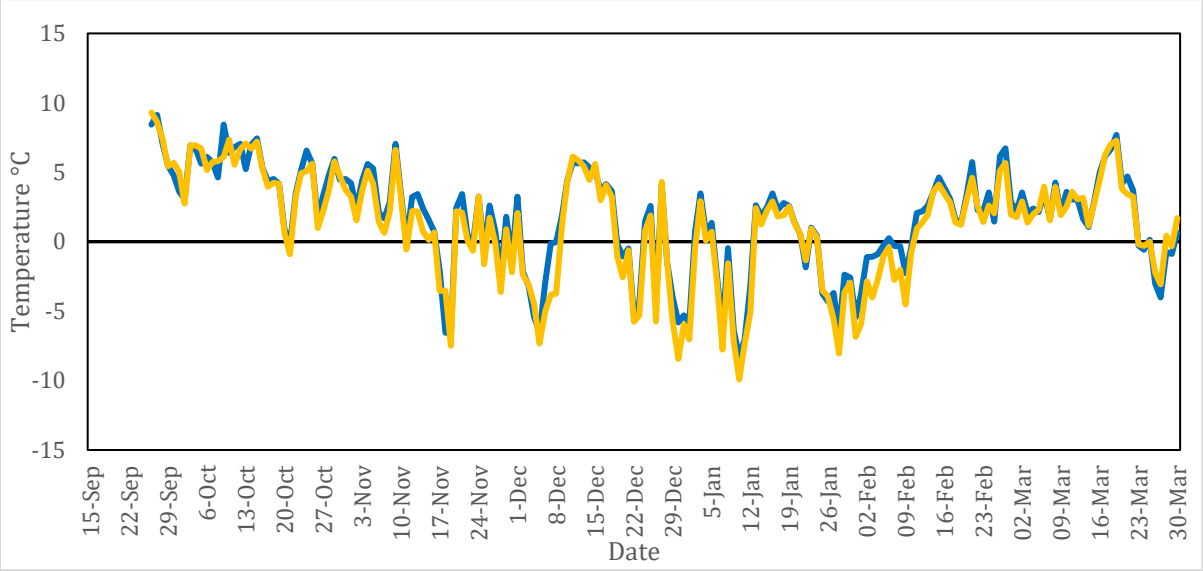

Figure 5.8 Daily mean air temperature patterns for the Laki lava field (yellow), Kirkjubæjarklaustur weather station (blue) during the study period.

Throughout the study period, the temperature monitored within the lava field was slightly lower than what was measured at Kirkjubæjarklaustur, however a Student T-test indicated that there was no significant temperature difference between the two locations ($p > 0.05$, $n=187$).

In the winter months (December 2020 to February 2021) air temperature tended to stay below 0°C, however fluctuations above 0°C were recorded. This was noticeable between December 8 -20, 2020. On December 11th, 2020, the average daily temperature rose to 5.7°C. The warmest day during the study was September 26th, 2020 (13.3°C) and the coldest day was January 10th, 2021 (-11.9°C). Average monthly air temperatures from September to January at the study site fell below the 30-year average recorded in Kirkjubæjarklaustur, whereas February and March were above average (Table 5.4).

When the average temperature is above 0°C, it is classified as a heating degree day, and below 0°C, it is classified as a cooling degree day. In total there were 434 heating degree days, and -217 cooling degree days recorded in the lava field, and 479 heating degree days and -157 cooling degree days recorded at Kirkjubæjarklaustur. Degree-days are often used in studies to assist in characterising regional climates (Schlenker *et al*., 2007).

Table 5.4 Average monthly temperature within the Laki lava field (during the study period) and Kirkjubæjarklaustur. The average monthly temperature for the last 30 years is also indicated. The temperature data from Kirkjubæjarklaustur was retrieved from the Iceland Meteorological Office IMO.

	Year	J	F	M	A	M	J	J	A	S	O	N	D	Yearly Avg
Laki Lava Field	2020									7.6	4.7	0.8	-0.7	
	2021	-2.0	0.8	2.3										
Kirkjubæjark.	2020	-0.3	-0.3	0.9	3.6	6.8	10.3	11.7	11.1	7.3	5.0	1.6	0.1	5.14
	2021	-1.4	1.8	2.2										
30-year avg. (1990 - 2020)		0.3	0.2	1.0	3.6	6.9	10.0	11.6	11.1	8.4	4.8	1.9	0.2	5.01

5.3.2 Relative Humidity

Relative humidity (%)over the study period, collected from the Lava field can be seen in Figure 5.9, plotted with air temperature (°C). September 2020 and February 2021 had the highest monthly averages of 85.6 and 87.4% versus December 2020 and January 2021 at 79.2 and 73.1%. Over the entire study period, the average relative humidity was 81.7%, which was 2.9% greater than the 15-year average (IMO).

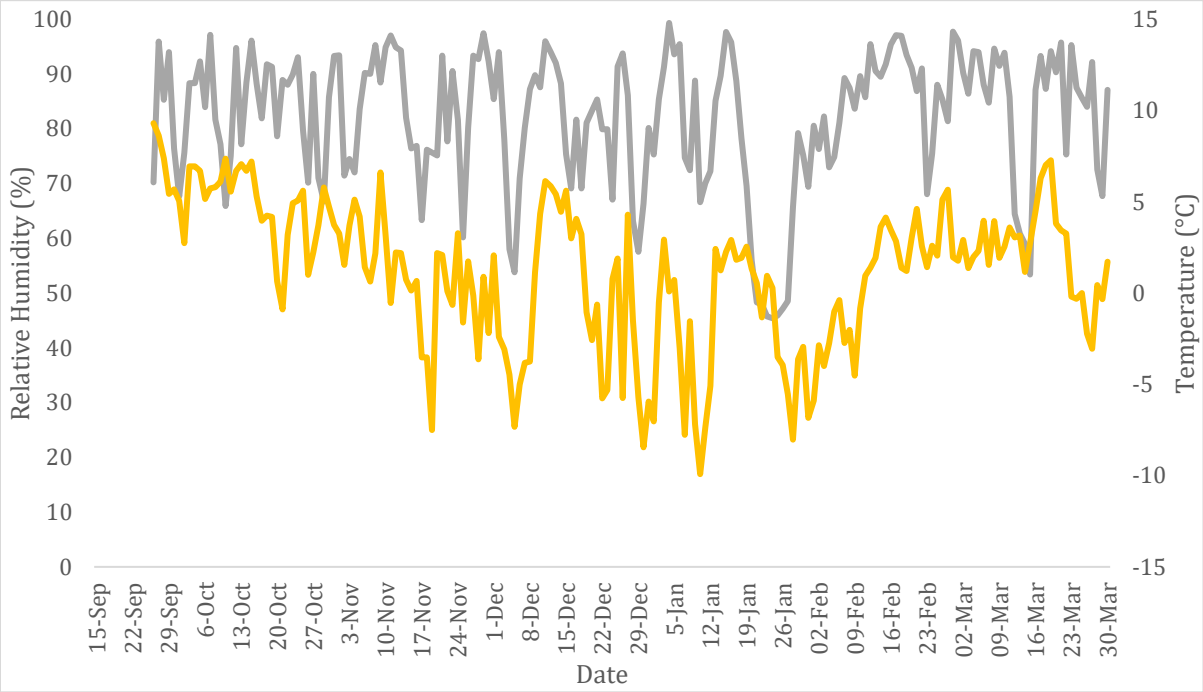

Figure 5.9 Relative humidity (%) (grey), air temperature (°C) (yellow) collected during the study period (September 26th, 2020 – March 30th, 2021) from the Laki lava field.

6.3.3 Windspeed

Windspeed data was not recorded in the field but was recorded at the nearby weather station in Kirkjubæjarklaustur as shown in Figure 6.10. Windspeeds fluctuated throughout the study with the lowest speeds occurring in October and March, with October 20th and 29th being the only two days during that timeframe where the daily windspeed average was above 12 m/s. The five (5) highest windspeed daily averages were record on December 2nd (14 m/s), 11th (13.1 m/s), 12th (12.6 m/s), 26th (13.5 m/s) and February 12th (12.6 m/s) (Figure 5.10). Windstorm events in Iceland commonly exceed 20 m/s (Gísladóttir *et al.*, 2005) and are usually more intense in the winter seasons, as hurricane type windspeeds can often occur due to the Icelandic Low (Hanna, 2004, Chapter 2.1). The greatest maximum windspeeds were on October 23rd (22.2 m/s), December 26th (26.5 m/s), January 8th (26.7 m/s) and March 26th (20.6 m/s) with both December 26th and January 8th having the highest recorded windspeed for the study period.

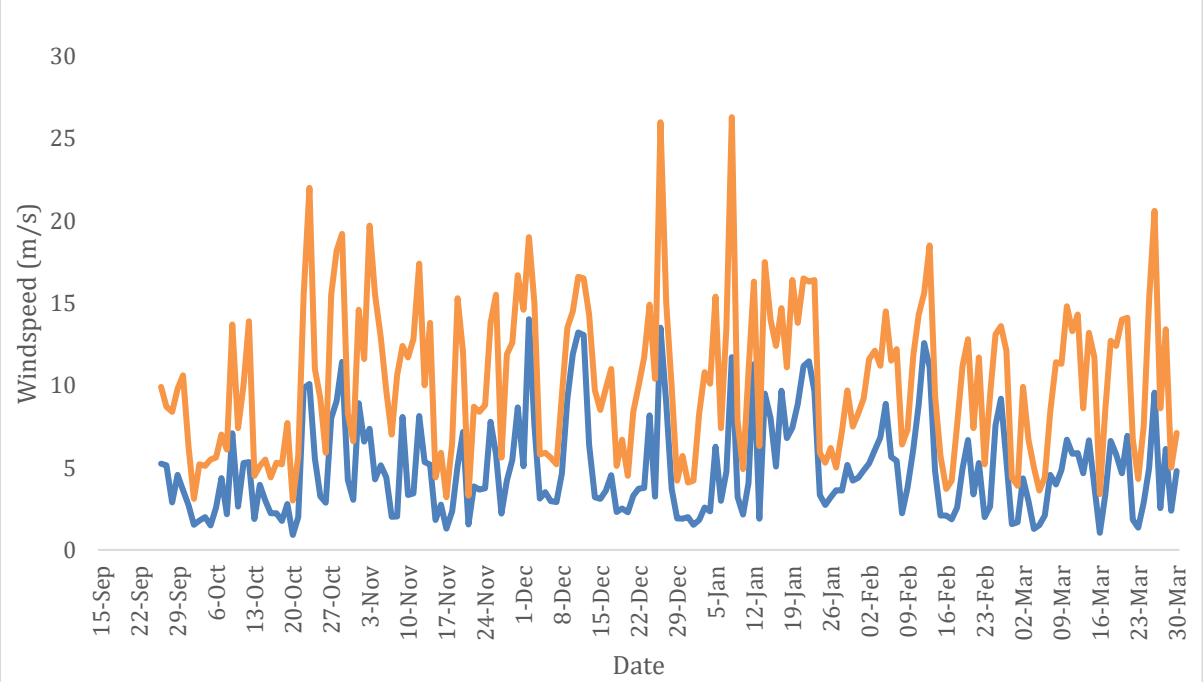

Figure 5.10 Average daily windspeed (blue) and the maximum daily windspeeds (orange) measured at the Kirkjubæjarklaustur weather station. Note windspeeds were measured at 10 m above ground surface.

5.4 Thermal Response of the Lava Rise Pits

Understanding the temperature regimes within the lava pits is important as they can be modified by various factors such as, topography, variable depth, opening (degree of shading), soil type (ash deposition), as well as vegetation and its distribution. Slight differences in temperature can result in frequent freeze-thaw cycles and numerous zero curtain episodes, where the air temperature lingers at 0ºC due to latent heat effects (Outcalt *et al.*, 1990; Hinkel and Outcalt, 1994) (see Figure 5.8).

5.4.1 Seasonal Near Surface Temperature Regimes of Lava Pits

The daily near surface (10 cm above substrate) temperatures recorded from the different depths of the pits (surface, middle, and bottom), are found in Figure 5.11 A. In the autumn months, the temperatures tended to stay above 0°C in September and early to mid-October, however, towards the end of October, temperatures below 0°C were more common. Temperatures generally fell below 0ºC during the winter, but several freeze-thaw events occurred in this season with the trend occurring on until the end of February. In March, temperatures above 0°C were the most common. However, being a transitional month from winter to spring, there were several days lingering at 0°C or below, especially at the end of March.

The -5 m pit had the lowest temperatures per day in comparison to the other pits, although an ANOVA indicated that the difference in overall temperature for the three lava rise pits were significant (n= 546, p= 0.0006). However, towards the end of the study, after February 19th, 2021, a notable difference occurred between the -5 and -7 m pit, where the latter pit become cooler, and this might be attributed to light conditions. The amount of light receipt and near surface temperatures followed a similar pattern. When these temperatures were higher in the pits,

light intensity also increased. The -5 m pit received the least amount of light exposure and had the lowest near-surface temperatures during the study (Figure 5.11 B). However, in the autumn, the -5 m pit had the highest light intensity, whereas the other pits received less. An ANOVA indicated that the intensity differences within the pits were statistically significant (n= 546, p= 0.004).

Within the lava pits the temperatures of the three pits tended to be colder at the bottom and warmer at the top (see Figs. 5.12 a-c).

In the -2 m pit this pattern was followed except from the 28th of January to the 9th of February 2021 at which point the middle of the pit was the coldest (Figure 6.12 a). However, between the three different layers there was no significant difference (n = 558, p=0.099). During the study, the bottom of the -2 m pit was frozen under ~40 cm of snow ice. Snow ice can occur when snow and water mix, forming slush, and then freezes as the surrounding air temperature decreases (Lepparanta, 1983). Being the smaller of the pits with a depth of only 2 m, the temperatures at the center and surface of the pit would have been similar to the atmospheric temperatures.

The temperature in the -5 m pit also followed a comparable trend with the bottom of the pit being colder than the surface (Figure 6.12 B). The middle (-3 m), however, began to surpass the temperature at the surface beginning on March 10th, 2021. While the temperature difference between the middle (-3 m) and the surface (0 m) of the pit ranged from ±0.5 to 2.1°C, the center of the pit was warmer than the surface and the bottom. However, an ANOVA indicated that this difference was not statistically significant (n= 524, p= 0.144).

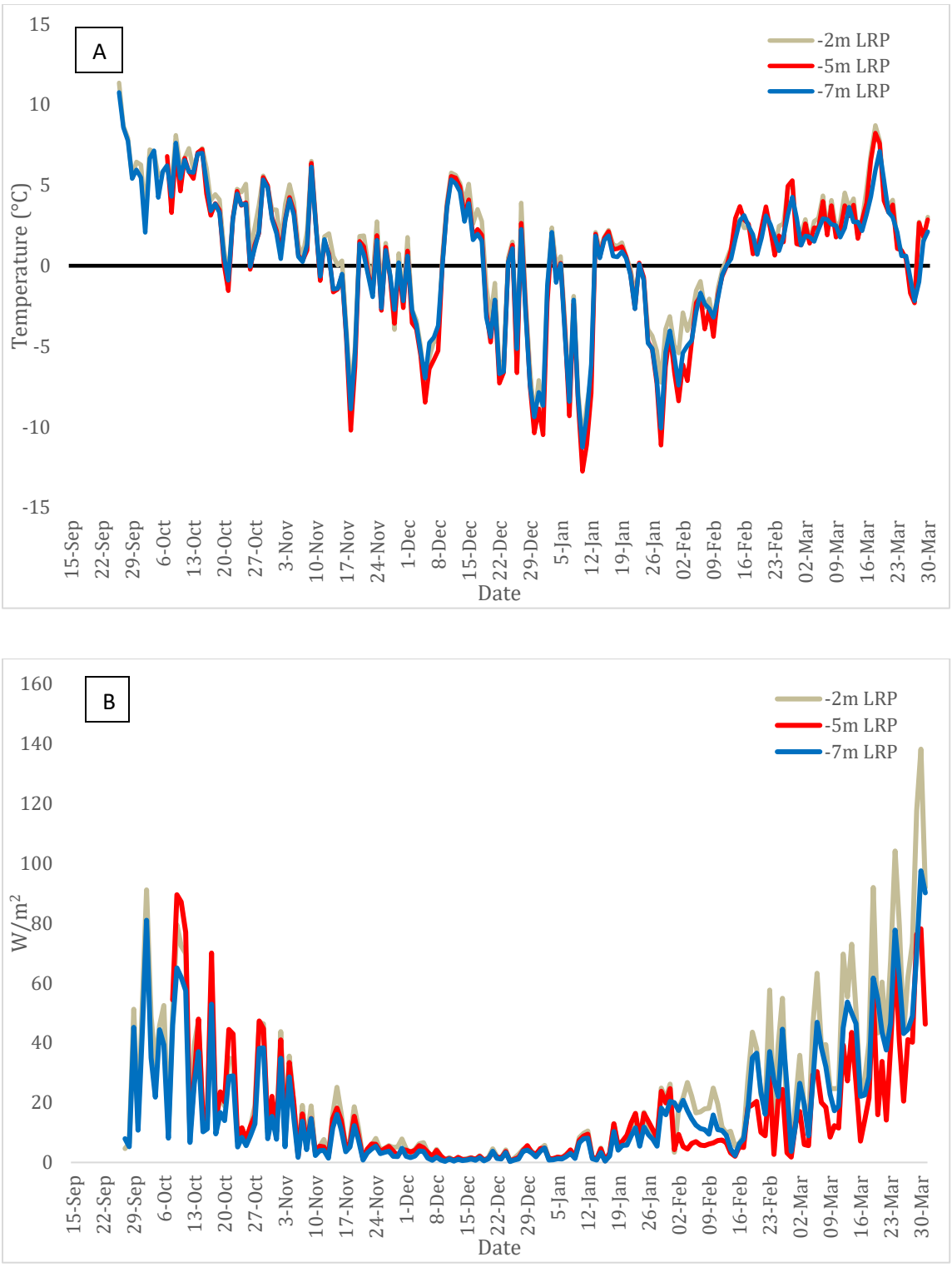

Figure 5.11 Daily average near surface temperature (8 cm above surface) of each pit (A). Light intensity (W/m^2) during the study period (B). Measurements were recorded in LUX and then converted into W/m^2.

The temperature regime of the -7 m pit was considerably more dynamic (Figure 5.12 C) than the other shallower pits. Like the other sites, the signal of temperatures being colder at the bottom and increasing towards the top was still present but temperatures in the middle section of the pit varied over the study. Up until October 24th, 2020, the temperatures at -4 m were colder than temperatures at -2 m. After November 14th, 2020, the middle section was warmer than the surface. A switch back to colder conditions did not occur until February 2021. An ANOVA indicated that there was a statistical difference in temperatures between the levels at the -7 m pit (n= 743, p=0.001).

Heating and cooling degree days were calculated for each pit over the study period using the average data from the different levels within the lava rise pits. In the -2 m pit there were 530 heating degree days, followed by 307 days in the -5 m pit and finally 358 days in the -7 m pit. There were -209 cooling degree days in the -2 m pit, -302 in the -5 m pit and -270 in the -7 m pit**.**

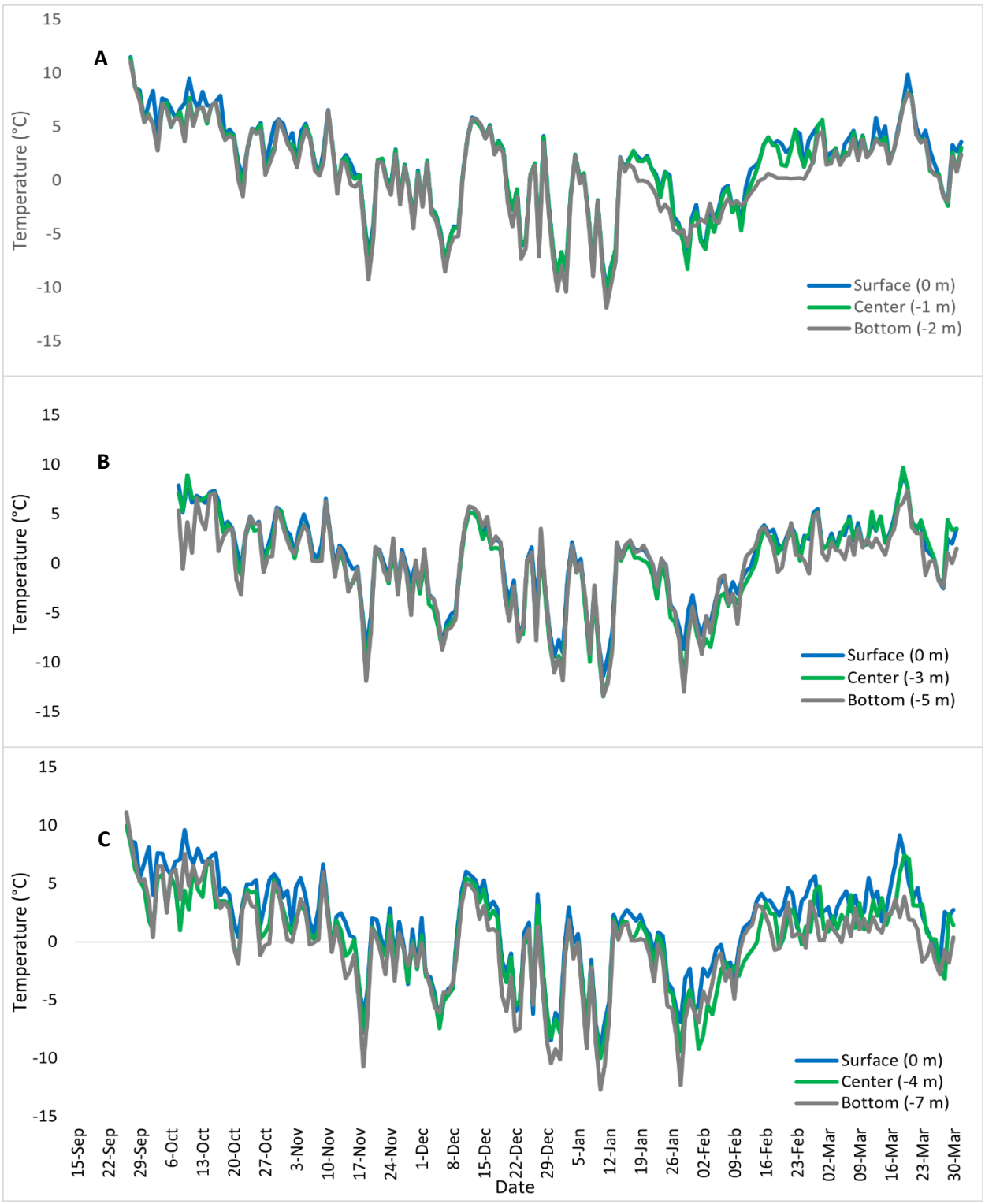

Figure 5.12 Temperatures recorded within the -2m (A), -5 m (B) and -7 m (C) lava rise pits, measured using HOBO Temperature/Light probes set 10 cm above the ground surface.

5.4.2 Ground Temperatures in Lava Pits (-0.05 m)

HOBO Smart Temperature probes were placed -0.05 m into the soil in each pit to measure ground temperature changes. Ground temperature, like near surface temperature, had a seasonal trend. In the earlier part of Fall (September – mid-October), daily ground temperatures averaged above 2-3°C occasionally decreasing to approximately 1°C. However, towards the end of the season (mid-October – November), the temperatures began to decrease to just above 0°C (Figure 6.13). Temperatures fell below 0ºC the second week of November. In the winter months, temperatures were generally below 0°C, with the highest temperatures of the season being 5°C and the lowest -13°C. The winter season, however, saw continuous fluctuations in temperature, seldomly passing 0.5°C. Towards the end of the winter season (mid-February), temperatures began to increase and not fall below 0°C. The beginning of the spring season (March) showed some variation in temperatures, but they stayed above 0°C, apart from the period (23 to 30 March) when temperatures went as low as -3°C. For the entire study period, an ANOVA indicated that the results between the sites were not statistically significant (n=546, p= 0.412).

The 'zero curtain effect' is created when ground temperatures reside at 0°C for a prolonged period due the latent heat effect. The effect can be described as a relationship between soil moisture content and temperature. Soils with a higher moisture content will stay at 0°C until frozen or thawed, while drier soils will result in them freezing or thawing faster (Farbrot *et al.*, 2007), often having no noticeable zero curtain effect. The 'zero curtain' effect took place in each of the pits, but it did not always occur simultaneously. A zero-curtain effect was noted at the bottom zone (-2 m) but it did not occur at the mid and upper levels in this pit (~Feb. 9 to Feb. 22). Small melting events occurred, as temperatures rose above 0°C, prior to the complete thawing of the ground (see Figure 5.13).

It was quite typical for zero curtain patterns to occur for two days before a notable increase or decrease in ground temperature. This effect was seen in the -7 m pit on November 26th – 28th, December 10th – 20th, February 13th – 26th and March 23rd – 30th. Zero curtain episodes were observed in the -5 m pit on November 21st – 24th, November 27th – December 3rd, December 10th – 19th, January 3rd – 7th and January 15th – 19th (Figure 5.6). At the -2 m pit ground temperatures lingered at 0°C from approximately January 17th to February 17th. However, as noted in section 5.2.1, the bottom of the -2 m pit was submerged under 40 cm of ice.

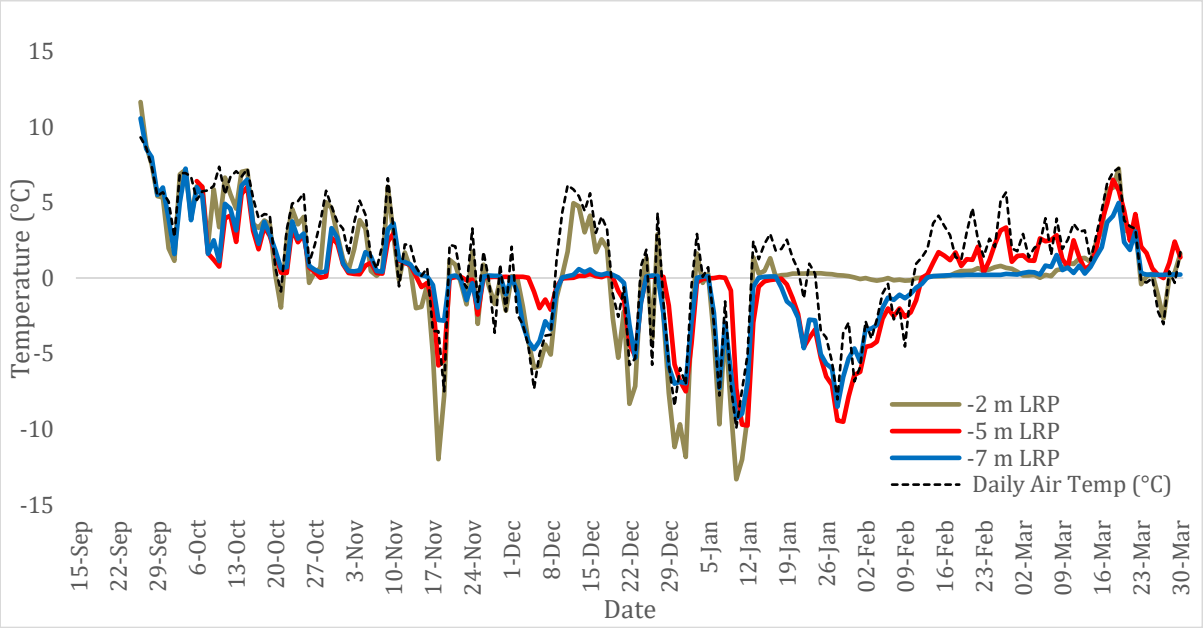

Figure 5.13 Recorded ground temperature during the study period. Temperature probes were placed 0.05 m into the ground of each lava rise pit. Air temperature is also plotted on this graph to compare the temperatures of the ground to what was recorded in the atmosphere.

During the study, heating degree days were calculated from these ground temperatures. In the -2 m pit there were 274 heating degree days, 171 in the -5 m pit and 193 in the -7 m lava rise pit. Cooling degree days were also identified, with the -2 m pit having -210 cooling degree days, -198 in the -5 m pit and finally -205 in the -7 m pit. Cooling and heating degree days were the most in the -2 m lava rise pit.

5.4.3 Spatial pattern of surface temperatures

Spot surface measurements were made from September 26th – October 8th, 2020, in each lava rise pit using an infrared thermometer. Overall, 222 samples were collected in each pit. The readings were focused on the main surface types of the pits (grass, moss, vascular plants, and bare ground). From Table 5.5, the -5 m pit had the largest temperature range for all four surface categories, followed by the -7 m and -2 m pits.

Table 5.5 Surface temperatures (°C) of ground cover in the rising lava pits. Surfaces were divided into four categories, grass, moss, vascular plants, and bare ground – ash. This table displays the range, mean and SD for the temperatures recorded from each lava rise pit.

	Grass			Moss			Vascular Plants			Bare Ground - Ash		
Lava Rise Pits	*Range*	$\bar{x}$	σ	*Range*	$\bar{x}$	σ	*Range*	$\bar{x}$	σ	*Range*	$\bar{x}$	σ
0 – -2 m (n = 210)	4.1 – 11.1	7.8	1.4	-1.0 – 12.2	8.5	1.8	3.1 –12.0	7.9	1.6	-1.0 – 12.6	8.1	2.3
0 – -5 m (n = 210)	-5.5 – 10.4	6.7	3.1	-5.0 – 12.3	7.4	3.5	-2.8 – 10.8	6.8	2.8	-7.4 – 12.5	7.1	3.9
0 – 7m (n = 210)	-1.2 – 11.2	6.7	2.6	-7.4 – 12.6	7.5	3.6	-2.2 – 11.0	7.0	2.9	-4.1 – 12.6	6.4	3.6

When comparing the temperature values recorded for each surface type within the pits, the -2 m lava rise pit had the highest mean temperature, no statistically significant difference could be identified ($p > 0.05$). The -5 and -7 m lava rise pits were close in their mean temperatures for each surface type, except for bare ground. The -5 m pit had a higher mean temperature (1.3°C) for bare ground, however, an ANOVA indicated that there was not a statistically significant difference ($n= 621$, $p = 0.910$). The changes in the temperature ranges of these pits can likely be linked to their topography. The -7 m is the largest of the three, and is

more open to the atmosphere, followed by the -2 m lava rise pit, whereas the -5 m pit has a smaller circumference resulting in less exposure to the changes in atmospheric temperature (see section 5.1). The elevated mean surface temperatures in the -2 m pit are driven by air temperature (see Figure 5.8). October 8th was the only day that near surface, ground and air temperatures were below 0°C at the time the measurements were recorded, otherwise the daily temperatures were above 0°C for all three sites.

5.5 Seasonal Hydrology

Due to Iceland's geographical location, the climate, wind, and precipitation are heavily impacted by the Gulf Stream on its west and southern shores, and the Icelandic Low (IL). This results in precipitation being very seasonal (See section 2.4). With warmer winter temperatures, and with temperatures around 0°C occurring in spring, fall and winter, it is not uncommon for Iceland to have both snow and rain events, especially in the winter. For this study, the seasonal hydrology of precipitation and soil moisture were investigated.

5.5.1 Precipitation

Rainfall events were quite significant in September and October, where the largest amounts of rainfall occurred. Days with continuous rain were recorded from September 26th, 2020 to September 30th, 2020, with a total of 104 mm measured at the lava field versus 122 mm at Kirkjubæjarklaustur (Figure 5.14). The highest precipitation days during the study occurred on September 27th (50 mm), 29th (30.8 mm), October 11th (25.6 mm) and 30th (29.2 mm) for a cumulative total of 136 mm. In Kirkjubæjarklaustur cumulative precipitation was slightly higher at 155 mm.

Cumulative rainfall for the lava field and Kirkjubæjarklaustur is also displayed on Figure 5.15. Over the study period a total of 670 mm of rain was observed at the lava field surface, 555 mm in the -7 m pit, 442 in the -5 m pit (underestimate due to gauge failure in February), 546 in the -2m pit, and 777 mm was recorded in Kirkjubæjarklaustur with approximately 50 % occurring in the autumn months (SON) and 50% in the winter (DJF). It should be noted that precipitation measurements in the lava field began on September 26th, 2020. Using precipitation data provided by IMO, it indicated that an additional 130 mm of rainfall occurred between September 1st – 25th, 2020. Differences in amounts can likely be attributed to wind, geomorphology, and location. Precipitation values indicated that the ratio of precipitation collected within the -7 m lava rise pit was 83%, while the -2 m pit collected 81% when compared to the total amount of precipitation collected at the surface.

As the rain gauges in the lava field dropped in accuracy below 0°C, the precipitation for these days were estimated (see methodology). Basically, a ratio was used to calculate the relationship between total rainfall collected in Kirkjubæjarklaustur and in the lava field on days that were > 0°C. This ratio was then applied to days below 0°C to estimate precipitation, and this is referred to as adjusted precipitation in Figures 5.14 and 5.15.

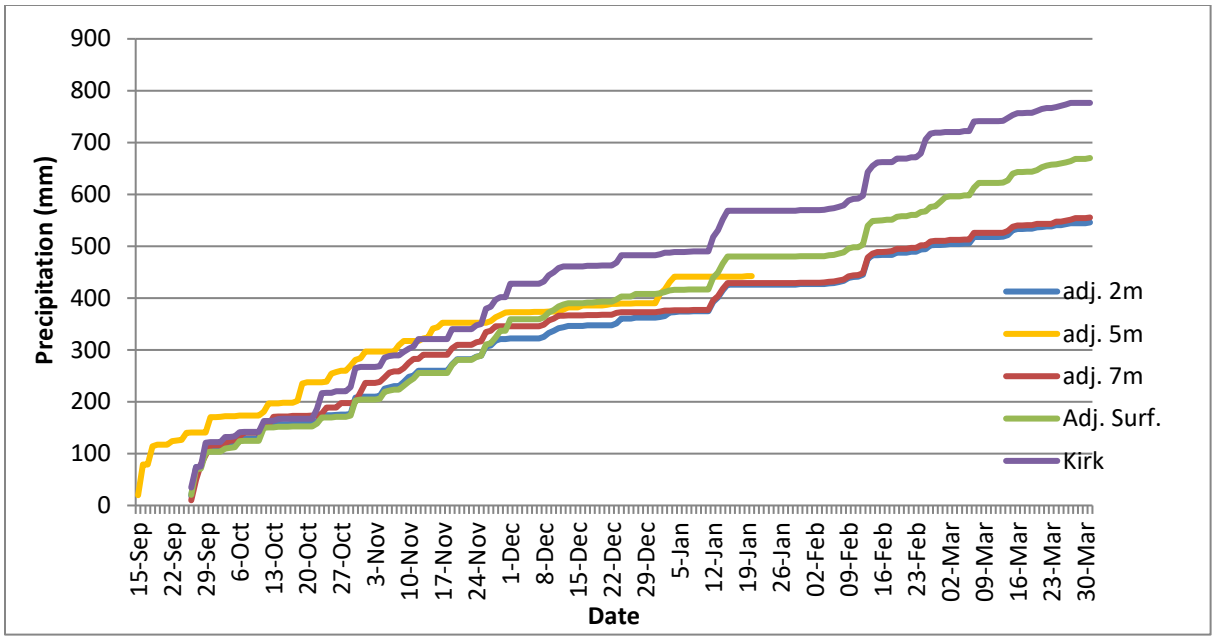

Figure 5.14 Daily precipitation recorded in both the Laki lava field and Kirkjubæjarklaustur weather station. Where blue indicates the adjusted precipitation for the -2 m pit, orange the adjusted precipitation for the -5 m pit (partial record), red the adjusted precipitation for the -7 m pit, green the adjusted precipitation for the surface and purple is the measured precipitation recorded at the Kirkjubæjarklaustur weather station.

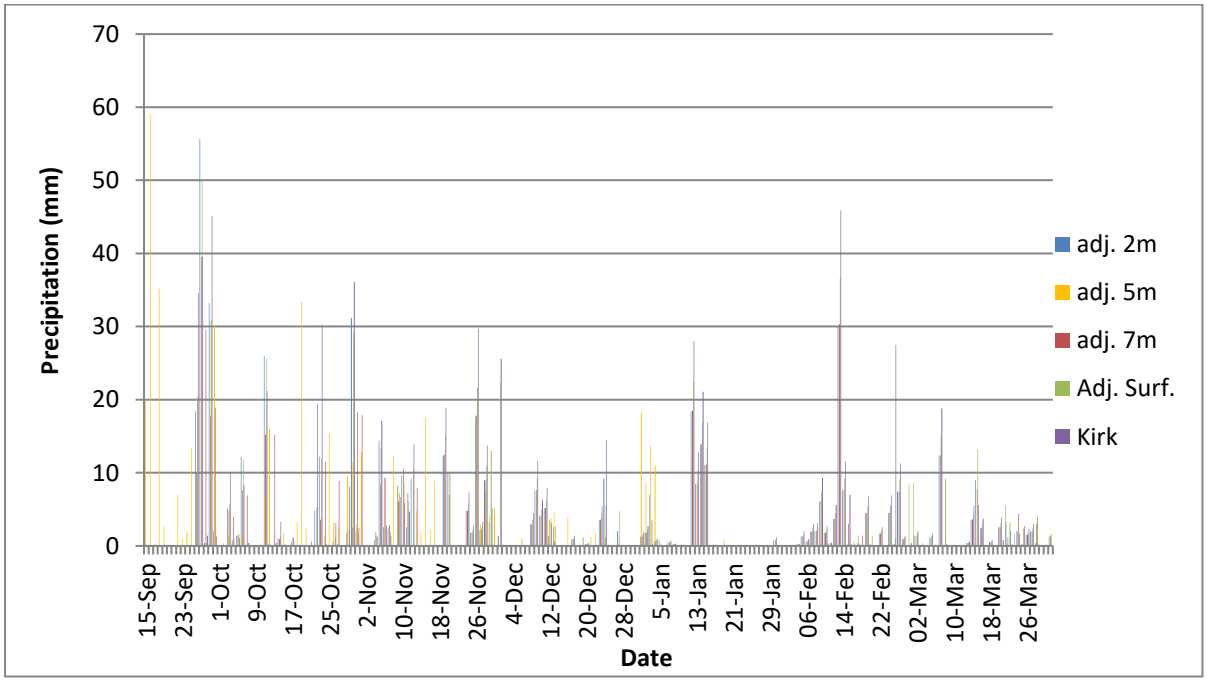

Figure 5.15 Cumulative precipitation recorded in the Laki lava field and Kirkjubæjarklaustur weather station. Where blue indicates the adjusted precipitation for the -2 m pit, orange the adjusted precipitation for the -5 m pit (partial record), red the adjusted precipitation for the -7 m pit, green the adjusted precipitation for the surface and purple is the measured precipitation recorded at the Kirkjubæjarklaustur weather station.

5.5.2 Infiltration

Infiltration tests were conducted twice at the bottom of each of the pits, before and after a rainfall event. The first infiltration test was conducted on September 25th, 2020, and this test was classified as the "before rainfall event" test. Within the four days prior to the commencement of this test, there was a total of 4 mm of rain. On October 2nd, 2020, another infiltration test was conducted. Between September 25th and October 1st, rainfall occurred every day resulting in a total of 126 mm.

The -2 and -5 m lava rise pits infiltrated more water than the -7 m lava rise pit both before and after the rainfall event (Figure 5.16 A-C). The pit with the greatest cumulative infiltration before rainfall was the -5 m pit with a total cumulative infiltration of 51.7 mm before the rainfall event, and 45.6 mm after (Figure 5.16 B). The -2 m pit accumulated 43.4 mm before the rainfall event and 45.8 mm after, which was the most recorded in the pit by 0.2 mm (Figure 5.16 A). Finally, the pit with the least was the -7 m pit (45.6 mm before and 32.9 mm after) (Figure 5.16 C).

Before the rainfall event, the -2 m pit had the lowest infiltration rate (2.9 mm/min), followed by the -7 m (3.1 mm/min), with the -5 m pit (3.4mm/min) having the highest rate. The infiltration rate for each pit after the rainfall event was in the same order as the time it took to plateau with -7 m (2.50 mm/min), -2 m (3.07 mm/min) and finally the -5 m pit (3.31 mm/min). The infiltration rates between the sites both before and after the rainfall were similar, and rainfall did not impact how quickly water infiltrated into the soils.

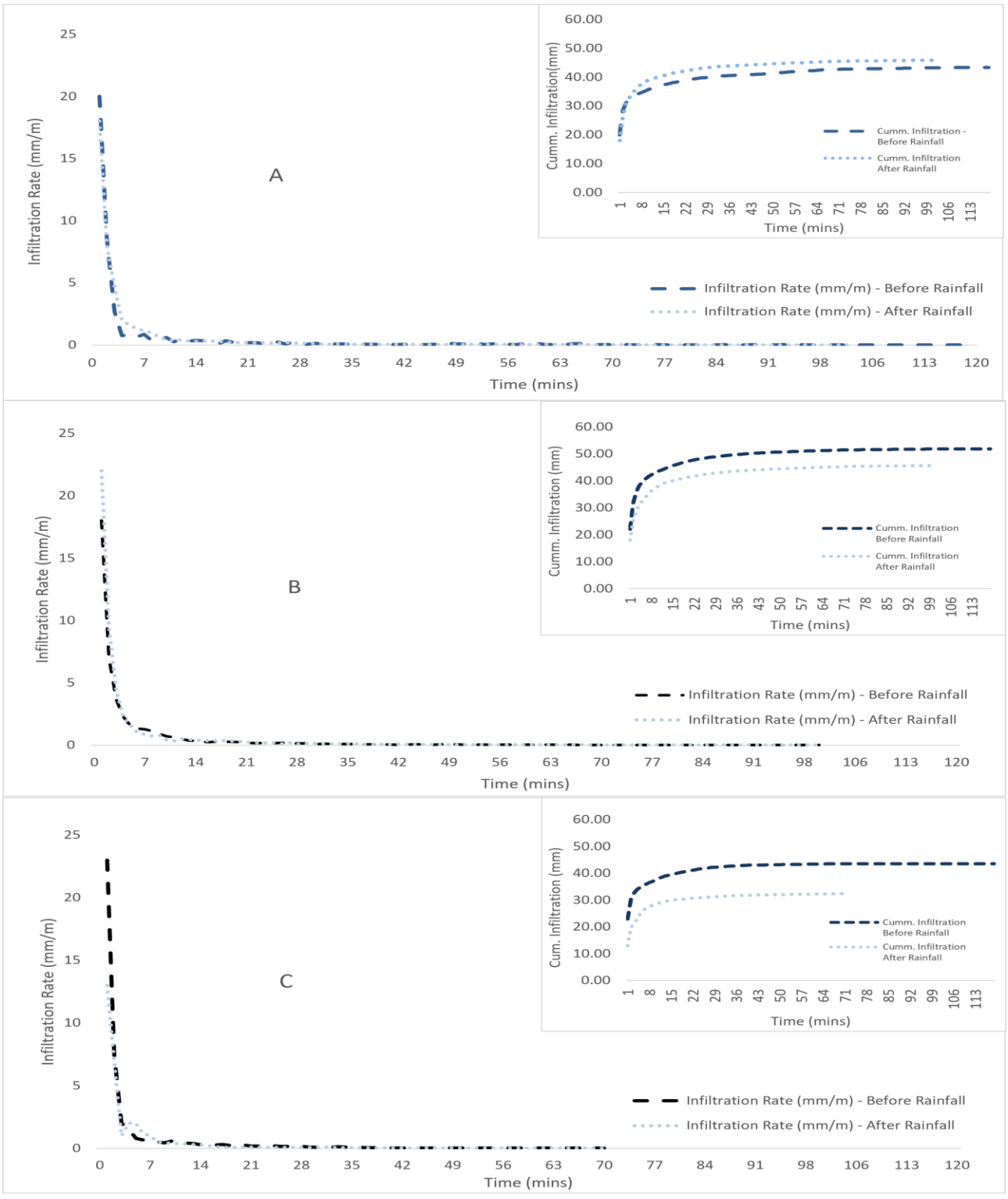

Figure 5.16 Infiltration rate (mm/min) is measured for all three pits, A. -2 m, B. -5 m, C. -7m. Cumulative infiltration (mm) was also measured and is displayed in an inset graph for each pit. For all pits the dashed line represents infiltration measured before rainfall and the dotted line represents infiltration measured after rainfall.

5.5.3 Moisture Content-Lava Rise Pits

Soil moisture samples with a Theta probe were taken throughout different depths within each pit, for a total of 231 samples per pit (Table 5.5). The samples were divided into the four categories, to correspond with the categories utilized for temperature samples: bare ground, moss, grass, and vascular plants.

Table 5.5 Field spot measurements of volumetric moisture content (%) (September 25th – October 9th, 2020) using a 6 cm theta probe. The table below displays the range, mean and standard deviation SD of volumetric moisture content within the Lava Rise Pits. Where x = mean, σ = standard deviation, and n=sample size.

	Grass			Moss			Vascular Plants			Bare Ground - Ash		
Lava Rise Pits	*Range*	*x*	*σ*	*Range*	*x*	*σ*	*Range*	*x*	*σ*	*Range*	*x*	*σ*
0 – -2 m (n=210)	4.6 - 28.8	13.1	3.5	10.0 - 45.4	22.3	7.5	7.1 - 46.3	15.9	7.0	6.9 - 31.1	15.8	4.7
0 – -5 m (n=210)	3.9 - 36.8	16.4	5.0	9.0 - 39.6	20.1	6.0	0.0 - 30.5	17.4	5.1	0.0 - 39.6	17.7	7.3
0 – -7 m (n=210)	13.4 - 51.1	31.1	7.5	11.3 - 51.0	31.2	7.9	13.2 - 48.9	29.0	7.9	0.0 - 57.1	37.5	11.0

Overall, these soil moisture content estimates indicated that the -7 m pit had the highest mean value in each category, followed by the -5 m pit, and finally the -2 m pit (Figure 5.17). The average moisture content for the moss was higher in the -2 m pit compared to the -5 m pit, which was the only deviation from the trend. Samples were collected daily, within a similar timeframe to avoid large differences due to rain. The volumetric moisture content between the different surfaces for both the -2 and -5 m pit were negligible, and not statistically significant (n= 630, p 0.129).

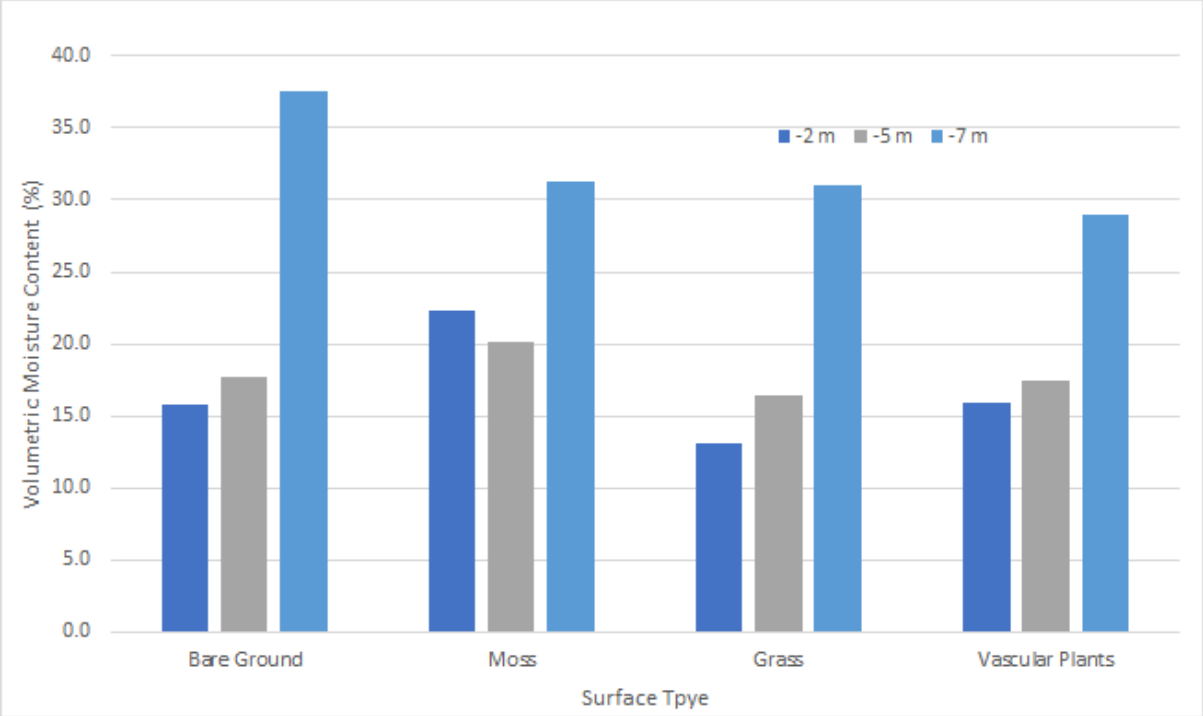

Figure 5.17 Average volumetric moisture content recorded in the field (September 25th – October 9th, 2020) – 231 moisture readings were recorded per pit using a 6 cm Theta Probe.

In both the -2 and -5 m pits, the higher moisture values were often measured at the surface of the individual pits, whereas the moisture content in the -7 m pit were elevated at the bottom.

When examining the lava rise pits individually, in the -2 m pit, volumetric moisture content decreased as the depth of the pit decreased (Figure 5.18 A). This applied to three of the four surface types. Moss was the only surface in this pit that increased in the center (-1 m depth), and then decreased again at the bottom. The changes in moisture content between the depths were not dramatic, with the exception being moss. Between -1 m and the bottom of the pit, there was a 12% change in the average volumetric moisture content. While the change was noticeable, it was not statistically significant (n= 630, p = 0.429).

In the -5 m lava rise pit, the volumetric moisture content decreased with depth (Figure 5.18 b). Decreases in volumetric moisture content were steady, with the moss and bare ground surface types experiencing the highest volumetric moisture content throughout each section of the pit.

The -7 m lava rise pit had the opposite trend compared to both the -2 m and -5 m pits. The volumetric moisture content tended to increase with depth (Figure 5.18 c). As noted earlier, the volumetric moisture content in this pit was nearly twice that of -2 and -5 m pits. Bare ground had the highest volumetric moisture content at each depth.

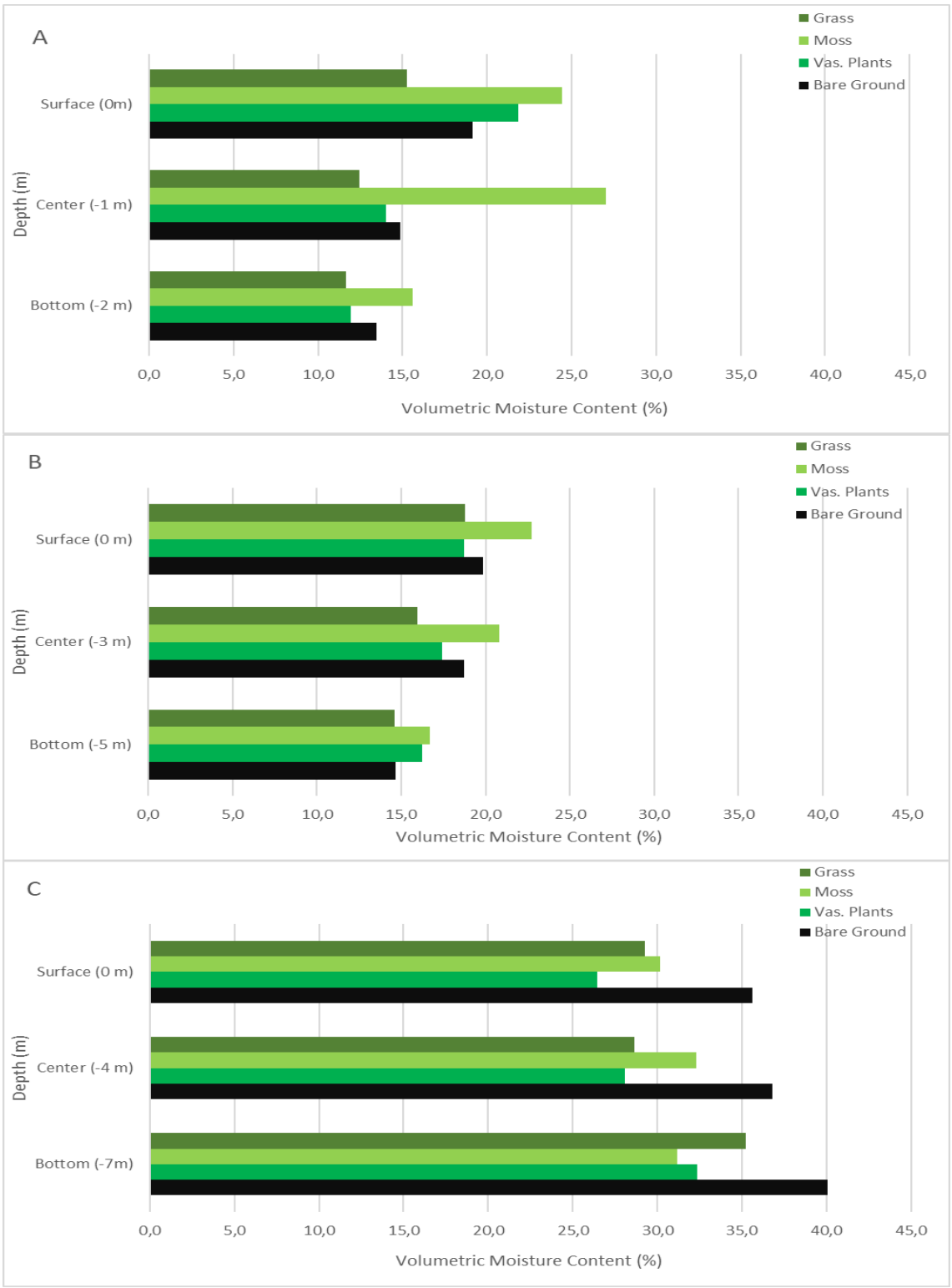

Figure 5.18 Volumetric moisture content (%) collected using a 6 cm Theta probe (± 1%) throughout the different depths within each lava pit (A=-2 m pit; B= -5 m pit and C= -7 m pit) categorized into four different categories: Grass, Moss, Vascular Plants and Bare Ground.

5.5.4 Continuous soil moisture levels in Lava Rise Pits.

Continuous moisture readings were recorded in all three pits, however, due to the sensor in the -2 m pit being submerged in ice, the continuous data logging device was destroyed here. The Smart HOBO Moisture Probes were placed at the bottom of each pit (-0.10 m) into the bare ground (soil/ash). Soil moisture was seen to increase when ground temperatures were above 0°C and during or after rain events. The direct response to rainfall events resulted in an increase in soil moisture (see Figure 5.19) unless the temperature of the ground was below 0ºC (Figures 5.20 and 5.12).

There were more fluctuations in soil moisture in the -5 m pit, especially in the autumn and early winter months than in the -7 m pit (Figure 5.19). During the winter season moisture content often fell below 0.1 m^3/m^3 and rose above 0.25 m^3/m^3 the following day. Elevated moisture contents occurred rapidly, however, after soil moisture levels fell, they would often remain low for a few days, and then spike up again.

In the middle of the winter season, moisture content within both pits remained stable, however, when approaching the winter to spring transition, the moisture content began to continuously increase. At the end of March 2021 there was an exception to this trend as there was a steep decline in soil moisture observed in the -5 m pit.

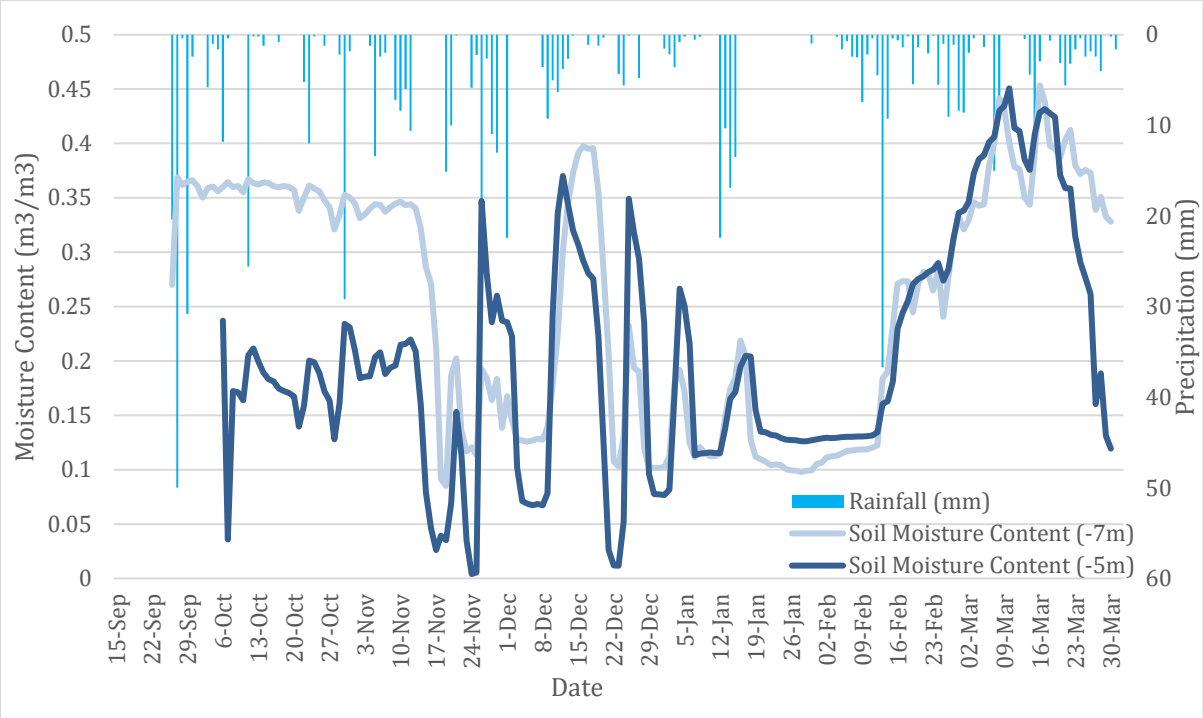

Figure 5.19 Continuous rainfall and soil moisture content measurements were collected over the study with sensors placed at bottom of each lava rise pit. Rainfall was measured using an ONSET HOBO RG3-M tipping-bucket rain gauge (±0.25 mm), and soil moistures was measured using a HOBO 10HS Smart Soil Moisture Sensor (± 3%).

When comparing the moisture content recorded in each pit and rainfall receipt, there was often an immediate response or a lag of several days. Soil moisture, however, is not just reliant on precipitation events, ground and air temperature are also significant, as warmer temperatures would lead to higher evaporation levels and drier ground (Dolschak *et al*.,2019).

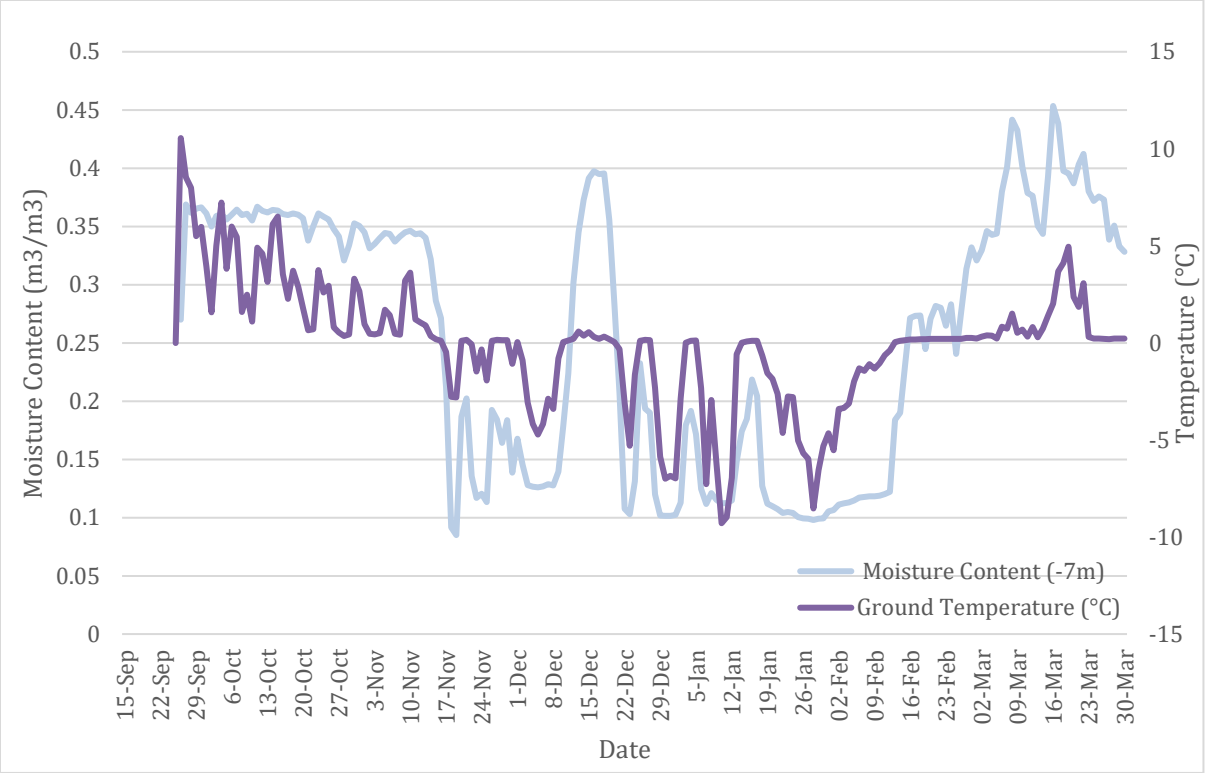

Figure 5.20 Ground temperature (Smart HOBO temperature sensor (±0.2°C)) (purple) and soil moisture content (HOBO 10HS Smart Moisture Sensor (± 3%) (blue) observed within the -7 m lava rise pit during the study period.

In the -7 m pit, soil moisture typically increased or remained relatively high when the ground temperature was above 0ºC, which can be seen in the initial and latter parts of the study period (Figure 6.20). The opposite can be observed during the cold winter season where the moisture content would drop due to frozen conditions. The relationship between increasing ground temperatures and moisture content can be observed starting December 22nd, 2020, to February 23rd, 2021, where eventually the ground reached above 0ºC, and the moisture content increased. While the relationship between frozen ground temperatures and moisture content has been established, precipitation does play a significant role during periods of frozen ground. From December 12th – 21st, 2020, there was a large spike in soil moisture just as the ground reached 0ºC, which was due to 129 mm of accumulated rainfall. However, small increases in the ground

temperature result in partial thawing, thus leading to small increases in moisture content. Cracks, crevices, and the structure of the soil can further enhance moisture content in soils during freeze-thaw events. Fraiser (1959) and Ymène *et al*., (2013) have also observed this in the Canadian Prairies.

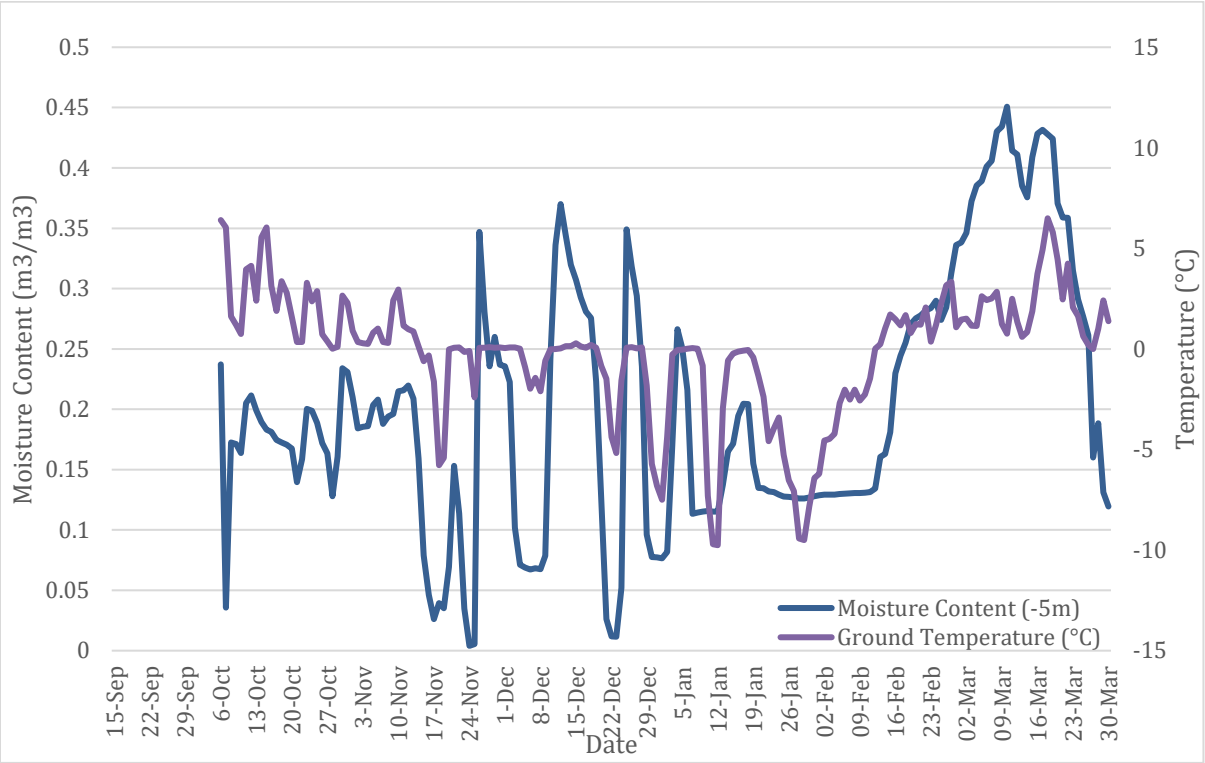

Figure 5.21 Ground temperature (Smart HOBO temperature sensor (±0.2°C)) (purple) and soil moisture content (HOBO 10HS Smart Moisture Sensor (± 3%) (blue) observed within the -5 m lava rise pit during the study period.

Soil moisture in the -5 m pit, also followed a similar trend to the -7 m pit where an increase in soil moisture occurred as the ground temperature rose above 0ºC (Figure 5.21). The peaks in moisture content in the -5 m pit were higher than moisture peaks in the -7 m pit, except from December 18th, 2020, January 16th, and March 16th, 2021. In the -5 m pit, the lowest moisture content observed was 0.01 m^3/m^3, whereas the lowest moisture content observed in the -7 m pit was 0.08 m^3/m^3. The fluctuations of soil moisture results in the -5 m pit varied much

more compared to the -7 m pit. However, during January 15th to February 17th, 2021, both lava pits had stable soil moisture regimes (Figure 5.10).

Chapter 6: Discussion

6.1 Introduction

The purpose of this study was to better understand the relationship between the geomorphology and hydrology of Lava Rise Pits found in the Laki lava field, Southeast Iceland. The thermal regimes of these landscapes were also investigated in this study.

Surface coverage (including vegetation identification, and density), ash dispersal and both 2D and 3D spatial maps were used to further identify and examine connections between the geomorphology and hydrology of these unique lava features. Measurements were collected using both smart technology and traditional field methods to better understand spatial and temporal patterns (both short- and long-term).

Analysing ground temperature, near surface above-ground temperature, and examining their relationship to air temperature was key to understanding the thermal regimes of these lava rise pits. A water budget framework was utilized to better understand the inputs, outputs, and storage pathways of water in these depressions. A great deal of focus centred on rainfall totals, infiltration, and water storage (soil moisture).

6.2 Surface Impacts

6.2.1 Surface Coverage

Surface coverage was examined in all three of the pits. While the pits had similar surface coverage composition (see study section), the amount of coverage and at what depth they occurred varied. When examining each of the lava rise pits (Figure 6.1), the -2 m and the -5 m lava rise pits, bare ground (ash and soils), and *Racomitrium lanuginosum* (Woolly Fringe Moss)

were the overall dominating surface types, which is common in vitrisols soils (Arnalds, 2004). Within the -7 m lava rise pit, *Racomitrium lanuginosum* (Woolly Fringe Moss) and *Empetrum nigrum (*Crowberry) were the dominating surface types. These patterns were expected as the -2 m and the -5 m were not as deep, and closer to both the glacial riverbank and the road, making it easier for winds to deposit glacial-fluvial sediments along with tephra (ash and dust) during aeolian activity (Arnalds *et al*, 2001). Plants are a great source of protection against erosion, as they help to keep soil in place thereby limiting wind erosion (Runólfsson 1987; Gísladóttir 2005). The most important factor in the placement of the vegetation was depth and distance from source areas, for example relative position of the pits to the glacial river and sandur. Those lava rise pits nearer to the river experience elevated deposits and coverage due to glacio-fluvial action (Arnalds, 2000 a; Arnalds, 2000 b). The distance from an ash source is critical as ash can damage vegetation through burial (Arnalds *et al*., 2000; Gísladóttir *et al*., 2005), inhibit photosynthesis, cause breakage, or increase heat (Young *et al.*, 2019). The lack of vascular plants here is a possible sign of erosion as they are likely uplifted and removed from the surface (Armbruster and Retta, 2000; Arnalds, 2004; Arnalds, 2010), or smothered by sand and ash (Arnalds, Sigurjónsson *et al*., 2000), resulting in bare ground.

Vascular plants, such as *Thymus praecox* (Wild Thyme), *Alchemilla alpina* (Alpine Lady's-Mantle) and large *Salix phylicifolia (Tea Leaved Willow)* bushes did not grow in the open, but rather in deeper pits. *Cladonia rangiferina* (Reindeer Lichen), *Racomitrium lanuginosum* (Woolly Fringe Moss), *Graminoid* (Grass), *Empetrum nigrum* (Crowberry), were the most common vegetation found at the surface, which aligned with findings by Arnalds and Kimble (2001).

6.2.2 Ash Dispersal

Ash distribution was important to this study, as one of the goals for this study was to understand how ash impacts the movement of water into groundwater reserves. While it was not possible to measure groundwater inputs and outputs, infiltration and moisture readings provided understanding of recharge processes in the lava rise pits. Soil moisture was an indicator of the amount of moisture within the ground. With coarser material, water can infiltrate into the ground faster, whereas finer materials (silts, clay) can hinder that movement (Orradóttir *et al.*, 2008). In the coarser material, voids and cracks in the ground would also further modify infiltration. As the lava rise pits have karst like features (Kiernan *et al.*, 2003), it is possible that cracks could have existed under the zones where the infiltration experiments occurred.

In the -2 m pit, ash coverage was the highest, followed by the -5 m pit and finally the -7 m pit. When examining the three pits individually, there are possible explanations for why ash distribution occurred the way it did. In the Laki lava field, aeolian activity is frequent in Southern Iceland as it experiences the most aeolian deposition (Arnalds, 2010). The inputs are from two main sources, glacio-fluvial deposits, and volcanic ash (Arnalds, 2001; Arnalds 2001a). Sand fields are aeolian sites and sand deposits can be redistributed over large areas. Wind erosion is also at its highest in the summer (Prospero *et al.*, 2012), and the least in the winter. However, in winter, frost heaving allows for more sand accumulation (Orvalle *et al.*, 2021), and the Laki lava field is in an area where wind erosion typically occurs (Arnalds, 2010).

The -2 m pit is the shallowest of the three, with the highest ash coverage, which may be due to its depth, resulting in decreased protection from wind events. Its proximity to the glacial river, also resulted in sandier soil composition. A lower percentage of vascular vegetation (*Graminoids*, *Salix phylicifolia*, *Empetrum nigrum* and *Juncus ranarius*) along with above 50%

ash surface coverage at the bottom signals a site prone to wind erosion and deposition (Greipsson, 2012). In the -5 m pit, as it was deeper, the surface covered by bare ground (ash and soils) began to increase, especially at the bottom (-5 m). This suggests that this pit is a sink for aeolian deposition verses a source due to it having a smaller opening (McTanish and Strong, 2007). Finally, although the -7 m pit is deeper than both the -2 and -5 m pit, the amount of surface area covered by ash was the lowest. This could be due to the increase coverage by moss and vascular plants, as well as the location of the pit. Vegetation commonly helps with the stabilization of aeolian activity (Youseff *et al.*, 2012). If there is more vegetation, then more stability is offered to an area, resulting in a decrease in wind activity and soil erosion (Youseff *et al.*, 2012.; Arnalds *et al.*, 2016). However, this is also dependent on vegetation type and height (Arnalds *et al.*, 2016). The vegetation in this study area was not tall, with ~30 cm height being the limit during random height measurements. With less vascular vegetation, an increase in ash dispersal and aeolian activity can occur (Ravi *et al*., 2010), which is more important when examining the -2 and 5 m pits.

6.3 Thermal Regimes

6.3.1 Thermal Regimes

The thermal regimes within the lava pits were impacted by many factors. Near surface and air temperatures generally decreased with elevation, however, the effect was commonly noticed during the night (Eneva and Collbaugh, 2009). During the day, areas that received larger amounts of sunlight, or areas that were shaded, distorted the relationship between temperature and elevation (Eneva and Collbaugh, 2009). While a study conducted by Eneva and Collbaugh (2009) did not analyse lava rise pits, a relationship between depth and openness was present. In this Icelandic study, it was found that the depth, pit openness (circumference) and air

temperature were the most important variables. Each pit had very distinct depths and openness. The importance behind pit openness suggests that the more open the pit is, the less shading would be present. These variables were noticed as the dominating factors for impacting near surface temperatures.

When examining the specifics of the pits, the smallest pit was -2 m deep, with a circumference of 101.8 m, whereas the -5 m pit had the smallest circumference (54.6 m). The -7 m was the deepest of the three and had the widest circumference 106.4 m. Near surface temperatures indicated that the coldest pit of the three was the -5 m pit (Figure 6.4 A), with the -2 m pit being the warmest. While an ANOVA did not indicate a statistically significant result, the temperatures of each pit did vary, showing slight temperature differences. This suggests that the circumference of the pits may have been a more important factor than depth, for near-surface temperatures here. Since the -2 and -7 m pits had the largest circumferences, this allowed the temperatures to be influenced by fluctuations in atmospheric air temperature. In the sheltered and deeper parts of the pits, air exchange was muted and ground temperatures were able to stay cooler or warmer than the atmosphere. The changes in temperature can be important when examining temperature inversions. For example, there was a switch in the temperature signal resulting in the -5 m pit becoming the coolest. Temperature inversions are frequently observed in the night and during the winter months (Eneva and Collbaugh, 2009).

It was determined that for all three pits there were more heating degree days than cooling degree days. For all three pits, an increase in warming degree days relative to the norm might provide an indication of climate change. From September 2020 to March 2021, temperatures were slightly higher than the 30-year trend (1990-2020 IMO), apart from November, December, and January. Although Iceland does have maritime like winters (Einarsson, 1984; Orradóttir,

2008), climate change continues to occur, which has been observed in the continuous loss of glacial mass (Aðalgeirsdóttir, Guðfinna, *et al*., 2020) and an increase in volcanic activity (Tinganelli, Leone, *et al*., 2018). Climate change, using glacial mass observations, have been heavily observed in the tourism industry as people react and adapt to the rapid retreat of glaciers, changes in landscape quality and attractiveness (Welling and Abegg, 2019; Welling, Árnason, and Ólafsdóttir *et al*., 2020).

6.3.2 Ground Temperature

Ground temperatures were highly dependent on the season, and there was a mixture of factors that impacted ground temperature. In Arctic regions, the main influence of the air-ground temperature relationship is insulation from snow or vegetation (in continental regions) (Smith and Riseborough, 2002; Farbrot *et al*., 2007). Other than insulation from vegetation, air temperature, ice or snow cover, variables such as depth, openness and/or slope angle, soil moisture, bulk density, and soil colour can also impact ground temperatures (Onwuka, 2016; Haskell *et al*., 2018). As noted earlier, water content affects the thermal properties of soil and mosses, and lichens can amplify winter warming of soils and summer cooling (Park *et al*., 2018).

The relationship between air temperature and vegetation cover was observed in this study. Air temperature primarily affected the smallest pit as it closely followed ground temperatures for most of the study, except when the probe was under ice (approximately 40 cm) in the -2 m pit, resulting in ground temperatures stabilizing at 0°C. The differences in ground temperatures can be the result of variations in depth and vegetation. After mid-March, the surface temperatures for all pits began to follow the fluctuations in air temperature. Studies have found that the energy exchange between the ground and the atmosphere is the primary driver to

ground temperature fluctuations (Onwuka, 2016) as well as soil moisture content (Janssen *et al*., 2004).

6.4 Hydrology

6.4.1 Soil moisture

Soil moisture can be impacted by topography, soil characteristics (Kaleita *et al.*, 2005), precipitation and vegetation (Yang *et al*., 2014), snowmelt (Harpold and Molotch *et al*., 2014), and can be spatially variable (Kaleita *et al.*, 2005). Rainfall and snowmelt were two of the most important variables influencing soil moisture levels in this study. However, a study completed by Yoo, *et al*. 1998, found that while rainfall is important, it is the water-diffusing mechanisms such as surface run-off or infiltration that are the real drivers of soil moisture, limiting the direct impact of rainfall. Yoo, *et al*. 1998 also found that soil texture, topography and evapotranspiration further diminished the impact of rainfall.

When the ground temperatures were above 0°C, increases in soil moisture responded faster to precipitation inputs. However, when ground temperatures were below 0°C and a precipitation event occurred, there was little to no increase in soil moisture until ground temperatures increased. A study conducted by Jiang *et al*. (2018) found that soil moisture was significantly lower during the freezing period or when the ground was frozen, as precipitation that was normally a source of recharge in the warmer months would be redirected or drained away. This was seen clearly in Figures 5.10 – 5.12, from January 17 to February 15th, 2021, as soil moisture was steady in the winter when the ground was frozen (Walsh *et al.*, 1985). In the autumn and winter seasons, when air temperatures were at or below 0°C, soil moisture content levels, maintained ground temperatures at 0ºC for extended periods of time, due to the zero-curtain effect (Domine *et al.*, 2018). However, when temperatures increased, snowmelt would be

the main driver for the increase in soil moisture, which was also observed by Harpold *et al*. (2014). Flint *et al*. (2017) found that soil moisture changes were consistent with the melting and freezing of snow resulting in an increase or decrease of infiltration into the soil.

During this study, zero-curtain effects were present but generally occurred in the smallest pit. This pattern reinforces the relationship between soil moisture and ground temperatures, which is found in other temperate and arctic locations (Jiang *et al*., 2018).

Research studies have indicated that areas where vegetation are present tend to show elevated soil moisture content compared to areas that are barren (e.g. D'Odorico *et al.*, 2007; Yang *et al*. 2008). The relationship between vegetated surfaces and soil moisture is evident as soil moisture was lower in both the -2 and -5 m pit. As moss and lichen have a high holding capacity, it can also increase the amount of water present, especially during the winter (Park *et al*., 2018).

6.4.2 Infiltration

Infiltration tests can foster a better understanding of the retention and movement of water through the soils. Orradóttir *et al.*, 2008 noted that an understanding of vegetation, land coverage changes, and hydrological processes, such as infiltration rates were critical to land management and development. For this study infiltration tests were conducted both before and after rainfall.

Infiltration can be altered by topography, vegetation, and current soil moisture and the coarseness of a material directly impacts the amount of moisture required for soils to reach full saturation (Gray and Norum, 1967; Tejedor *et al*., 2013; Orradóttir, 2008). Lower moisture measurements and longer infiltration tests are indicators of coarse material, or the potential of a

smaller voids under the surface, like in a clay. Andosols are known to have both high infiltration rates and soil water retention (Orradóttir *et al.*, 2008).

The importance behind conducting a test before and after precipitation was to see how the moisture content within the soils would change after a 'natural' input of moisture. After the rainfall event, it was observed that infiltration rates were similar to infiltration rates before a rainfall event, with all three pits showing a steady rate or cumulative plateau of within 5 – 11 minutes. This is indicative that water was infiltrated at a quick rate initially, which supports the finding made by Yoo *et al*., (1998) that while precipitation is important, soil characteristics can impact infiltration, thus having a direct effect on soil moisture. While the sharp drop in infiltration at the sites would suggest that that infiltration might be 'poor' in these soils the fact that these soils were able to infiltrate ~30+ mm over 100 minutes (see infiltration diagrams), supports the high infiltration nature of Andosols (Orradottir *et al.,* 2008).

6.4.3 Seasonal impacts of precipitation

Overland flow was observed at the lava field surface and within the -7 m lava rise pit. Due to the size of the pits, and the varying topography, calculating total overland flow into the lava rise pits was not possible. Overland flow was only noticed at the surface due to incised channels that developed around surface vegetation. It was also only observed during the autumn and winter seasons, as the soils reached full saturation in the autumn, and froze over in the winter (Figure 6.1).

Where this study was conducted, in the southern region of Iceland typically has some of the highest levels of precipitation within the country (Phillips and Thorpe, 2005). In their study, Phillips and Thorpe (2005) found that >50% of precipitation occurred from October to March. Total rainfall measured during this study was similar, as each season (autumn and winter) had

50% of the collected rainfall respectively. Rainfall is also impacted by the Icelandic Low (Crochet, 2007), which can be very localized (Hanna *et al.* 2004).

Figure 6.1 Photos taken displaying the movement of water throughout the lava field. The first picture was taken on September 27th, 2020, the second on October 6th, 2020, and the third picture was taken on January 30th, 2021.

Freeze-thaw cycles are common in Iceland due to the rapid changes in temperatures, and precipitation, and modified by soil characteristics (Hall, 2007; Arnalds, 2015). Freeze-thaw action occurred throughout this study, as it is common in Iceland due to the maritime like climate during the winter (Einarsson, 1984; Orradóttir 2008). In this study there were seven freeze thaw events that took place during the winter season. Kværno and Øygarden (2006) found that freeze-thaw effects were more disruptive when temperatures lingered around -4°C and were less impactful when temperatures were colder i.e. -18°C. The potential for freeze-thaw events increases when the ground is not covered by snow, as snow and ice can help insulate the ground thus resulting in temperature stability (Gatto, 1995; Kværno and Øygarden, 2006; and Li, 2012). Freeze-thaw events are driven by soil structure, water content and the presence of vegetation.

The interaction between heating and cooling degree days, and precipitation resulted in snow ice. The -2 m lava rise pit was frozen under ~40 cm of snow ice, which can be seen in (Figure 6.2). Snow ice occurs when snow and water mix, forming slush, and then freezes as the surrounding air temperature decreases (Lepparanta, 1983). Snow ice was not found in the larger pits and was only noticeable in the smaller pits closest to the glacial river. This could be due to wind blowing water from the near-by glacial river, overland flow at the surface, or a frozen ground layer that decreased moisture capacity resulting in water pooling, and then freezing. Thus, upon melting, this snowpack or ice layer would be a source of water to recharge soil moisture in the lava pit (Flint *et al*., 2008; Harpold *et al*., 2014).

Figure 6.2 Ice coverage in the small pit when the entire (or bottom) of the pit was covered by ~40 cm of ice. In the right picture, equipment used to measure ground and near surface temperature were submerged in the ice. The photo on the left showed the occurrence of snow ice.

6.5 Climate Warming

As noted by Kieran et al., (2003), lava rise pits may play a large role in contributing water to groundwater replenishment. However, to fully assess this, the ability to access the groundwater system within these lava rise pits is crucial. Monitoring ground temperatures in the lava rise pits is important as it could give rise to further research. As global temperatures continue to increase with climate change (Welling and Abegg, 2019; Welling *et al*., 2020), it is highly likely that increases in freeze-thaw events in cold regions will continue to occur (Wang *et al.*, 2020). Cracks in soils may potentially be impactful on climate change as it releases stored carbon, especially since soils, after oceans are the largest carbon reservoirs on the planet (Arnalds *et al.*, 2000).

Cracks in soil will also increase soil erosion as freeze-thaw cycles will alter the structure of the soil (Wang et al., 2020).

As these lava fields have very little amounts of vegetation with root systems to stabilize soils, erosion will be an important concern moving forward (Yang *et al.,* 2003). More than one third of Iceland is covered in some form of volcanic landscape, much of which can be considered as deserts (Arnalds and Kimble, 2001). Erosion has been and continues to be one of the most important environmental threats (Mauffi *et al.,* 2022). Lava rise pits will be affected by climate change through the intensification of precipitation and stronger winds (Nearing et al., 2004; Dore, 2005; Trenberth, 2011; Donat *et al.,* 2015; Gorman, 2015), which will further increase soil erosion and sediment deposition across the landscape (Yang *et al.,* 2003; Wang *et al.,* 2020). Frequent and more intense rain events will result in saturated soils that initiate saturation overland flow and soil erosion through the movement of sediment and material swept away during overland flow (Nearing *et al.,* 2004). Vegetation helps stabilize the negative effects of erosion (Youseff *et al.,* 2012.; Arnalds *et al.,* 2016), however, continuous aeolian activity will cause plants to be buried or smothered by sandy material (Arnalds *et al.,* 2000; Gísladóttir *et al.,* 2005; Arnalds *et al.,* 2016). As this area is classified as a sandy desert, this area is already prone to sandstorms and windstorms due to its andic soil composition and regional climate (Gísladóttir *et al.,* 2005; Arnalds, 2010; Prospero *et al.,* 2012). Arnalds *et al.,* (2000) found that carbon release within andic soils will increase if the land continues to face degradation via erosion, heavy rainfall, and continued loss of plants. This will allow this site to continue as a source for the release of carbon emissions rather than being a sink (Arnalds *et al.,* 2000).

6.6 Study Limitations and Future Work

Limitations can always be found when conducting field research, and this study was not an exception. We employed a container to collect drip (condensation and overland flow) into the pit. However, due to the rough topography of the lava rise pits, it was only possible to capture a small portion of overland flow coming from the lava surface and draining into the cracks and lava tunnels below the ground. The inability to assess groundwater was another limitation of this study and should be examined in the future. Without having any boring equipment to bore down and access the groundwater below the lava rocks, it was not possible to implement wells to observe water levels and estimate groundwater flow. As these are a porous area, with lots of surface cracks and crevasses, the presence of groundwater recharge and discharge is extremely likely.

Increasing the number of soil samples per pit, across the different depths would be important to identify if there are any significant differences within the soils, especially due to the differences in surface coverage. This may help clarify the observation that lava rise pits on the interior of the lava field contain a higher diversity of vascular plants and greater coverage of non-vascular plants.

For this study, evaporation was not measured in the field. Einarsson (1972) found that due to low temperatures during the fall and winter season, evapotranspiration rates are relatively low. In the future, other methods could be explored: temperature-based approaches to assess potential evaporation or the use of lysimeters (Dingman, 2002).

Chapter 7: Conclusions

The purpose of this study was to better understand the relationship between the geomorphology and hydrology of Lava Rise Pits found in the Laki lava field, Southeast Iceland during a fall-winter period. The thermal regimes of these landscapes were also investigated in this study.

The main findings of this study are as follows:

1. Ash and surface coverage showed that more ash was deposited in the pits as the depth decreased. The deepest of the three pits had the least ash coverage while the shallowest pit had the most. The study also noted significant differences in surface coverage within the lava rise pits and with depth.

2. Thermal regimes were primarily impacted by depth, pit openness and the relations between the ground and air temperature signals. In pits that were more open and exposed to the atmosphere, the near surface above ground temperatures, and below ground temperatures mimicked the trends in air temperature.
3. Precipitation (rainfall) was the most important input of water into these depressions, and soil moisture fluctuations were linked to ground temperature conditions. When ground temperatures were below 0°C and frozen, soil moisture levels were low despite large precipitation events. However, once ground temperatures increased, soil moisture levels rose due to snow and ice melt infiltration.
4. While rainfall was the primary input of water into the lava rise pit system, other water pathways besides infiltration, such as overland flow, groundwater may play a significant role in water movement in these features. Additional effort should be found to better evaluate them

5. Finally, to better understand the hydrology of these lava rise pits and their role in the larger Laki lava field hydrogeology, strategic and long-term studies of their groundwater regime should be mounted. Ongoing climate warming, frequent volcanic activity together with enhanced aeolian activity and flood events here makes this a dynamic Low Arctic landscape deserving of greater inquiry.

Chapter 8: References

Aðalgeirsdóttir, G., Magnússon, E., Pálsson, F., Thorsteinsson, T., Belart, J., Jóhannesson, T., & Björnsson, H. (2020). Glacier changes in Iceland from~ 1890 to 2019. *Frontiers in Earth Science*, 520.

Armbrust, D. V., Retta, A. (2000). Wind and sandblast damage to growing vegetation. *Annals of Arid Zone*, *39*(3), 273-284.

Arnalds, O. (2000 a). Desertification: an appeal for a broader perspective. In Rangeland desertification (pp. 5-15). *Springer*, Dordrecht.

Arnalds O. 2010. Dust sources and deposition of aeolian materials in Iceland. *Icelandic Agricultural Sciences*, 23, 3–21.

Arnalds, O. (2000 b). The Icelandic 'rofabard'soil erosion features. *Earth Surface Processes and Landforms: The Journal of the British Geomorphological Research Group*, *25*(1), 17-28.

Arnalds, O. (2004). Volcanic soils of Iceland. *Catena*, *56*(1-3), 3-20.

Arnalds, O. (2008). Soils of Iceland. *Jökull*, *58*, 409-421.

Arnalds, O., & Kimble, J. (2001). Andisols of deserts in Iceland. *Soil Science Society of America Journal*, *65*(6), 1778-1786.

Arnalds, O., Dagsson-Waldhauserova, P., and Ólafsson, H. (2016). The Icelandic volcanic aeolian environment: Processes and impacts—A review. *Aeolian Research*, *20*, 176-195.

Arnalds, O., Gisladottir, F. O., & Sigurjonsson, H. (2001). Sandy deserts of Iceland: an overview. *Journal of Arid Environments*, *47*(3), 359-371.

Arnalds, O., Guðbergsson, G., & Guðmundsson, J. (2000). Carbon sequestration and reclamation of severely degraded soils in Iceland. *Icelandic Agricultural Sciences*, *13*, 87-97.

Arnalds, O., Gudmundsson, J., Oskarsson, H., Brink, S. H., & Gisladottir, F. O. (2016). Icelandic inland wetlands: characteristics and extent of draining. *Wetlands*, *36*(4), 759-769.

Belart, J., Magnússon, E., Berthier, E., Gunnlaugsson, Á. Þ., Pálsson, F., Aðalgeirsdóttir, G., & Björnsson, H. (2020). Mass balance of 14 Icelandic glaciers, 1945–2017: spatial variations and links with climate. *Frontiers in Earth Science*, 163.

Bjarnason, Á. H. (1991). Vegetation on lava fields in the Hekla area, Iceland. (Doctoral dissertation, Sv. växtgeografiska sällsk.). *Acta phytogeogr. suec*. 1-114 Full Reference?

Björnsson, H., & Einarsson, P. (1990). Volcanoes beneath Vatnajökull, Iceland: Evidence from radio echo-sounding, earthquakes and jökulhlaups. *Jökull*, *40*, 147-168.

Björnsson, H., & Pálsson, F. (2008). Icelandic glaciers. *Jökull*, *58*(58), 365-386.

Bouwer, H. (1986). Intake rate: cylinder infiltrometer. Methods of Soil Analysis: Part 1. *Physical and Mineralogical Methods*, *5*, 825-844.

Cade-Menun, B. J., Bell, G., Baker-Ismail, S., Fouli, Y., Hodder, K., McMartin, D. W., & Wu, K. (2013). Nutrient loss from Saskatchewan cropland and pasture in spring snowmelt runoff. *Canadian Journal of Soil Science*, 93(4), 445-458.

Cech, T. V. (2009). Principles of water resources: history, development, management, and policy. *John Wiley & Sons*. ISBN 0-471-43861-8 446 pp

Chen, Z., Chen, W. E., Leblanc, S. G., Henry, G. H., & Chen, W. (2010). Digital photograph analysis for measuring percent plant cover in the Arctic. *Arctic, 63(*5*)*, 315-326.

Crochet, P. (2007). A study of regional precipitation trends in Iceland using a high-quality gauge network and ERA-40. *Journal of Climate*, *20*(18), 4659-4677.

Davies, S. M., Larsen, G., Wastegård, S., Turney, C. S., Hall, V. A., Coyle, L., & Thordarson, T. (2010). Widespread dispersal of Icelandic tephra: how does the Eyjafjöll eruption of 2010 compare to past Icelandic events? *Journal of Quaternary Science*, *25*(5), 605-611.

de Trincheria Gomez, J., Dawit, D., Famba, S., Leal Filho, W., Malesu, M., Mussera, P. V., & Oguge, N. (2018). Using rainwater for off-season small-scale irrigation in arid and Semi-arid Areas of Sub-Saharan Africa: Key Working Principles and Best Practices. *Rainwater-Smart Agriculture in Arid and Semi-Arid Areas* (pp. 9-36).

Dilley, A. C. (1968). On the computer calculation of vapor pressure and specific humidity gradients from psychrometric data. *Journal of Applied Meteorology*, *7*(4), 717-719.

Dingman, S. L. (2002). Physical Hydrology . Long Grove, IL, New Jersey.

Dingman, S. L. (2015). Physical hydrology. Waveland press., New Jersey.

D'Odorico, P., Caylor, K., Okin, G. S., & Scanlon, T. M. (2007). On soil moisture–vegetation feedbacks and their possible effects on the dynamics of dryland ecosystems. *Journal of Geophysical Research: Biogeosciences*, *112*(G4).

Dolschak, K., Gartner, K., & Berger, T. W. (2019). The impact of rising temperatures on water balance and phenology of European beech (Fagus sylvatica L.) stands. *Modeling earth systems and environment*, 5(4), 1347-1363.

Domine, F., Belke-Brea, M., Sarranzin, D., Arnaud, L., Barrere M., & Poirier, M. (2018). Soil moisture, wind speed and depth hoar formation in the Arctic snowpack. *Journal of Glaciology*, 64(248), 990-1002.

Donat, M. G., Lowry, A. L., Alexander, L. V., O'Gorman, P. A., & Maher, N. (2016). More extreme precipitation in the world's dry and wet regions. *Nature Climate Change*, *6*(5), 508-513.

Dore, M. H. (2005). Climate change and changes in global precipitation patterns: what do we know? *Environment International*, *31*(8), 1167-1181.

Dragosics, M., Meinander, O., Jónsdóttír, T., Dürig, T., De Leeuw, G., Pálsson, F., & Thorsteinsson, T. (2016). Insulation effects of Icelandic dust and volcanic ash on snow and ice. *Arabian Journal of Geosciences*, *9*(2), 1-14.

Dubbert, M., & Werner, C. (2019). Water fluxes mediated by vegetation: emerging isotopic insights at the soil and atmosphere interfaces. *New Phytologist*, *221*(4), 1754-1763.

Einarsson, B. (2009). "Jökulhlaups in Skaftá: A study of a jökulhlaup from the Western Skaftá cauldron in the Vatnajökull ice cap, Iceland." *Icelandic Meteorological Office*. 1-74.

Einarsson, M. Á. (1984). Climate of iceland. *World survey of climatology*, 15(110), 673-697.

Einarsson, M. Á. (1972). Potential evapotranspiration and water balance in Iceland. *Hydrology Research*, *3*(4), 183-198.

Eneva, M., & Coolbaugh, M. (2009). Importance of elevation and temperature inversions for the interpretation of thermal infrared satellite images used in geothermal exploration. *GRC Transactions*, 33, 467-470.

Farbrot, H., Etzelmüller, B., Schuler, T. V., Guðmundsson, Á., Eiken, T., Humlum, O., & Björnsson, H. (2007). Thermal characteristics and impact of climate change on mountain permafrost in Iceland. *Journal of Geophysical Research: Earth Surface*, *112*(F3).

Flint, A. L., Flint, L. E., & Dettinger, M. D. (2008). Modeling soil moisture processes and recharge under a melting snowpack. *Vadose Zone Journal*, *7*(1), 350-357.

Gatto, L. W. (1995). Soil freeze-thaw effects on bank erodibility and stability. *Army Cold Regions Research and Engineering Laboratory (USA) Not a complete reference*

Gisladottir, F. O., Arnalds, O., & Gisladottir, G. (2005). The effect of landscape and retreating glaciers on wind erosion in south Iceland. *Land Degradation & Development*, *16*(2), 177-187

Glaze, L. S., Anderson, S. W., Stofan, E. R., Baloga, S., & Smrekar, S. E. (2005). Statistical distribution of tumuli on pahoehoe flow surfaces: Analysis of examples in Hawaii and Iceland and potential applications to lava flows on Mars. *Journal of Geophysical Research: Solid Earth*, *110*, 1- 14.

González-Correa, S., Lapuerta, M., Ballesteros, R., Pacheco-Ferrada, D., Castro, L., & Cereceda-Balic, F. (2022). Impacts of Soot, Ash, Sand, and Haze on Snow Albedo in Sierra Nevada, Spain. *Atmosphere*, *13*(11), 1903.

Gray, D. M., & Norum, D. I. (1967, November). The effect of soil moisture on infiltration as related to runoff and recharge. In *Proceedings of hydrology symposium* Vol. 6, pp. 133-153

Green, S. J., Demes, K., Arbeider, M., Palen, W. J., Salomon, A. K., Sisk, T. D., & Ryan, M. E. (2017). Oil sands and the marine environment: current knowledge and future challenges. *Frontiers in Ecology and the Environment*, *15*(2), 74-83.

Greipsson, S. (2012). Catastrophic soil erosion in Iceland: Impact of long-term climate change, compounded natural disturbances and human driven land-use changes. *Catena*, *98*, 41-54.

Guilbaud, M. N., Self, S., Thordarson, T., & Blake, S. (2005). Morphology, surface structures, and emplacement of lavas produced by Laki, AD 1783–1784. *Geological Society of America Special Papers*, *396*, 81-102.

Hall, K. (2007). Evidence for freeze–thaw events and their implications for rock weathering in northern Canada: II. The temperature at which water freezes in rock. *Earth surface processes and Landforms*, *32*(2), 249-259.

Hameed, S., & Piontkovski, S. (2004). The dominant influence of the Icelandic Low on the position of the Gulf Stream northwall. *Geophysical research letters*, *31*(9), need to put in page numbers.

Hamilton, C. W., Scheidt, S. P., Sori, M. M., de Wet, A. P., Bleacher, J. E., Mouginis-Mark, P. J., & Crumpler, L. S. (2020). Lava-rise plateaus and inflation pits in the McCartys lava flow field, New Mexico: An analog for pāhoehoe-like lava flows on planetary surfaces. *Journal of Geophysical Research: Planets*, *125*(7).

Hanna, E., Jónsson, T., & Box, J. E. (2004). An analysis of Icelandic climate since the nineteenth century. *International Journal of Climatology: A Journal of the Royal Meteorological Society*, *24*(10), 1193-1210.

Harpold, A. A., Molotch, N. P., Musselman, K. N., Bales, R. C., Kirchner, P. B., Litvak, M., & Brooks, P. D. (2015). Soil moisture response to snowmelt timing in mixed-conifer subalpine forests. *Hydrological Processes*, *29*(12), 2782-2798.

Haskell, D. E., Bales, A. L., Webster, C. R., Meyer, M. W., & Flaspohler, D. J. (2018). Effectiveness of bare-root and gravel-culture shrubs used in wildlife habitat restoration on lakeshores in Northern Wisconsin. Ecological Restoration, 36(2), 134-144.

Hinkel, K. M., & Outcalt, S. I. (1994). Identification of heat-transfer processes during soil cooling, freezing, and thaw in central alaska. *Permafrost and Periglacial Processes*, *5*(4), 217-235.

Hunt, R. J., Krabbenhoft, D. P., & Anderson, M. P. (1996). Groundwater inflow measurements in wetland systems. *Water Resources Research*, *32*(3), 495-507.

Icelandic Meteorological Office (IMO). (2020). Climate Report. Retrieved from - https://en.vedur.is/climatology/iceland/climate-report

Janssen, H., Carmeliet, J., & Hens, H. (2004). The influence of soil moisture transfer on building heat loss via the ground. *Building and Environment*, 39(7), 825-836.

Jónsdóttir, J.F. & Uvo, C.B., 2009. Long-term variability in precipitation and streamflow in Iceland and relations to atmospheric circulation. *International Journal of Climatology*, *29*(10), 1369-1380.

Kaleita, A. L., Tian, L. F., & Hirschi, M. C. (2005). Relationship between soil moisture content and soil surface reflectance. *Transactions of the ASAE*, *48*(5), 1979-1986.

Kane, D. L., & Stein, J. (1983). Water movement into seasonally frozen soils. *Water Resources Research*, *19*(6), 1547-1557.

Katla GeoPark. (2017). Skaftá River. Retrieved from - http://www.katlageopark.com/geosites/skafta/

Keszthelyi, L. P., & Pieri, D. C. (1993). Emplacement of the 75-km-long Carrizozo lava flow field, south-central New Mexico. *Journal of volcanology and geothermal research*, *59*(1-2), 59-75.

Khan, R. A., Islam, S., & Singh, R. K. (2015). Methods of Estimating Ground water Recharge. *International Journal of Engineering Associates*, *5*(2), 6-13.

Kiernan, K., Wood, C., & Middleton, G. (2003). Aquifer structure and contamination risk in lava flows: insights from Iceland and Australia. *Environmental Geology*, *43*, 852-865.

Klove, B., Kvitsand, H.M.L., Pitkänen, T., Gunnarsdottir, M.J., Gaut, S., Gardarsson, S.M., Rossi, P.M., & Miettinen, I. (2017). Overview of groundwater sources and water-supply systems, and

associated microbial pollution, in Finland, Norway and Iceland. *Hydrogeology Journal,* 25, 1033-1044.

Koc, B., Eren, I., & Ertekin, F. K. (2008). Modelling bulk density, porosity and shrinkage of quince during drying: The effect of drying method. *Journal of Food Engineering*, *85*(3), 340-349.

Köhler, L. (2003). Epiphyte biomass and its hydrological properties in old-growth and secondary montane cloud forest, Monteverde, Costa Rica. Not a complete reference

Kværnø, S. H., & Øygarden, L. (2006). The influence of freeze–thaw cycles and soil moisture on aggregate stability of three soils in Norway. *Catena*, *67*(3), 175-182.

Langmann, B. (2013). Volcanic ash versus mineral dust: atmospheric processing and environmental and climate impacts. *ISRN Atmospheric Sciences*, *2013*, 1-17.

Leppäranta, M. (1983). A growth model for black ice, snow ice and snow thickness in subarctic basins. *Hydrology Research*, *14*(2), 59-70.

Li, X., Jin, R., Pan, X., Zhang, T., & Guo, J. (2012). Changes in the near-surface soil freeze–thaw cycle on the Qinghai-Tibetan Plateau. *International Journal of Applied Earth Observation and Geoinformation*, *17*, 33-42.

Magilligan, F. J., Gomez, B., Mertes, L. A. K., Smith, L. C., Smith, N. D., Finnegan, D., & Garvin, J. B. (2002). Geomorphic effectiveness, sandur development, and the pattern of landscape response during jökulhlaups: Skeiðarársandur, southeastern Iceland. *Geomorphology*, *44*(1-2), 95-113.

Marsh, P., Rouse, W. R., & Woo, M. K. (1981). Evaporation at a High Arctic site. *Journal of Applied Meteorology*, *20*(6), 713-716.

Maruffi, L., Stucchi, L., Casale, F., & Bocchiola, D. (2022). Soil erosion and sediment transport under climate change for Mera River, in Italian Alps of Valchiavenna. *Science of The Total Environment*, 806, 150651.

McTainsh, G., & Strong, C. (2007). The role of aeolian dust in ecosystems. *Geomorphology*, 89(1-2), 39-54.

Harun, N., & Kamaruddin, A. H. C. (2016). Groundwater Level Monitoring using Levelogger and the Importance of Long-Term Groundwater Level Data. In MALAYSIAN NUCLEAR AGENCY R&D SEMINAR 2016At: Malaysian Nuclear agency. WHY CAPS?

Nearing, M. A., Pruski, F. F., & O'neal, M. R. (2004). Expected climate change impacts on soil erosion rates: a review. *Journal of soil and water conservation*, *59*(1), 43-50.

Óladóttir, B. A., Larsen, G., & Sigmarsson, O. (2011). Holocene volcanic activity at Grímsvötn, Bárdarbunga and Kverkfjöll subglacial centres beneath Vatnajökull, Iceland. *Bulletin of Volcanology*, *73*(9), 1187-1208.

Ólafsson, H., Furger, M., & Brümmer, B. (2007). The weather and climate of Iceland. *Meteorologische Zeitschrift*, *16*(1), 5-8.

Onwuka, B.M. (2016). Effects of soil temperature on some soil properties and plant growth. *Scholarly Journal of Agricultural Science* 6(3), 89-93.

Orradottir, B., Archer, S. R., Arnalds, O., Wilding, L. P., & Thurow, T. L. (2008). Infiltration in Icelandic Andisols: the role of vegetation and soil frost. *Arctic, Antarctic, and Alpine Research*, *40*(2), 412-421.

Outcalt, S. I., Nelson, F. E., & Hinkel, K. M. (1990). The zero-curtain effect: Heat and mass transfer across an isothermal region in freezing soil. *Water Resources Research*, *26*(7), 1509-1516.

Park, H., Launiainen, S., Konstantinov, P. Y., Iijima, Y., & Fedorov, A. N. (2018). Modeling the effect of moss cover on soil temperature and carbon fluxes at a tundra site in northeastern Siberia. *Journal of Geophysical Research: Biogeosciences*, 123(9), 3028-3044.

Phillips, I. D., & Thorpe, J. (2006). Icelandic precipitation—North Atlantic sea-surface temperature associations. *International Journal of Climatology: A Journal of the Royal Meteorological Society*, *26*(9), 1201-1221.

Poesen, J. W., Torri, D., & Bunte, K. (1994). Effects of rock fragments on soil erosion by water at different spatial scales: a review. *Catena*, *23*(1-2), 141-166.

Prospero, J. M., Bullard, J. E., & Hodgkins, R. (2012). High-latitude dust over the North Atlantic: inputs from Icelandic proglacial dust storms. science, 335(6072), 1078-1082.

Ravi, S., Breshears, D. D., Huxman, T. E., & D'Odorico, P. (2010). Land degradation in drylands: interactions among hydrologic–aeolian erosion and vegetation dynamics. *Geomorphology*, 116(3-4), 236-245.

Roberts, M. J., Russell, A. J., Tweed, F. S., & Knudsen, Ó. (2001). Controls on englacial sediment deposition during the November 1996 jökulhlaup, Skeiðarárjökull, Iceland. *Earth Surface Processes and Landforms*, *26*(9), 935-952.

Rowland, S. K., & Walker, G. P. (1990). Pahoehoe and aa in Hawaii: volumetric flow rate controls the lava structure. *Bulletin of Volcanology*, *52*(8), 615-628.

Runólfsson, S. (1987). Land reclamation in Iceland. Arctic and Alpine Research, 19(4), 514-517.

Scheffel, H. A., & Young, K. L. (2021). Water level and groundwater dynamics across a Sandur-wetland landscape in response to seasonal and episodic events, South-East Iceland. *Wetlands*, *41*(2), 27.

Scheidt, S. P., Hamilton, C. W., Zimbelman, J. R., Bleacher, J. E., Garry, W. B., deWet, A. P., & Crumpler, L. S. (2014). Lava-rise plateaus and inflation pits within the McCartys flow, New Mexico. In *Lunar and Planetary Science Conference*, *45*, 1491-1492.

Schlenker, W., Hanemann, W. M., & Fisher, A. C. (2007). Water availability, degree days, and the potential impact of climate change on irrigated agriculture in California. *Climatic Change*, *81*(1), 19-38.

Self, S., Keszthelyi, L., & Thordarson, T. (1998). The importance of pāhoehoe. *Annual Review of Earth and Planetary Sciences*, *26*(1), 81-110.

Senjobi, B. A., & Ogunkunle, O. A. (2010). Effect of land use on soil degradation and soil productivity decline on alfisols and ultisols in Ogun State in South Western, Nigeria. *Agriculturae Conspectus Scientificus*, *75*(1), 9-19.

Serreze, M. C., Carse, F., Barry, R. G., & Rogers, J. C. (1997). Icelandic low cyclone activity: Climatological features, linkages with the NAO, and relationships with recent changes in the Northern Hemisphere circulation. *Journal of Climate*, *10*(3), 453-464.

Sethi, R. R., Kumar, A., Sharma, S. P., & Verma, H. C. (2010). Prediction of water table depth in a hard rock basin by using artificial neural network. *International Journal of Water Resources and Environmental Engineering*, *2*(4), 95-102.

Smith, M. W., & Riseborough, D. W. (2002). Climate and the limits of permafrost: a zonal analysis. *Permafrost and Periglacial Processes*, *13*(1), 1-15.

Tejedor, M., Neris, J., & Jiménez, C. (2013). Soil properties controlling infiltration in volcanic soils (Tenerife, Spain). *Soil Science Society of America Journal*, *77*(1), 202-212.

Thompson, S. E., Harman, C. J., Heine, P., & Katul, G. (2010). Vegetation-infiltration relationships across climatic and soil type gradients. *Journal of Geophysical Research: Biogeosciences*, *115*(G2).

Thorarinsdottir, E. F., & Arnalds, O. (2012). Wind erosion of volcanic materials in the Hekla area, South Iceland. *Aeolian Research*, *4*, 39-50

Thordarson, T., & Self, S. (1993). The Laki (Skaftár fires) and Grímsvötn eruptions in 1783–1785. *Bulletin of Volcanology*, 55, 233-263.

Thórdarson, T., & Höskuldsson, Á. (2008). Postglacial volcanism in Iceland. *Jökull*, *58*(198), e228.

Thordarson, T., & Larsen, G. (2007). Volcanism in Iceland in historical time: Volcano types, eruption styles and eruptive history. *Journal of Geodynamics*, *43*(1), 118-152.

Thorhallsdóttir, T. (2007). Environment and energy in Iceland: A comparative analysis of values and impacts. *Environmental Impact Assessment Review*, *27*(6), 522-544.

Timoney, K. P., & Lee, P. (2009). Does the Alberta tar sands industry pollute? The scientific evidence. *The Open Conservation Biology Journal*, *3*(1).

Tinganelli, L., Erlendsson, E., Eddudóttir, S. D., & Gísladóttir, G. (2018). Impacts of climate, tephra and land use upon Holocene landscape stability in Northwest Iceland. *Geomorphology*, 322, 117-131.

Trenberth, K. E. (2011). Changes in precipitation with climate change. *Climate research*, *47*(1-2), 123-138.

Van Stan, J. T., Stubbins, A., Bittar, T., Reichard, J. S., Wright, K. A., & Jenkins, R. B. (2015). Tillandsia usneoides (L.) (Spanish moss) water storage and leachate characteristics from two maritime oak forest settings. *Ecohydrology*, *8*(6), 988-1004.

Vilmundardóttir, O. K., Sigurmundsson, F. S., Møller-Pedersen, G. B., Belart, J. M. C., Kizel, F., Falco, N., & Gísladóttir, G. (2018). Of mosses and men: Plant succession, soil development and soil carbon accretion in the sub-Arctic volcanic landscape of Hekla, Iceland. *Progress in Physical Geography: Earth and Environment*, *42*(6), 765-791.

Walker, G. P. (1991). Structure, and origin by injection of lava under surface crust, of tumuli,"lava rises", "lava-rise pits", and "lava-inflation clefts" in Hawaii. *Bulletin of Volcanology*, *53*(7), 546-558.

Walsh, J. E., Jasperson, W. H., & Ross, B. (1985). Influences of snow cover and soil moisture on monthly air temperature. *Monthly Weather Review*, *113*(5), 756-768.

Wang, Q., Qi, J., Wu, H., Zeng, Y., Shui, W., Zeng, J., & Zhang, X. (2020). Freeze-Thaw cycle representation alters response of watershed hydrology to future climate change. *Catena*, *195*, 104767.

Wang, S., Huang, J., Yang, D., Pavlic, G., & Li, J. (2015). Long-term water budget imbalances and error sources for cold region drainage basins. *Hydrological processes*, *29*(9), 2125-2136.

Ward, R.C. and M. Robinson. (2000). Principles of Hydrology, 4th Edition. *McGraw Hill*, 450 pp.

Welling, J., & Abegg, B. (2021). Following the ice: Adaptation processes of glacier tour operators in Southeast Iceland. *International Journal of Biometeorology*, *65*, 703-715.

Welling, J., Árnason, Þ., & Ólafsdóttir, R. (2020). Implications of climate change on nature-based tourism demand: A segmentation analysis of glacier site visitors in southeast Iceland. *Sustainability*, *12*(13), 5338.

Westman, C. N., & Joly, T. L. (2019). Oil sands extraction in Alberta, Canada: A review of impacts and processes concerning Indigenous peoples. *Human Ecology*, *47*, 233-243.

Whitehead, P. W., & Stephenson, P. J. (1998). Lava rise ridges of the Toomba basalt flow, north Queensland, Australia. *Journal of Geophysical Research: solid earth*, *103*(B11), 27371-27382.

Yang, D., Kanae, S., Oki, T., Koike, T. and Musiake, K., 2003. Global potential soil erosion with reference to land use and climate changes. *Hydrological processes*, *17*(14), 913-2928.

Yang, L., Wei, W., Chen, L., Chen, W., & Wang, J. (2014). Response of temporal variation of soil moisture to vegetation restoration in semi-arid Loess Plateau, China. *Catena*, 115, 123-133.

Yoo, C., Valdés, J. B., & North, G. R. (1998). Evaluation of the impact of rainfall on soil moisture variability. *Advances in Water Resources*, *21*(5), 375-384.

Young, K. L., Assini, J., Abnizova, A., & De Miranda, N. (2010). Hydrology of hillslope-wetland streams, Polar Bear Pass, Nunavut, Canada. *Hydrological processes*, *24*(23), 3345-3358.

Young, K. L., Scheffel, H. A., Abnizova, A., & Siferd, J. R. (2017). Spatial and temporal dynamics of groundwater flow across a wet meadow, Polar Bear Pass, Bathurst Island, Nunavut. *Permafrost and Periglacial Processes*, *28*(2), 405-419.

Youssef, F., Visser, S. M., Karssenberg, D., Erpul, G., Cornelis, W. M., Gabriels, D., & Poortinga, A. (2012). The effect of vegetation patterns on wind-blown mass transport at the regional scale: A wind tunnel experiment. *Geomorphology*, 159, 178-188.

Zhang, X., Walsh, J. E., Zhang, J., Bhatt, U. S., & Ikeda, M. (2004). Climatology and interannual variability of Arctic cyclone activity: 1948–2002. *Journal of climate*, *17*(12), 2300-2317.

Appendix I: Sampling strategy in the study lava rise pits

Lava Rise Pit (-2 m)				
Type	Sample Size	Paramters/Variables Measured	Location in Lava Rise Pit	Sampling Approach
Soil Sample	2	Bulk Density (g/cm^3), Porosity (%), Volumetric Water Content (%), Particle Size	Surface (0m)	Stratified-random sampling
	2		Center (-1 m)	
	2		Bottom (-2 m)	
Surface Type Spot Measurement: Moisture Content	70	Volumetric Moisture Content (%)	Surface (0m)	Stratified-random sampling
	70		Center (-1 m)	
	70		Bottom (-2 m)	
Surface Type Spot Merasurement: Temperature	70	Temperature (°C)	Surface (0m)	Stratified-random sampling
	70		Center (-1 m)	
	70		Bottom (-2 m)	
Surface Type Coverage	30	Surface Coverage Type Distribution (%)	Surface (0m)	Stratified-random sampling
	30		Center (-1 m)	
	30		Bottom (-2 m)	

Lava Rise Pit (-5 m)				
Type	Sample Size	Paramters/Variables Measured	Location in Lava Rise Pit	Sampling Approach,
Soil Sample	2	Bulk Density (g/cm^3), Porosity (%), Volumetric Water Content (%), Particle Size	Surface (0m)	Stratified-random sampling
	2		Center (-3 m)	
	2		Bottom (-5 m)	
Surface Type Spot Measurement: Moisture	70	Volumetric Moisture Content (%)	Surface (0m)	Stratified-random sampling
	70		Center (-3 m)	
	70		Bottom (-5 m)	
Surface Type Spot Merasurement: Temperature	70	Temperature (°C)	Surface (0m)	Stratified-random sampling
	70		Center (-3 m)	
	70		Bottom (-5 m)	
Surface Type Coverage	30	Surface Coverage Type Distribution (%)	Surface (0m)	Stratified-random sampling
	30		Center (-3 m)	
	30		Bottom (-5 m)	

Lava Rise Pit (-7 m)				
Type	Sample Size	Paramters/Variables Measured	Location in Lava Rise Pit	Sampling Approach
Soil Sample	2	Bulk Density (g/cm^3), Porosity (%), Volumetric Water Content (%), Particle Size	Surface (0m)	Stratified-random sampling
	2		Center (-4 m)	
	2		Bottom (-7 m)	
Surface Type Spot Measurement: Moisture	70	Volumetric Moisture Content (%)	Surface (0 m)	Stratified-random sampling
	70		Center (-4 m)	
	70		Bottom (-7 m)	
Surface Type Spot Merasurement: Temperature	70	Temperature (°C)	Surface (0 m)	Stratified-random sampling
	70		Center (-4 m)	
	70		Bottom (-7 m)	
Surface Type Coverage	30	Surface Coverage Type Distribution (%)	Surface (0m)	Stratified-random sampling
	30		Center (-1 m)	
	30		Bottom (-2 m)	